

SUMARY

1	INTRODUCTION	1
2	MINAS GERAIS – GEOGRAPHY AND GEOLOGY	2
3	WORK METHODOLOGY	5
3.1	MAGNETOTELLURIC DATA PROCESSING	6
3.1.1	1D MT Modelling	6
4	ELECTRODE SITE SELECTION	11
5	GEOPHYSICAL SOUNDINGS	14
5.1	EL04 – SANTA RITA DE JACUTINGA	22
5.1.1	Combined (ER + MT) Model	27
5.2	EL38C – ANDRELÂNDIA	28
5.3	EL39C – ANDRELÂNDIA	29
5.3.1	Combined (ER + MT) Model	36
5.4	EL43 – SÃO VICENTE DE MINAS	36
5.4.1	Combined (ER + MT) Model	43
5.5	EL42 – SÃO VICENTE DE MINAS	43
5.5.1	Combined (ER + MT) Model	49
5.6	EL46 – CARRANCAS	49
5.6.1	Combined (ER + MT) Model	54
6	ELECTRODE SIMULATION	55
6.1	STATION 39	63
6.2	STATION 43	63
6.3	STATION 42	63
6.4	STATION 46	63
7	CONCLUSION	69

1 INTRODUCTION

This report presents the processing of the geophysical data acquired for stations 04, 39c, 43, 42 and 46, and the simulations for the selection of the best site for the Terminal Rio electrode.

2 MINAS GERAIS – GEOGRAPHY AND GEOLOGY

The most striking geomorphological features of Rio de Janeiro are the mountain ranges Serra do Mar and Serra da Mantiqueira, separated by the inter plateau depression Paraíba do Sul. The Rio de Janeiro Desktop Study showed that there is no way to locate a HVDC ground electrode in Rio de Janeiro state, given its geoFigurey and geology. It was thus proposed the search for a reasonable site South of Minas Gerais State, to where the HVDC line towers can carry the electrode line, after the Serra da Mantiqueira.

Figure 2.1 presents the HVDC line and the geologic map of the west area of the line, which is the search area for the Minas Gerais electrode. To East of the line there is the pipeline that goes to Belo Horizonte, making this side of the HVDC line a risky location for the electrode, because of the interference with the pipeline.

A geoFigureic evaluation of this area shows that it does not have big cities and is not crossed by pipelines, in spite of being a hilly area. The geologic evaluation shows an area of metamorphic rocks, submitted to a wide folding, compressing and shear process, within the Brasília belt, Tocantins geologic province. The unities of the Tonian Period, identified by NPcgx (Group Carrancas) and NPax (Group Andrelândia) may have schist, a rock that hosts carbon, and thus may present Figureite veins.

The sites in general are located within hilly areas (so called “half oranges”), with flatter areas near the flooding zone of the rivers or over dry meanders.

For the Minas Gerais electrode, considering preliminarily the same electrical performance calculated for the Rio de Janeiro electrode, it is advisable to keep a clearance distance of at least 40 km from any pipeline, while it is not available a magnetotelluric sounding at this area.

South of Minas Gerais state there are records of the occurrence of Figureite in the region of São João Del Rey, about 150 km from Terminal Rio. Groups Andrelândia (Npax) and Carrancas (NPcgx) contain schist, a rock that may host Figureyte veins (Figure 2.2). It is important to note that schist is a highly anisotropic rock, what means that the soil surface potential profile will be assymmetric, with a shorter range along the strike direction and a wider range in the perpendicular direction.

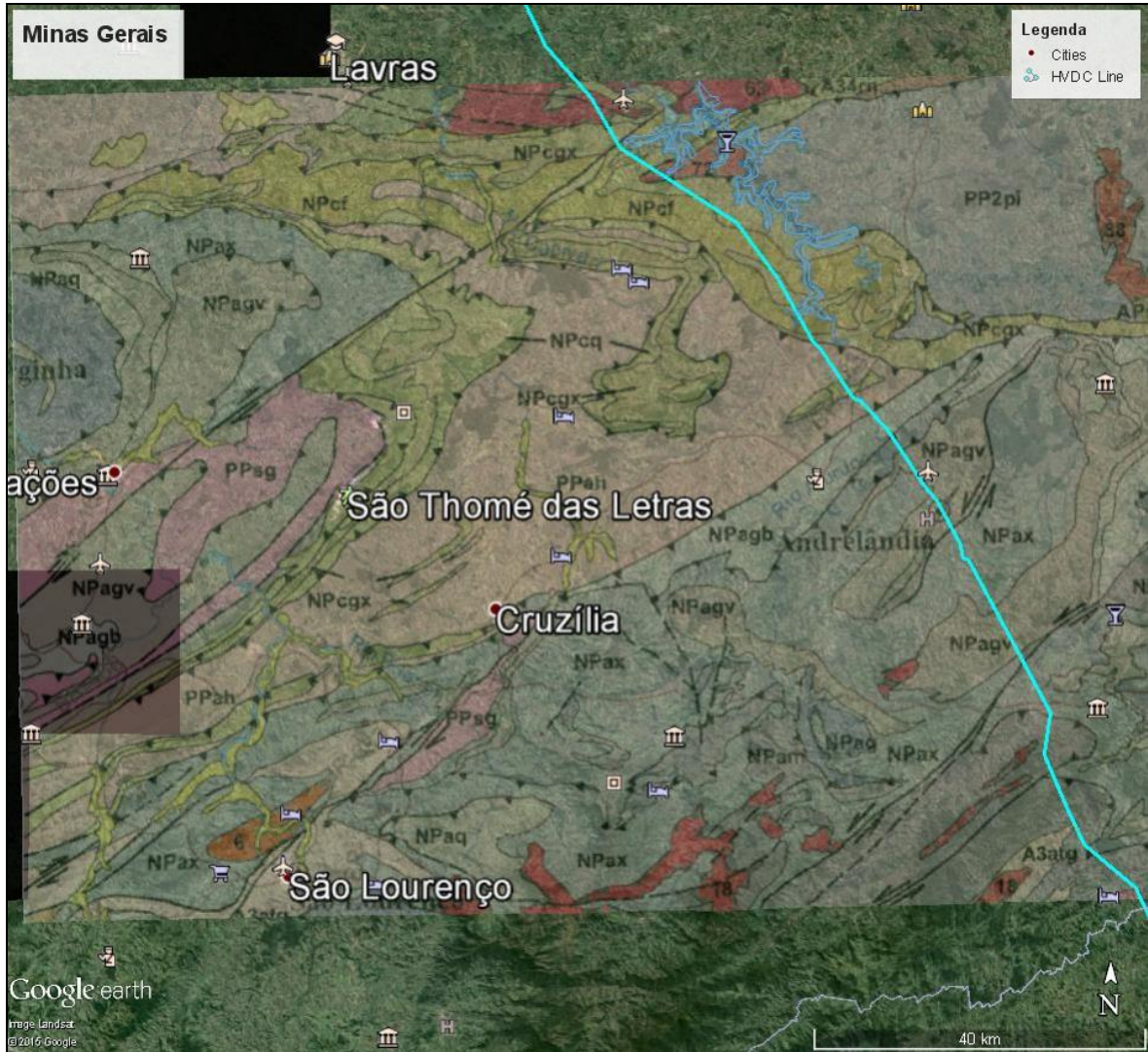


Figure 2.1: South of Minas Gerais with the HVDC line and its West area.

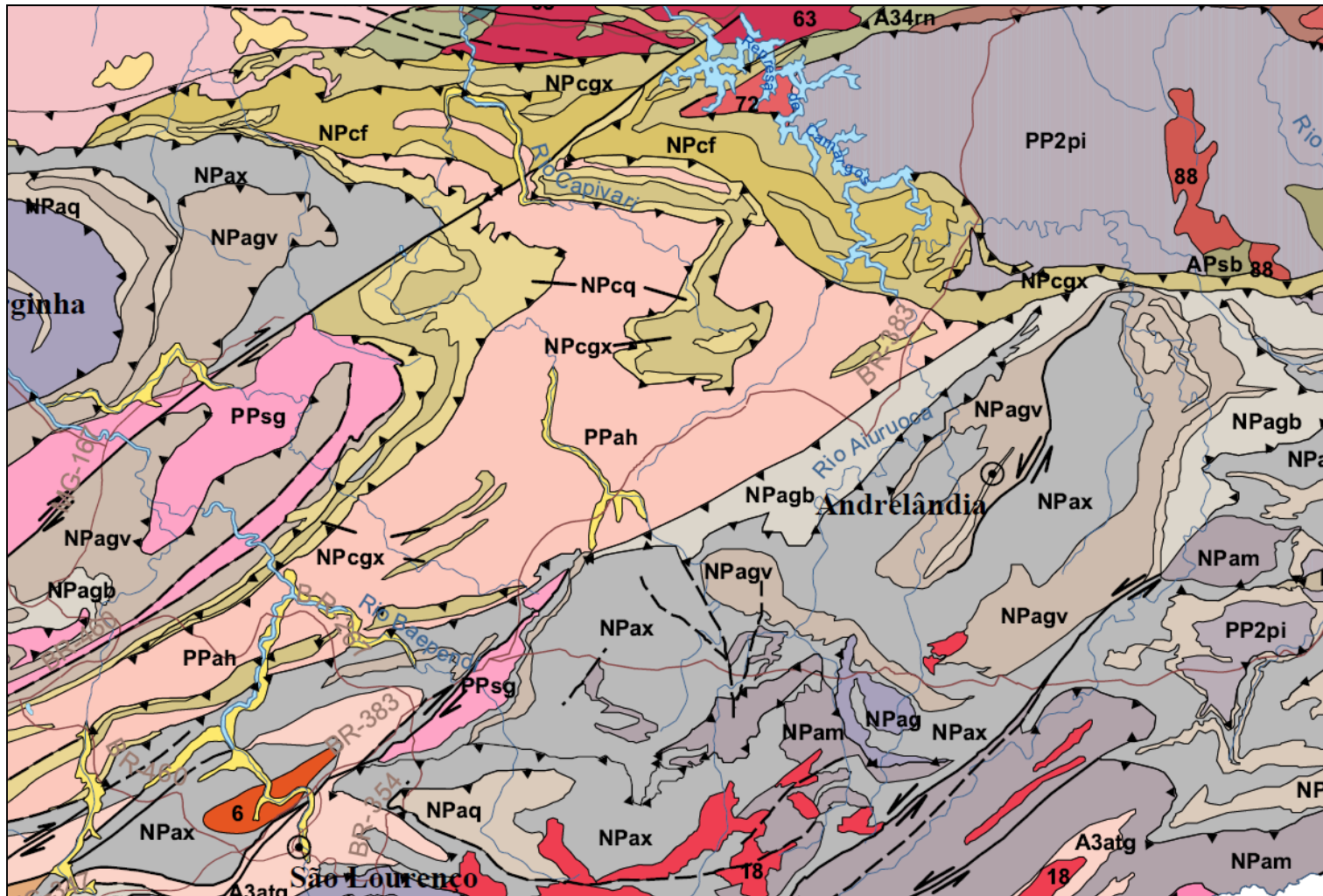


Figure 2.2: geological map of the south-western part of Minas Gerais – the HVDC line comes from close to the dam (central North) down to the Southeast corner, where it enters into Rio de Janeiro.

3 WORK METHODOLOGY

Site Selection for a HVDC ground electrode is an elaborate and iterative process, as many different issues have to be taken into account. The surveys to be developed for this search can be divided into three categories: GeoFigureical Survey, Geophysical Survey and Geotechnical Survey.

The geoFigureical survey is the first to be considered for the selection of the candidate areas to host the electrode. Among the many criteria that can be established, the main important are:

- located outside a ring 15 km around the converter station, and as far as possible from public or private facilities that could be adversely affected by interferences, such as pipelines, urban gas distribution, water and sewer lines, buried cables, transmission lines, well casings, buried metal tanks, bridges, power and distribution substations, power distribution and telephone lines from urban areas and from pipelines;
- reasonably flat, without erosion signs or rocky outcrops and not excessively dry;
- readily accessible by a secondary road (it is not advisable to select a site close to main roads);
- available for purchase and presenting no legal, environmental or archeological restrictions for hosting a ground electrode;
- not a touristic place and with no plans for development of major facilities at its vicinity;
- a reasonably straight line to the converter substation, without the need to cross cities, villages, protected areas, mauntain ranges etc.

For the conventional electrode, the traditional way of site selection is to pre-select a number of areas, with the above geoFigureical characteristics expected for hosting the electrode, and then go to the geophysical survey, starting with the magnetotelluric (MT) survey at the pre-selected areas.

This survey will indicate the two that present the best deep geoelectric structure, which will be subjected to a preliminary shallow geophysical survey, for the identification of the site with the best overall geoelectric structure.

For the application on ground electrode design, it is needed the construction of 1D layered ground models, that shall be locally representative for the shallow layers about 1-2 km around the electrode center, and regionally representative for the deep layers for a radius of a few tens around the electrode.

This model can be achieved by the combination of the subsurface models prospected by the electroresistivity (ER) and magnetotellurc sounding methods. It is necessary to compile a geoelectrical model from the soil surface down to a depth that is much larger than the dimensions of the electrodes in order to achieve a proper model, and this model shall be fairly detailed at the shallow ground layers, where the electrode is buried.

The results from magnetotelluric (MT) stations give information from the surface down to depths from one to many km. TDEM and audio-magnetotelluric soundings guive information from near-surface (few hundred meters) layers and electroresistivity soundings (Schlumberger or Wenner) guive information from shallow layers (few tens of meters). These methods are thus complementary to each other.

These techniques, due to the diffuse propagation of the electric and magnetic fields in the Earths's crust (governed by diffusion equations, associated to fields that present exponential attenuation with depth), present low resolution capacity but are quite suitable for the characterization of the resistivity of wide ground volumes, as needed for grounding studies.

3.1 MAGNETOTELLURIC DATA PROCESSING

The raw data includes five temporal series (Ex, Ey, Hx, Hy and Hz), which are submitted to a heavy data processing, by means of filtering and Fast Fourier Transform, for noise elimination and conversion to the frequency domain. Once in the frequency domain, the data is processed for the production of the EDI file with the power spectra for each frequency.

The power spectra is exported, in EDI format, to the software where it is calculated the apparent resistivity and phase curves for components XY and YX. In this process it is made the conversion of the measuring alignment from magnetic North to geographic North, considering the local declination. The software allows for the post-processing of the apparent resistivity and phase curves, such as:

- rotation to the main axis of the impedance matrix, in order to align with the dominant strike of the area and to maximize the curves separation, and thus, the 2D dimensionality (Figure 3.3);
- rotation to the minimum curves separation (about 45 degrees from the maximum separation), in order to maximize the 1D dimensionality;
- for both curves - editing to eliminate outliers and smoothing to eliminate noise oscillations (Figure 3.4).

For the Minas Gerais data, which presents multidimensional characteristics with MT stations approximately aligned, it was performed a 2D inversion, which enables a preliminary static-shift correction with the selection of appropriate parameters (Figure 3.5).

The correction of static shift is a need in geophysical surveys involving electric field measurements on the soil surface, as is the case of electroresistivity and magnetotelluric surveys. This type of deviation occurs due to the existence of surface inhomogeneities on the ground, with size and depth below the prospecting scale. These shallow inhomogeneities leads to the accumulation of electric charges at its interfaces with the predominant media, resulting on local electric fields that are added to the natural fields associated to the deeper crust layers.

3.1.1 1D MT Modelling

The physical principle that governs induction in a discontinuity is conservation of current. As the current must be kept constant through the discontinuity, the change in conductivity requires the E_y electric field to be discontinuous. In the TM mode the electrical field E_y is perpendicular to the discontinuity, and the need for current conservation in the direction perpendicular to lateral discontinuities (considering that there are no charge sources), results in the E_y electric field presenting strikingly different values on both sides of the interface (due to electrical charges accumulation), and thus in data distortion. All other components of the electromagnetic field are continuous along the discontinuity.

Figure 3.1 shows a 2D model with a vertical contact between two different conductivity zones and Figure 3.2 shows the behavior of the electric field before and after the discontinuity. If the resistivities are $\rho_1 = 10 \text{ } \Omega\text{m}$ and $\rho_2 = 1000 \text{ } \Omega\text{m}$, the following relations applies:

$$- J_y = \sigma E_y \rightarrow 0.1 * E_1 = 0.001 * E_2 \rightarrow E_2 > E_1$$

If the MT data shows a 2D pattern, for the calculation of the 1D geoelectric model of the station it is needed the rotation of the curves to an azimuth where they present minimum separation (about 45 degrees from the maximum separation), in order to maximize the 1D dimensionality and minimize the data distortion.

Data distortion when averaging the two apparent resistivity curves is a consequence of the fact that the horizontal axis of these curves is period (s) and not depth (m). The physical interpretation of averaging in this case means paralleling layers. The way to minimize the data distortion is then by approximating the two curves in order to parallel layers of depths as close as possible.

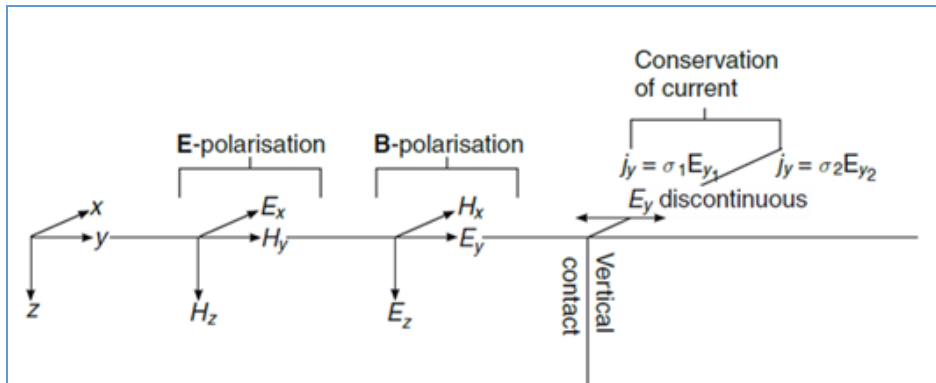


Figure 3.1: bidimensionality (2D) and polarization modes - E (mode TE) and B (mode TM).

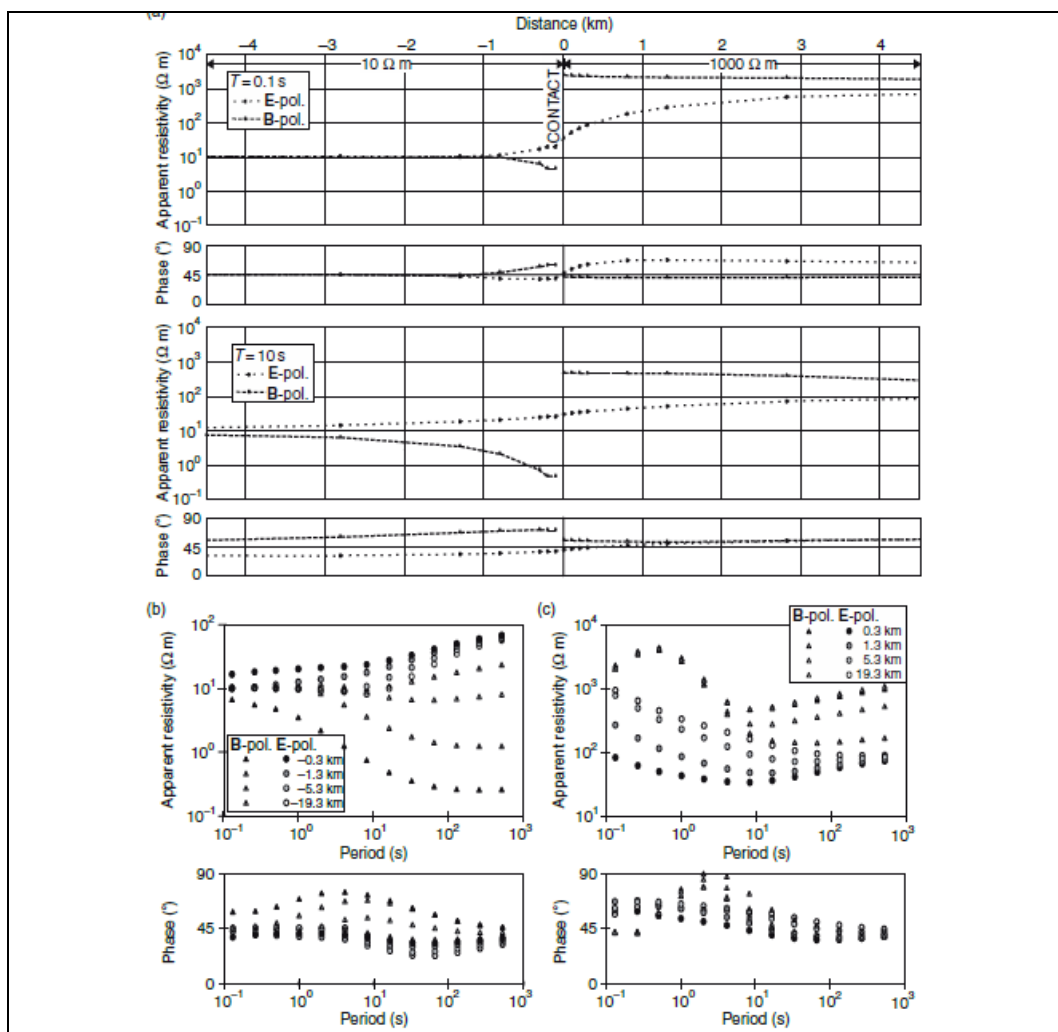


Figure 3.2: bidimensionality (2D) and polarization modes - E (TE mode) and B (TM mode).

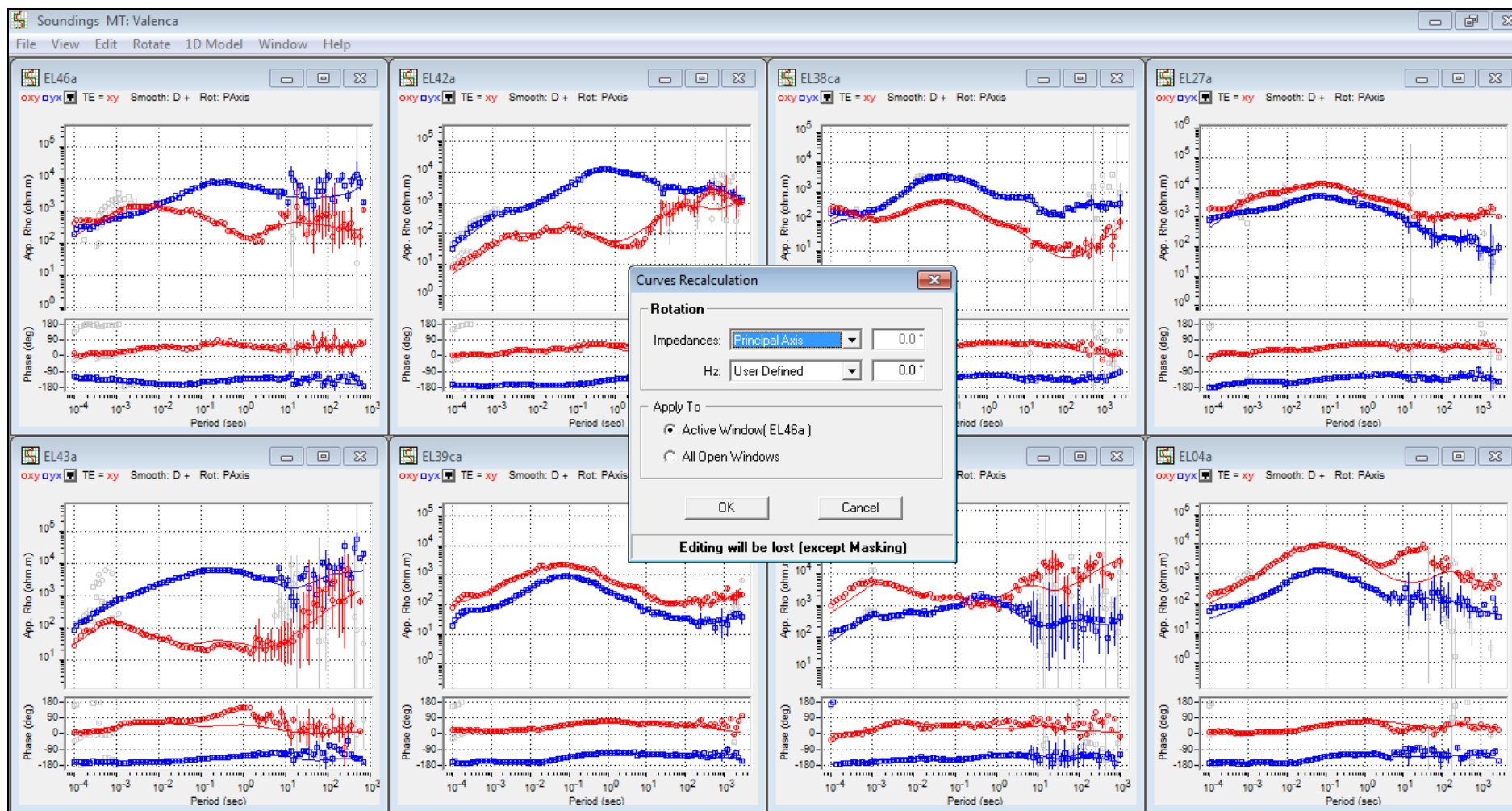


Figure 3.3: edited apparent resistivity and phase curves (TM and TE modes), smoothed and rotated to the dominant strike.

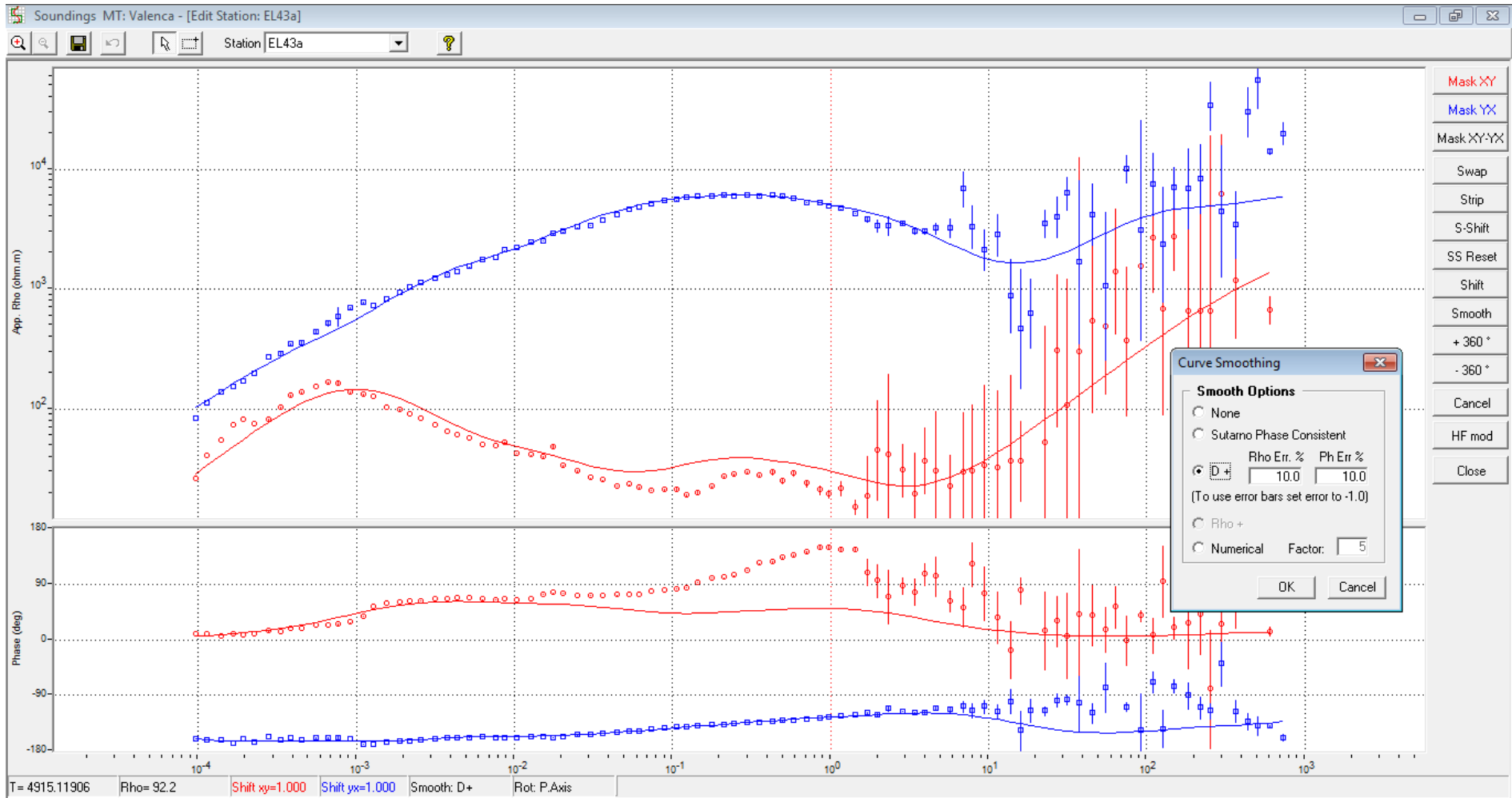


Figure 3.4: edited apparent resistivity and phase curves (TM and TE modes) smoothed by the D+ method and rotated to the dominant strike.

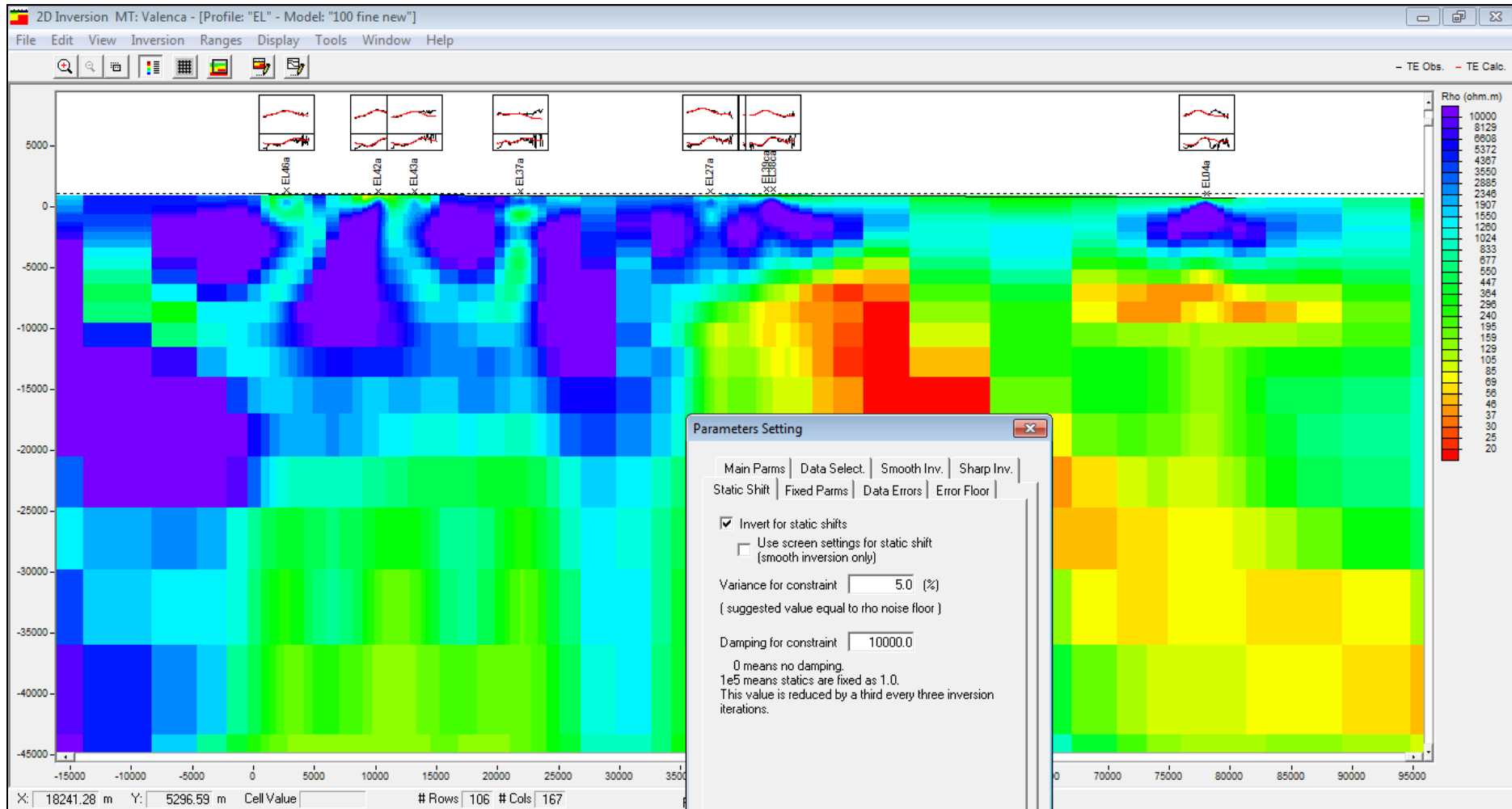


Figure 3.5: 2D inversion with simultaneous static-shift correction.

4 ELECTRODE SITE SELECTION

For the Rio Madeira HVDC transmission system, at Porto Velho, the geologic setting is similar to Minas Gerais (crystalline basement with shallow overburden). Bipole 1 electrode is located about 70 km away from the converter substation and is composed by 60 vertical electrodes, 90 m deep. Bipole 2 is a horizontal electrode with perimeter about 6 km wide, what means an equivalent circle about 2 km diameter.

For the Site Selection of the Belo Monte, Bipole 1 electrodes, it was made 12 MT soundings for the Estreito electrode and 8 MT soundings for the Xingu electrode. The Xingu electrode, of Belo Monte Bipole 1, is a double ring horizontal type and occupies a 1 km² area, presenting a design resistance close to the 0.35 Ω established by the tender documentation, in spite of being located at the Alter do Chão sedimentary basin.

The search for the Rio de Janeiro electrode site shall start with the definition of what kind of land electrode is to be designed – conventional or Figureite vein electrode. As it was shown by the Rio de Janeiro Desktop Study, the search methodology for the Figureite vein electrode is quite complex, depending on a preliminary aerial survey, by means of an electromagnetic sounding method (TDEM or Slingram), complemented by a land based survey. Due to this complexity, which is money and time consuming, and to the fact that there is no guarantee that a suitable site for the electrode will be found, it was decided to make the conventional site selection survey.

The high resistivity geoelectric models obtained for both MT stations at Paraiba do Sul river, and the proximity of the Transpetro pipelines, and also of the Terminal Rio itself, about 45 km away, make this area not compatible with a HVDC ground electrode.

Due to the restriction of Rio de Janeiro state, to host the ground electrode, it was developed the Minas Gerais survey, including the following sequence of activities:

- development of the MT survey at 8 stations by Strataimage – near-surface (AMT) and deep (MT) magnetotelluric soundings,
- processing of the field data by Strataimage and issuing of the correspondent apparent resistivity curves;
- evaluation of the data collected by Strataimage and selection of the two best stations;
- development of the shallow vertical electrical soundings (VES - Schlumberger) at the two best stations by Geoanalysis;
- at both best stations, combination of the shallow (ER) and deep (MT) apparent resistivity curves into a single curve and its inversion for the construction of the 1D model;
- interpretation of the 1D model, based on the known geologic structure at the surveyed area, for the inferring of the aquifer and basement depths;
- evaluation of the best station for hosting the Rio de Janeiro ground electrode.

Figure 4.1 presents the HVDC line and the 8 selected sites for the magnetotelluric survey (Stations 4, 27, 37, 38c, 39c, 42, 43 and 46). The circles with 15 km radiuses are centered in the main cities of the area, and should be avoided, in order to minimize the risk of interference on the cities facilities. The white line defines a clearance between 5 to 7 km around the HVDC line. Figure 4.2 presents the HVDC line and the 8 MT stations over the geologic map of the area.

It was very difficult to find reasonable areas for this survey, due to the hilly topography of all this area. The selected sites (except 38c and 39c) where inspected by a CSEPDI and CET Brazil team, among many other sites.

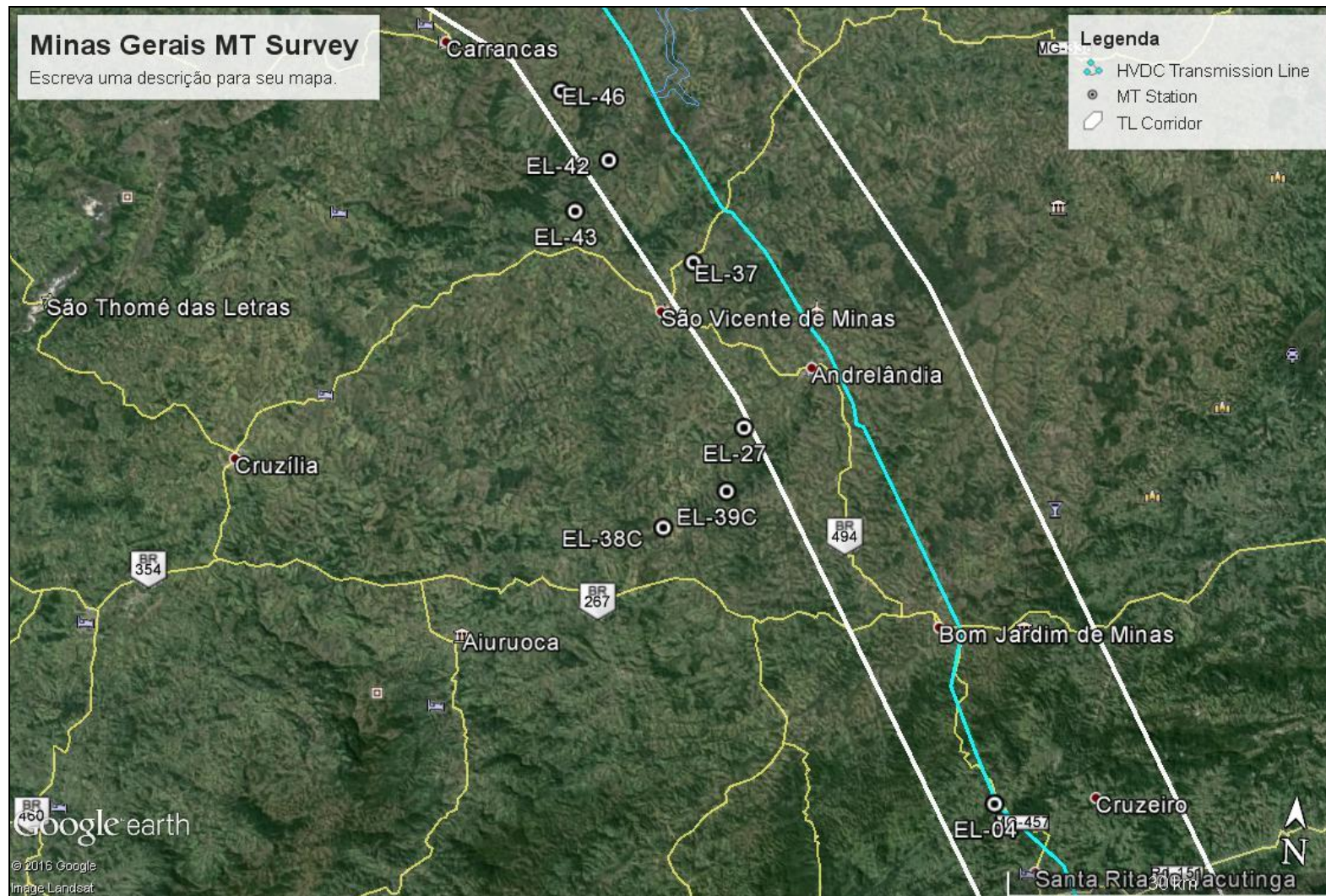


Figure 4.1: 8 MT stations South Minas Gerais, HVDC line (blue) and its corridor (white).

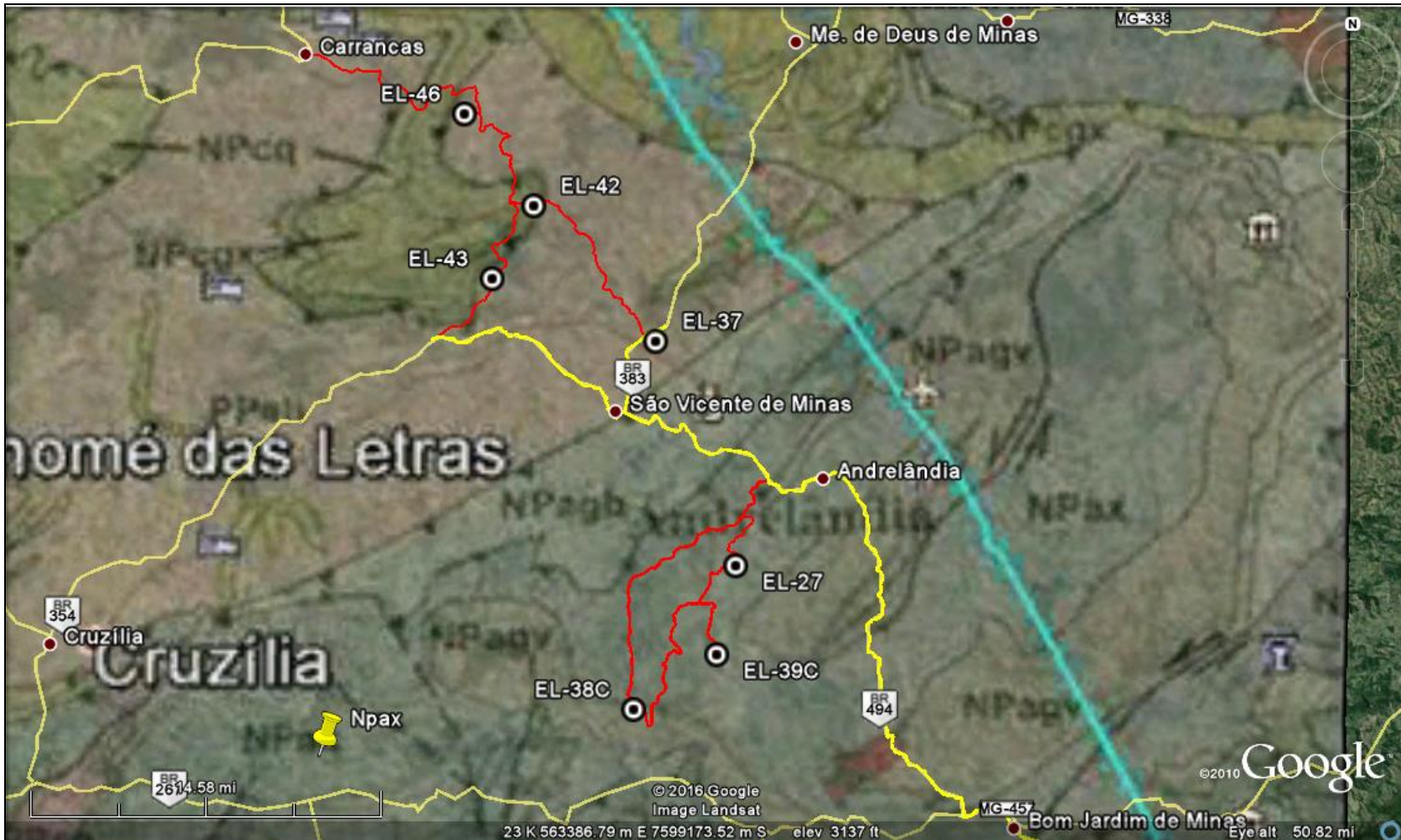


Figure 4.2: 8 MT stations South Minas Gerais and the HVDC line (green) over the geologic map.

5 GEOPHYSICAL SOUNDINGS

Table 5.1 and Figure 5.1 present the UTM coordinates and the localization of the 10 stations where it was developed the MT survey:

- Rio de Janeiro (close to Paraíba do Sul river) – stations EV01 and EV05;
- Minas Gerais – the other 8 stations.

The acquisition time for each MT sounding was 24 hours, with half one hour for the AMT sounding. The AMT soundings allowed for the prospection of the near-surface ground layers and also for the static shift adjustments. The aligned stations at each direction allowed for the construction of two 2D sections MT with the static shift correction.

It was acquired AMT and MT data in 8 stations, close to the cities Santa Rita de Jacutinga, Andrelândia and Carrancas, south of Minas Gerais state. It was measured the electric and magnetic fields Ex, Hy, Ey and Hx with equipment from Phoenix Geophysics. The frequency range goes from 10 kHz to 0.0034 Hz. All the stations presented high resistivities (around 1.000 Ω m) because the stations are within the Brasília mobile belt, South of São Francisco craton.

Figure 5.2 present the apparent resistivity curves of the 6 MT stations at Minas Gerais, where it was made the geometric average between the TM and TE modes.

Figures 5.3 and 5.4 present the smoothed apparent resistivity curves and phase curves (TM and TE modes) for the 8 stations, for two different alignments of the measuring axis:

- Figure 5.3 - the axis was rotated to maximize the curves separation, what means that the TE mode is aligned with the dominant strike of the area;
- Figure 5.4 - using the geological map as a guide, it was tested several rotation angles for each particular station, until it was found one that joined the TE and TM modes, minimizing the curves separation, allowing for the 1D (average) modelling.

The analysis of these curves allow the following general findings:

- the stations are not too noisy, mainly for the short and median periods (from 10^{-4} to 1 s);
- the separation of TM and TE modes show a 2D geoelectric structure;
- the curves generally start with an upward inclination, what means that there is no basin with sediments, but only a shallow overburden;
- the opening of the curves for TE and TM modes over longer periods, may indicate lateral variation that can be associated with deep geologic faults.

The aligned stations allowed for the construction of a crust section (40 km deep, 80 km wide). Figure 5.5 presents the resistivity section from the combination of 1D Occam layered models of the MT stations. Figure 5.6 presents the 2D resistivity section, obtained from a 2D inversion with simultaneous static-shift correction, and Figure 5.7 presents this same section smoothed. For the 2D inversion the curves were softened by the D+ method, in order to eliminate oscillations due to noise. For all the section presented, the geoelectric structure between stations EL04 and EL38 is not reliable, due to the wide distance between these two stations, without any intermediate station. All the stations present a 2D geoelectric structure.

From these 10 MT soundings, it was selected 5 stations (yellow in Table 5.1), which presented the possibility of hosting a HVDC ground electrode, and at each station it was done four VES - Vertical Electrical Soundings, for the determination of the shallow geoelectric model. All the shallow soundings were made with Schlumberger arrangement, with current probes separation up to 1 km wide.

For combination with the ER apparent resistivity curve, the XY and YX curves of the MT sounding for each station was rotated in order to present the minimum separation and then it was done the geometric average of both curves.

The next sub-items present the results of the geophysical surveys done at these five selected stations and the combined geoelectric model, which allowed for the electrode simulations.

Station	S	E	Height
EL04	7556921	589770	736
EL38c	7580605	558600	1113
EL39c	7584175	564133	1059
EL27	7590012	565408	944
EL37	7604760	560108	940
EL43	7608905	549230	954
EL42	7613671	552026	932
EL46	7619742	547402	971

Table 5.1: coordinates of the 8 MT stations in Minas Gerais.

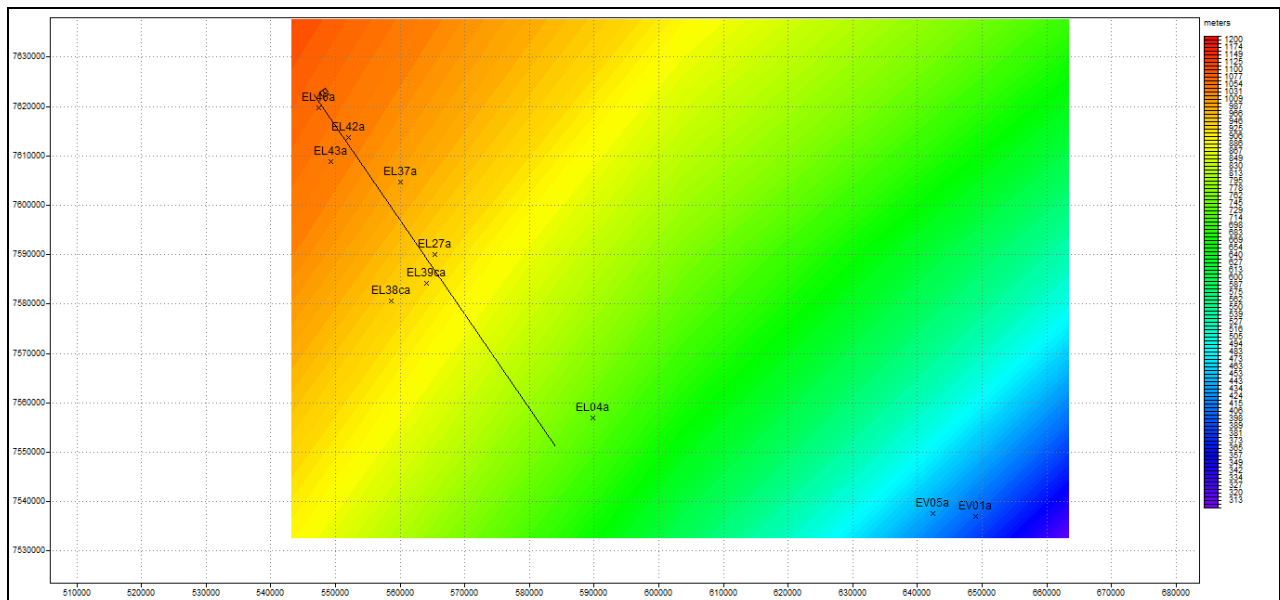


Figure 5.1: sounding line of the 8 MT stations in Minas Gerais.

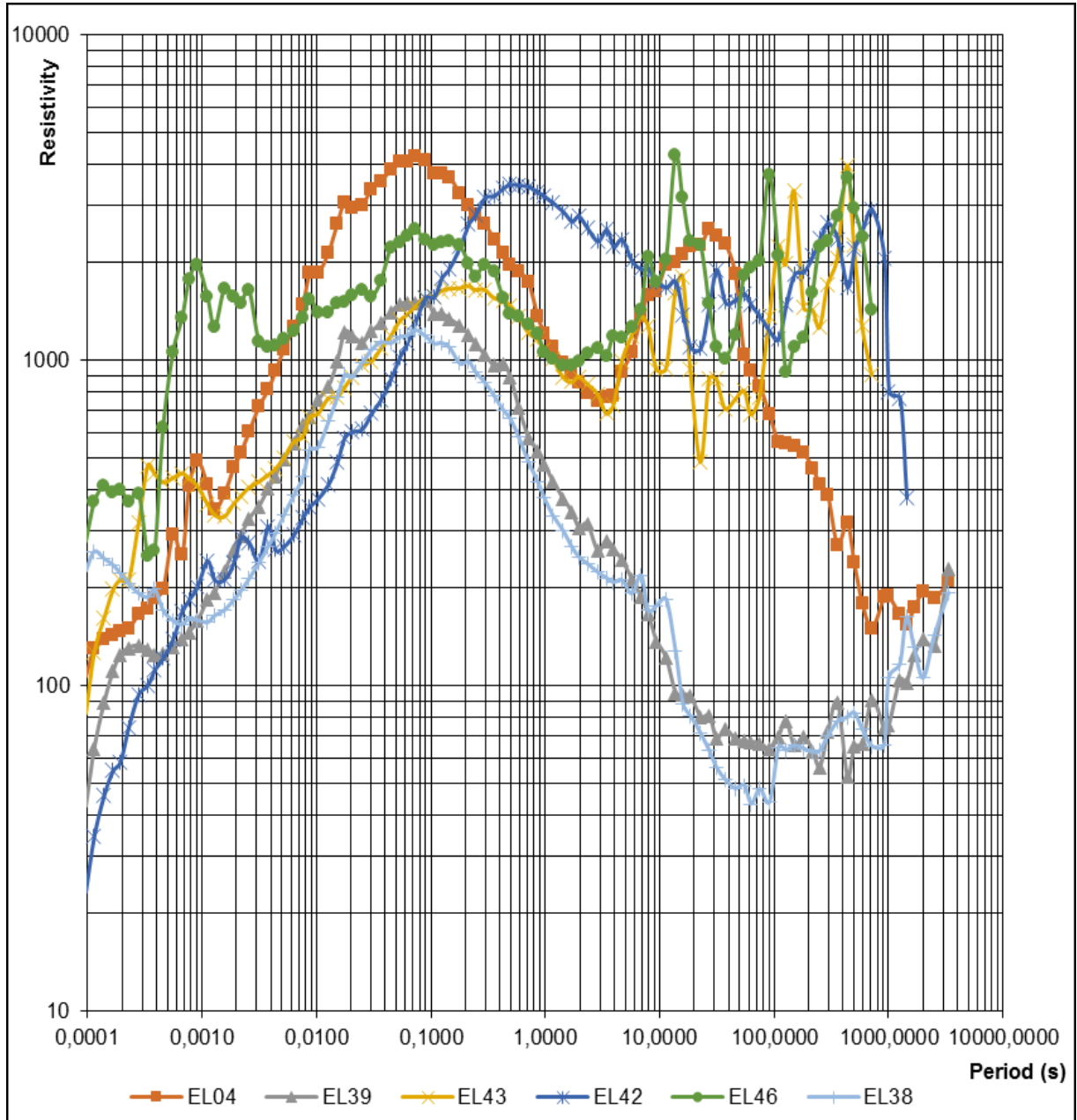


Figure 5.2: 1D apparent resistivity (Ωm) x period (s) curves.

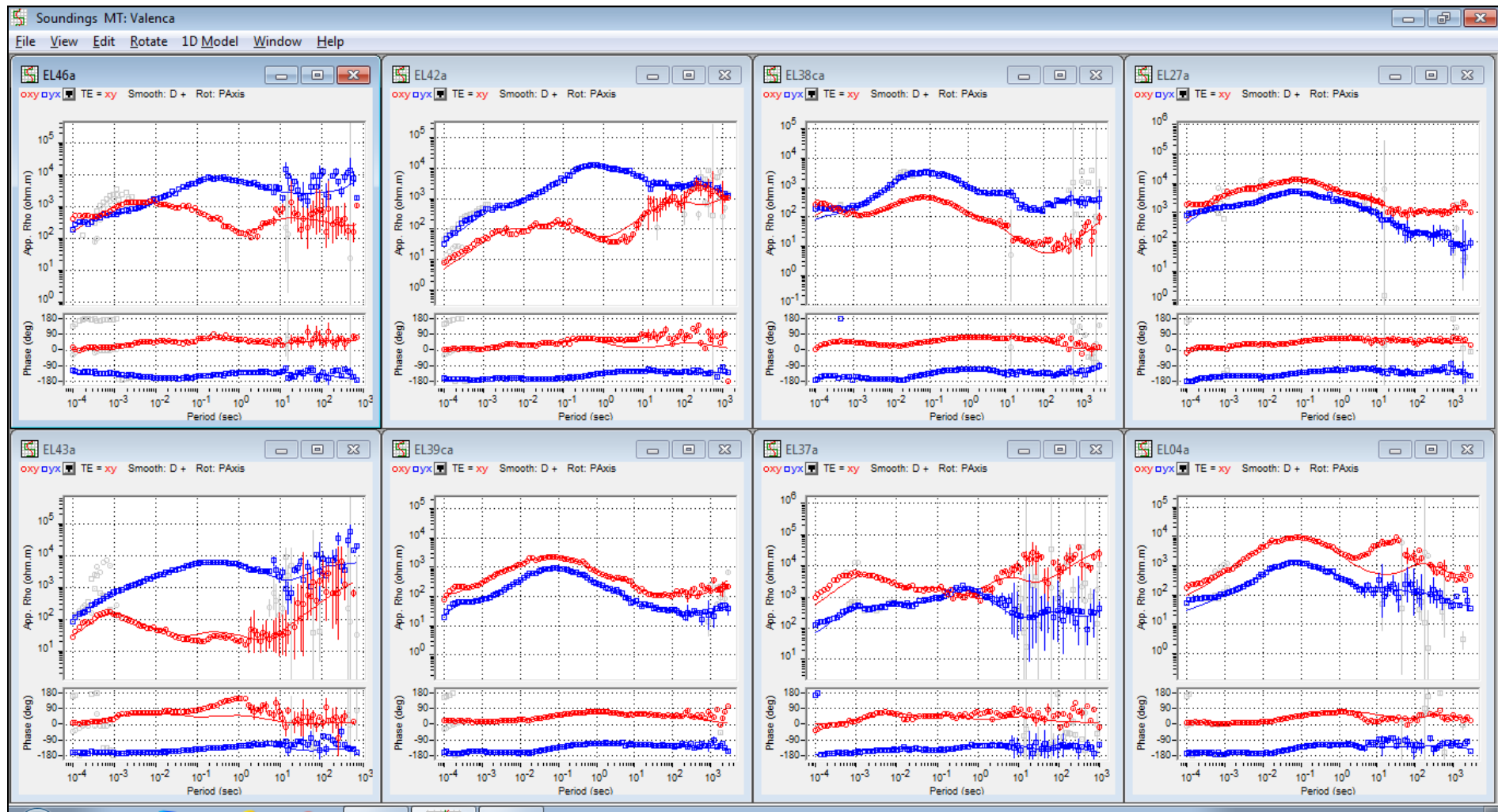


Figure 5.3: TM and TE modes of the apparent resistivity and phase curves for the 8 stations, smoothed and rotated to the dominant strike.

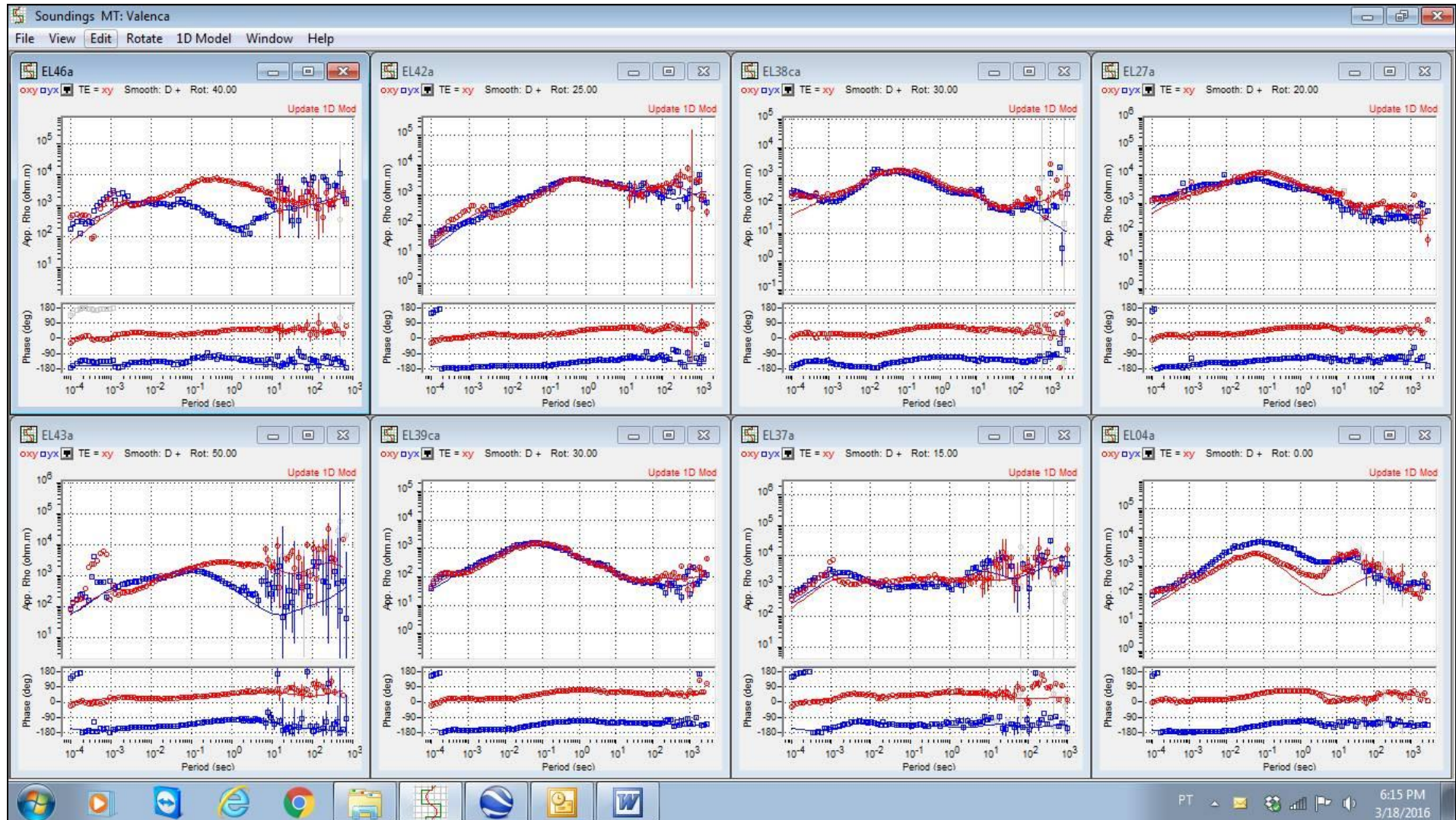


Figure 5.4: XY and YX apparent resistivity and phase curves for the 8 stations, smoothed and rotated for 1D modelling.

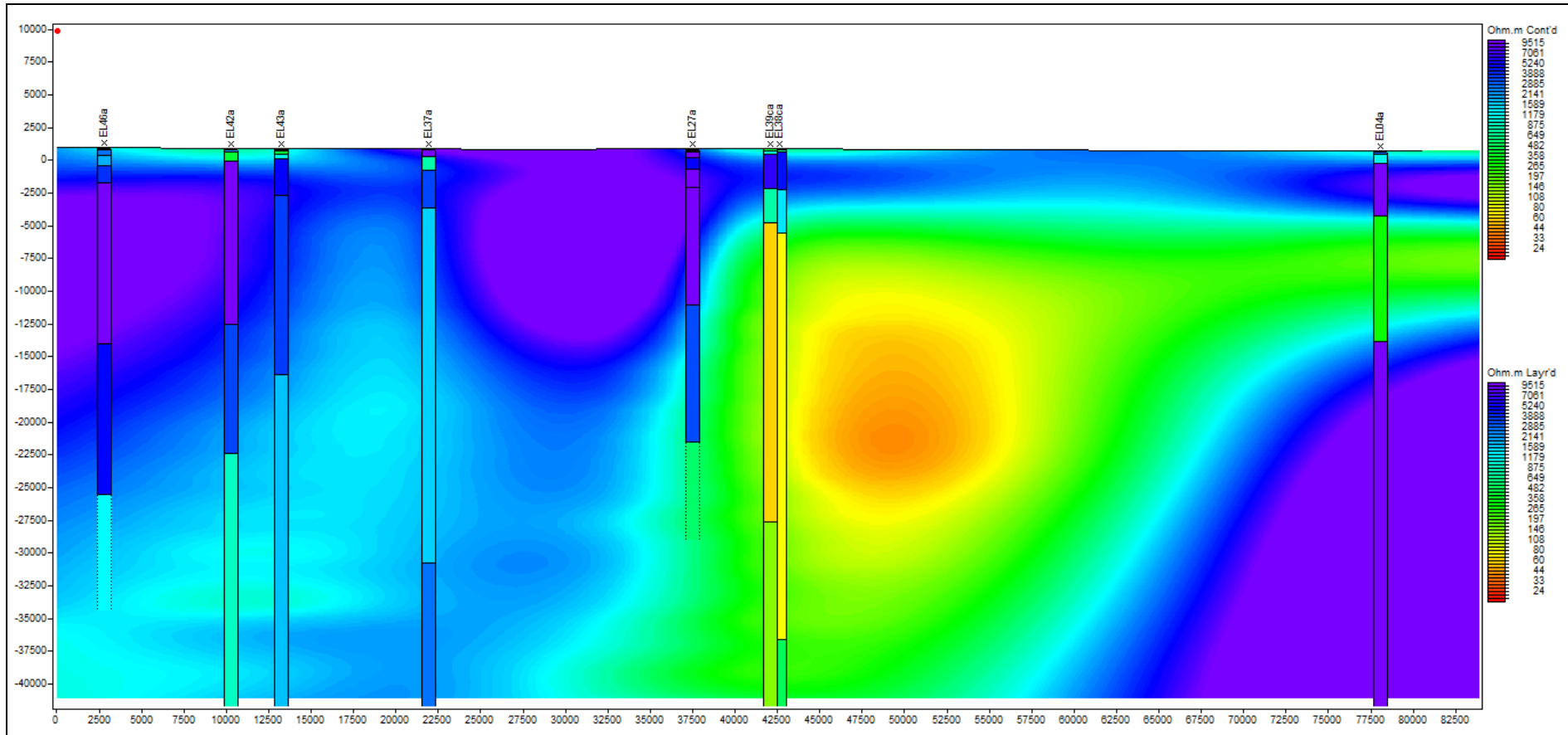


Figure 5.5: resistivity section from the combination of 1D Occam layered models of the MT stations.

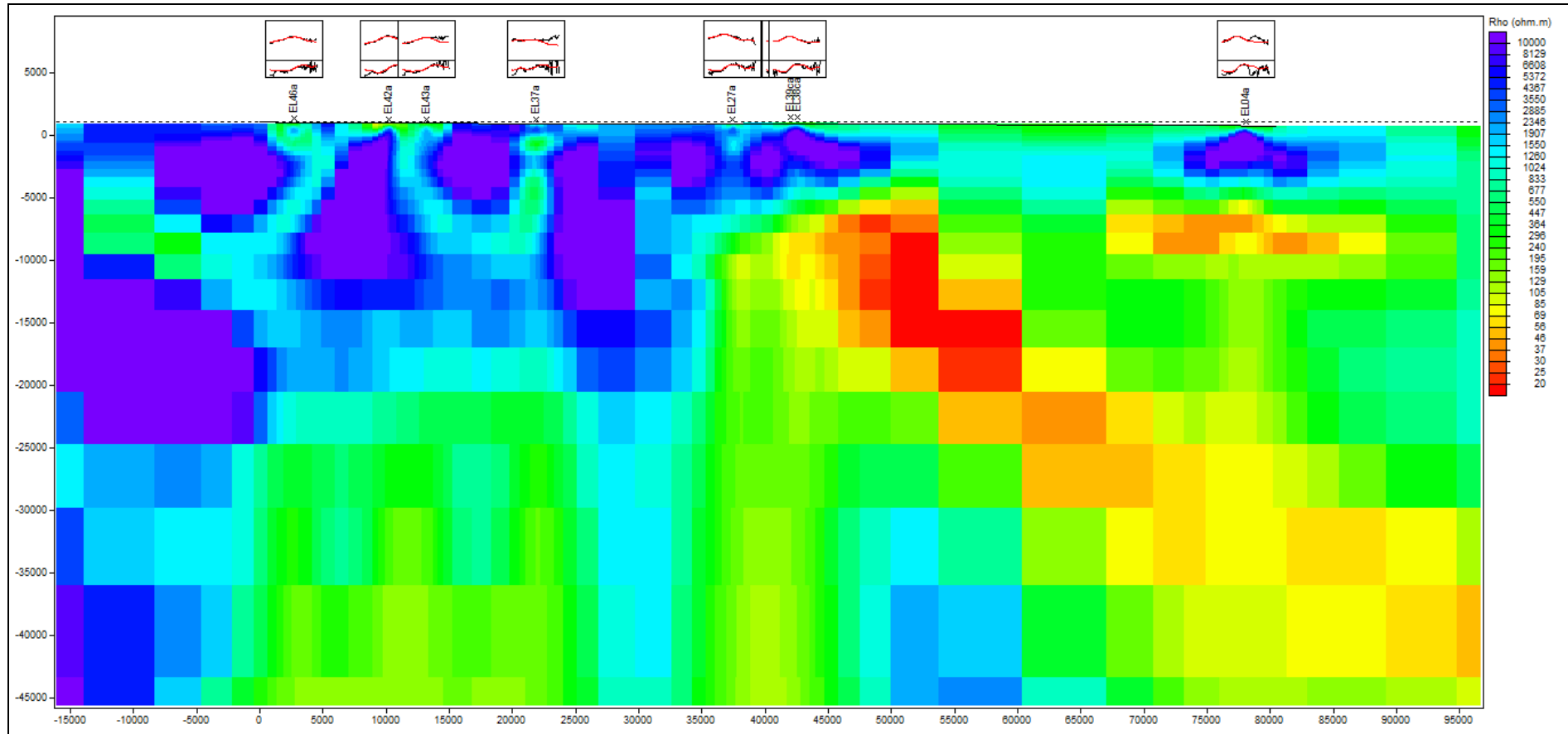


Figure 5.6: 2D resistivity section.

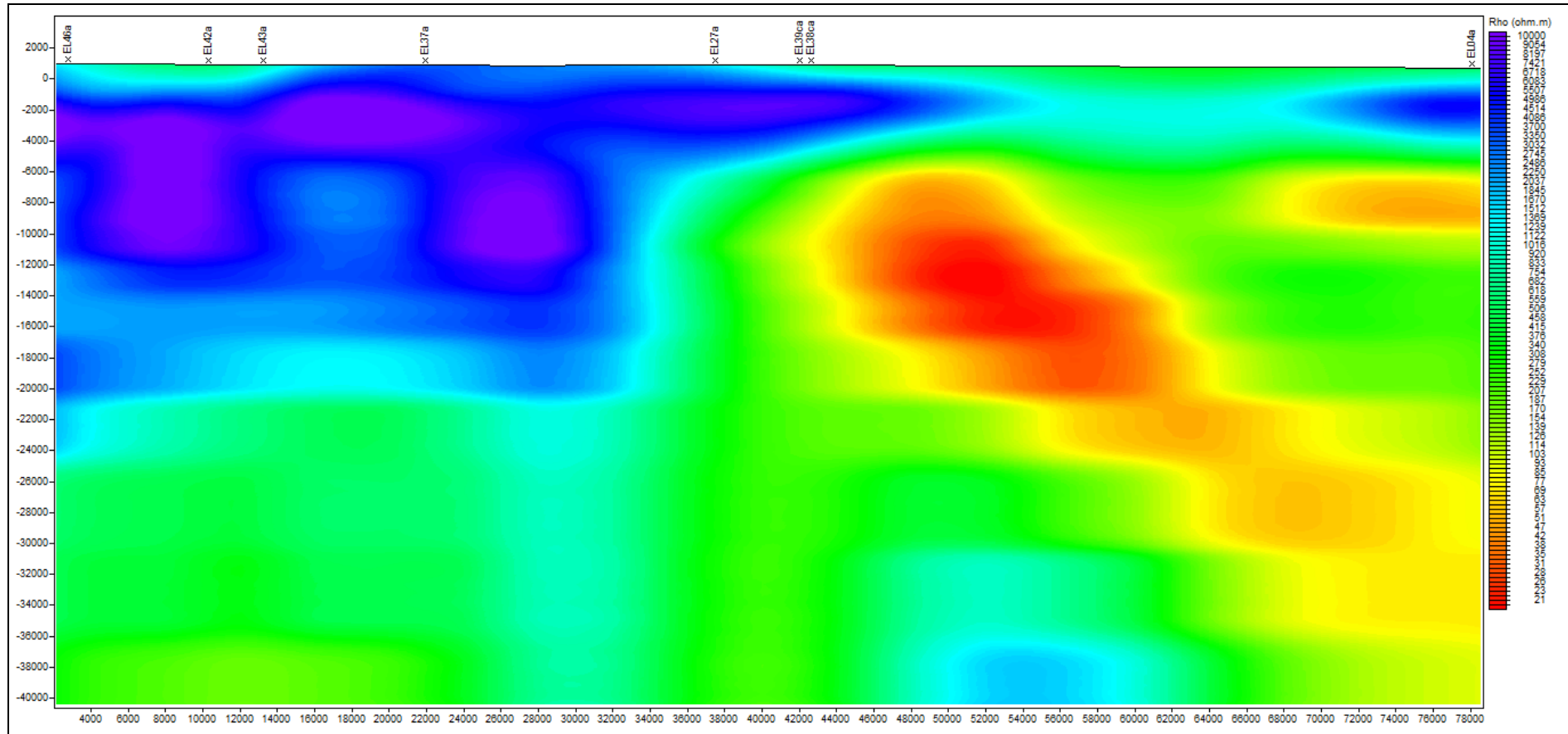


Figure 5.7: smoothed 2D resistivity section.

5.1 EL04 – Santa Rita de Jacutinga

Photo 5.1 shows a view of the field team during the MT survey – it can be seen that the site is undulated and does not have outcrops. The soil is sandy and was flooded around the river that crosses the area.

Figure 5.8 presents the four apparent resistivity curves and its geometric average, which was inverted, resulting on the model presented in Figure 5.9. This model shows an 84 m sediments layer above the basement.

Figure 5.10 presents the apparent resistivity and phase curves (TM and TE) for Station EL04, with noise appearing for frequencies above 0.1 Hz. The curves start upwards, what is indicative of a shallow basement, compatible with the undulated topoFigure of the area.

Figure 5.11 presents the apparent resistivity and phase curves rotated for 1D modeling and Figure 5.12 presents the rotated apparent resistivity and phase curves (XY and YX) and 1D magnetotelluric geoelectric model.



Photo 5.1: view of Station EL04.

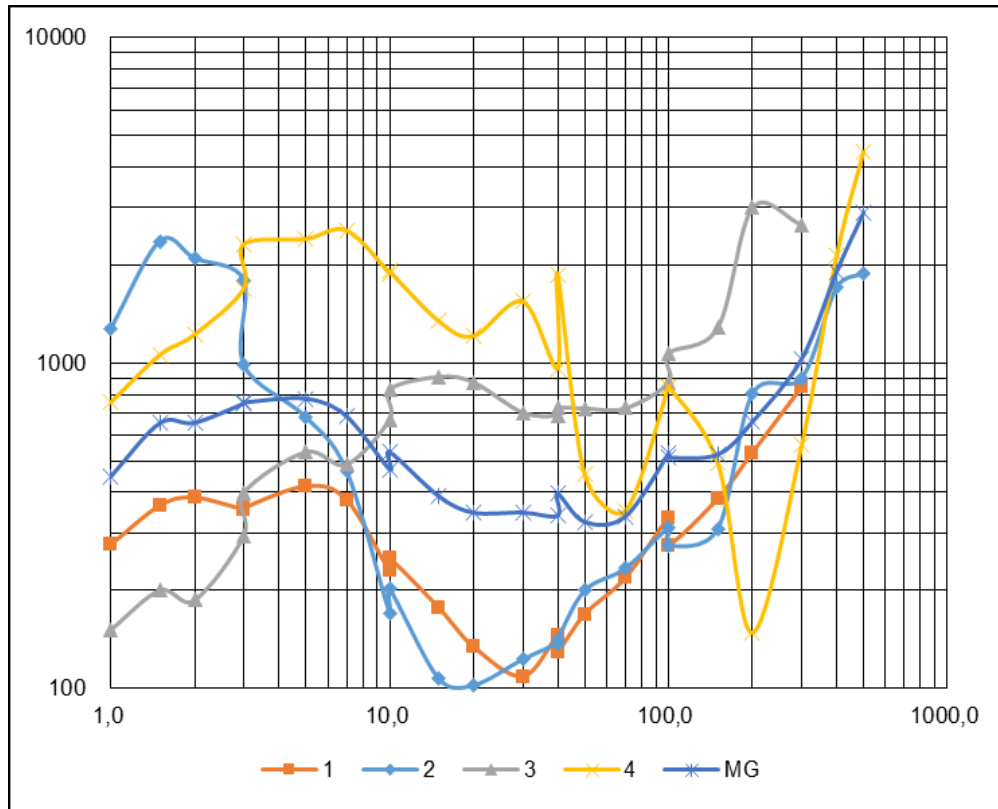
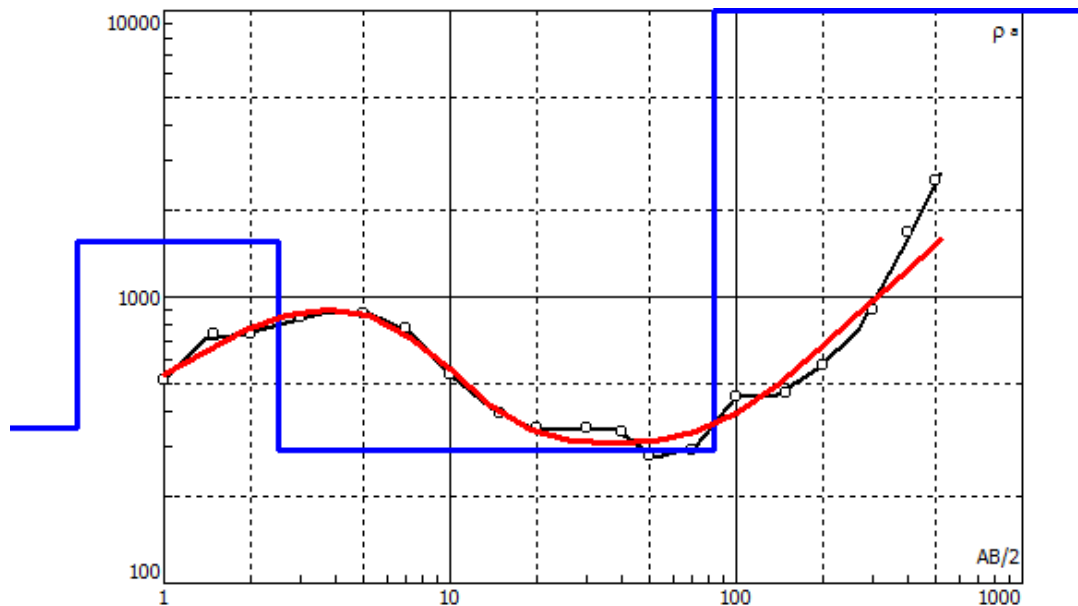


Figure 5.8: four shallow apparent resistivity curves and its geometric average at site EL04.



N	ρ	h	d	Alt
1	350	0.5	0.5	-0.5
2	1566	2	2.5	-2.496
3	293	81.6	84.1	-84.13
4	10000			

Figure 5.9: average apparent resistivity curve of the shallow ground layers – measured (black) and calculated (red) and geoelectric model (black).

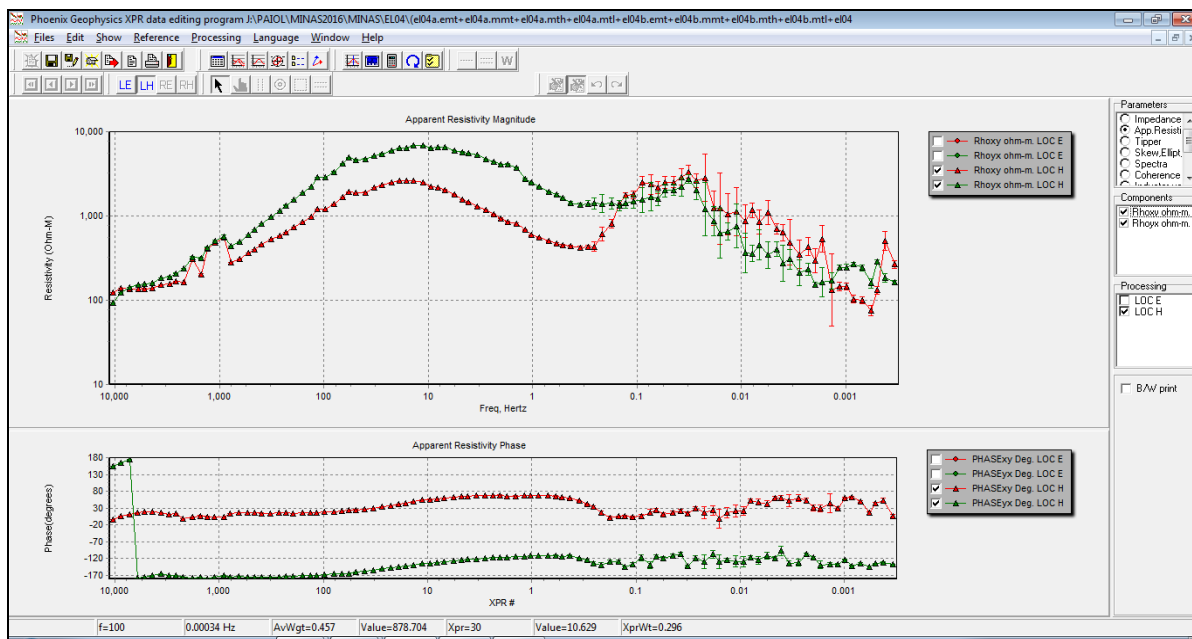


Figure 5.10: TM and TE modes of the apparent resistivity and phase curves for Station EL04.

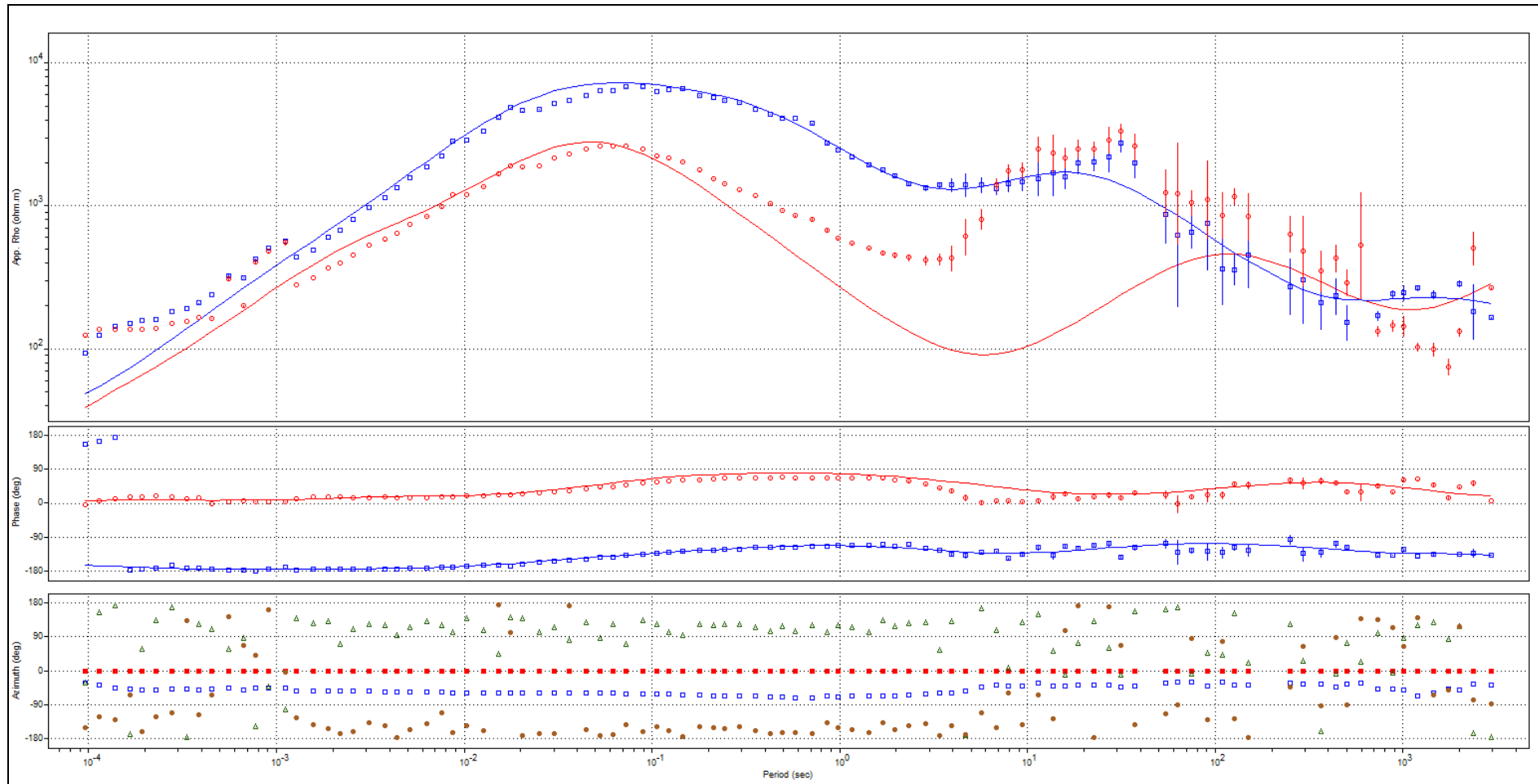


Figure 5.11: station EL04 - apparent resistivity and phase curves rotated for 1D modeling - measured (points) and smoothed (lines).

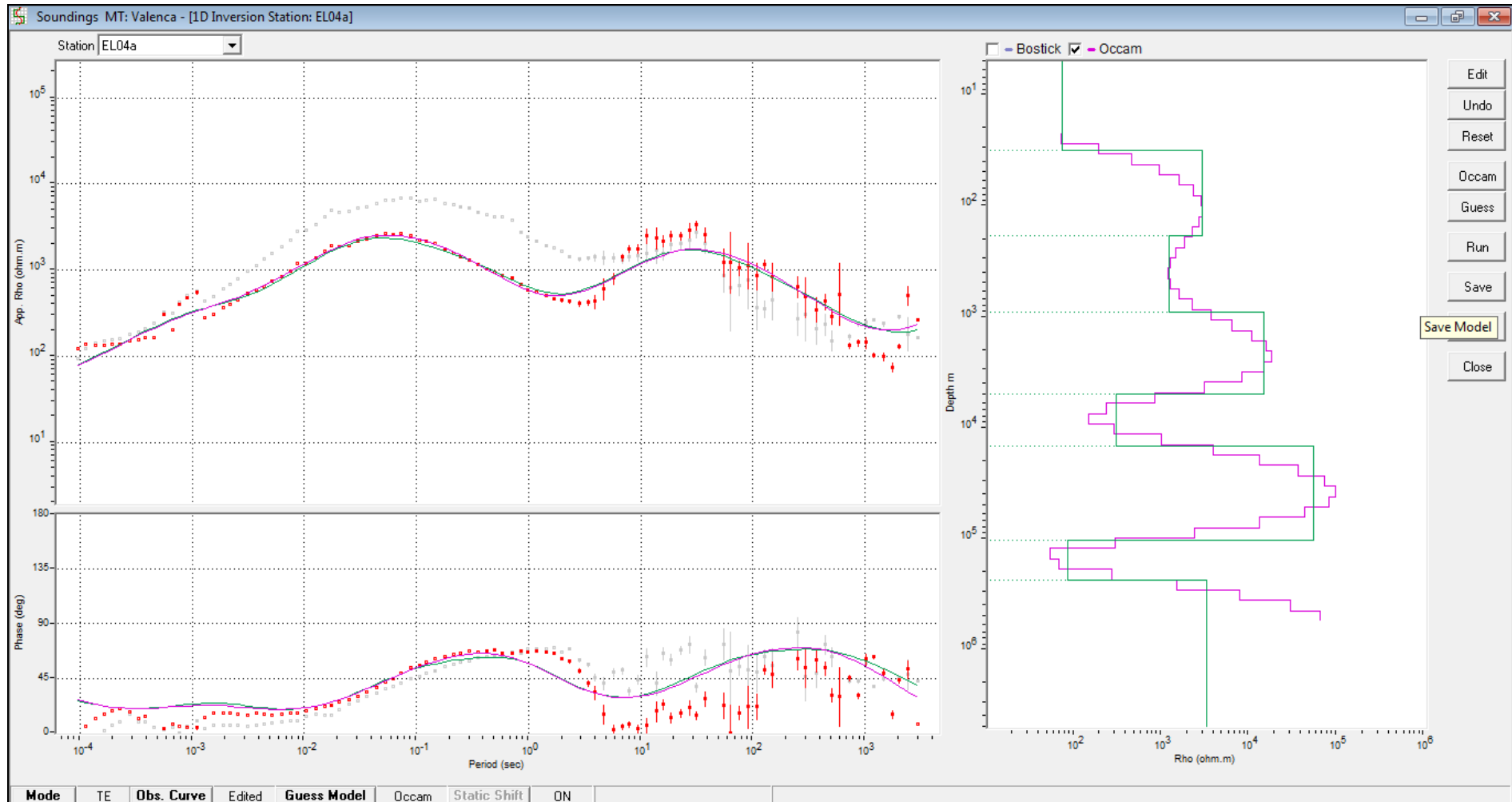


Figure 5.12: Station EL04 - XY and YX apparent resistivity and phase curves (rotated) and 1D MT geoelectric model.

5.1.1 Combined (ER + MT) Model

Figure 5.13 presents the combined ER and MT curves, with expected maximum (yellow) and minimum (gray) boundaries for the 1D apparent resistivity curves at site EL04.

Figure 5.14 presents the average apparent resistivity and phase curves, and the geoelectric model (blue). This model, with a 10000 Ωm x 10 km ground layer, shows that site EL04 presents no condition to host a HVDC ground electrode.

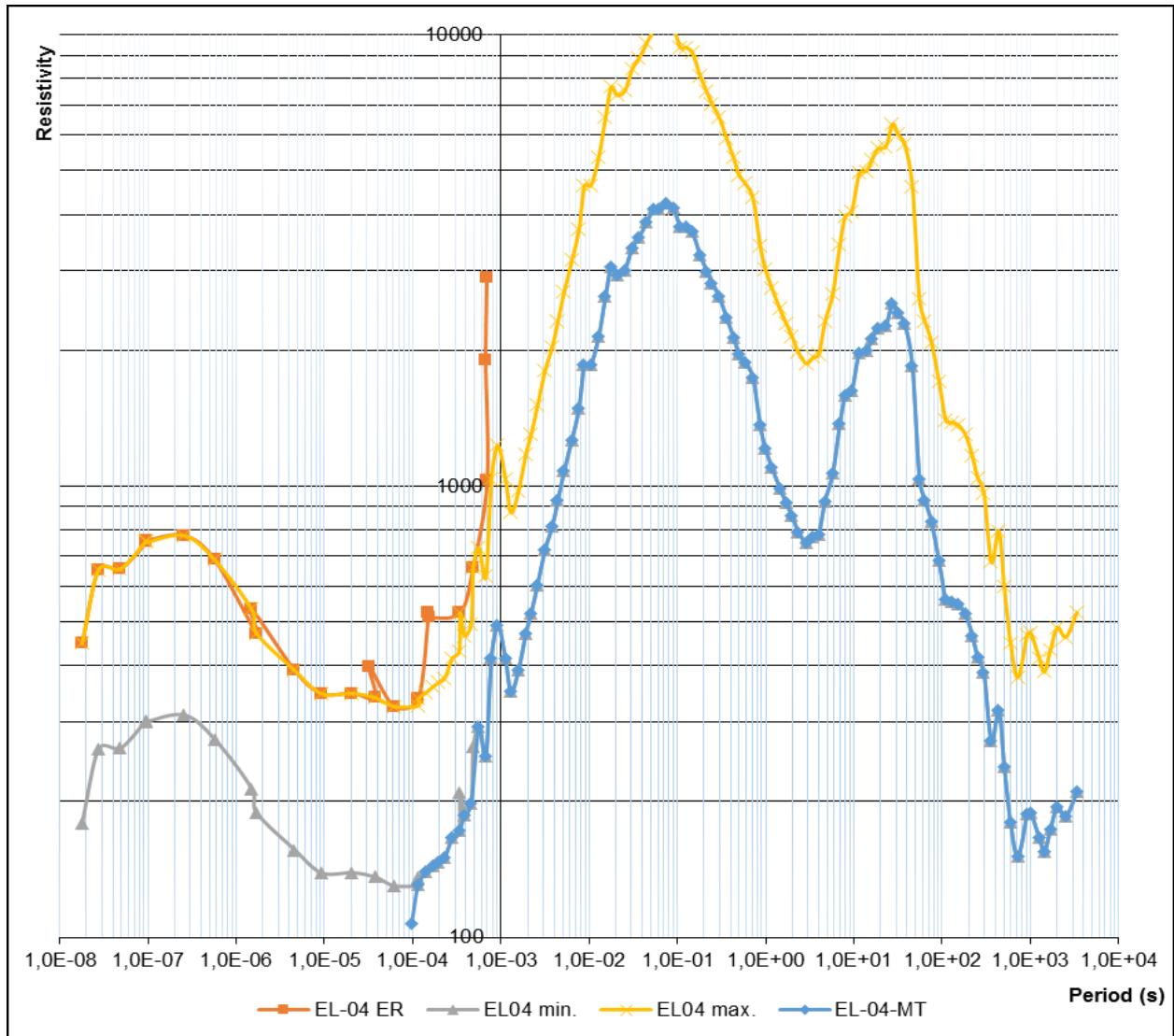


Figure 5.13: Site EL04 - combined ER (orange) and MT (blue) curves – expected maximum (yellow) and minimum (gray) boundaries for apparent resistivity curves.

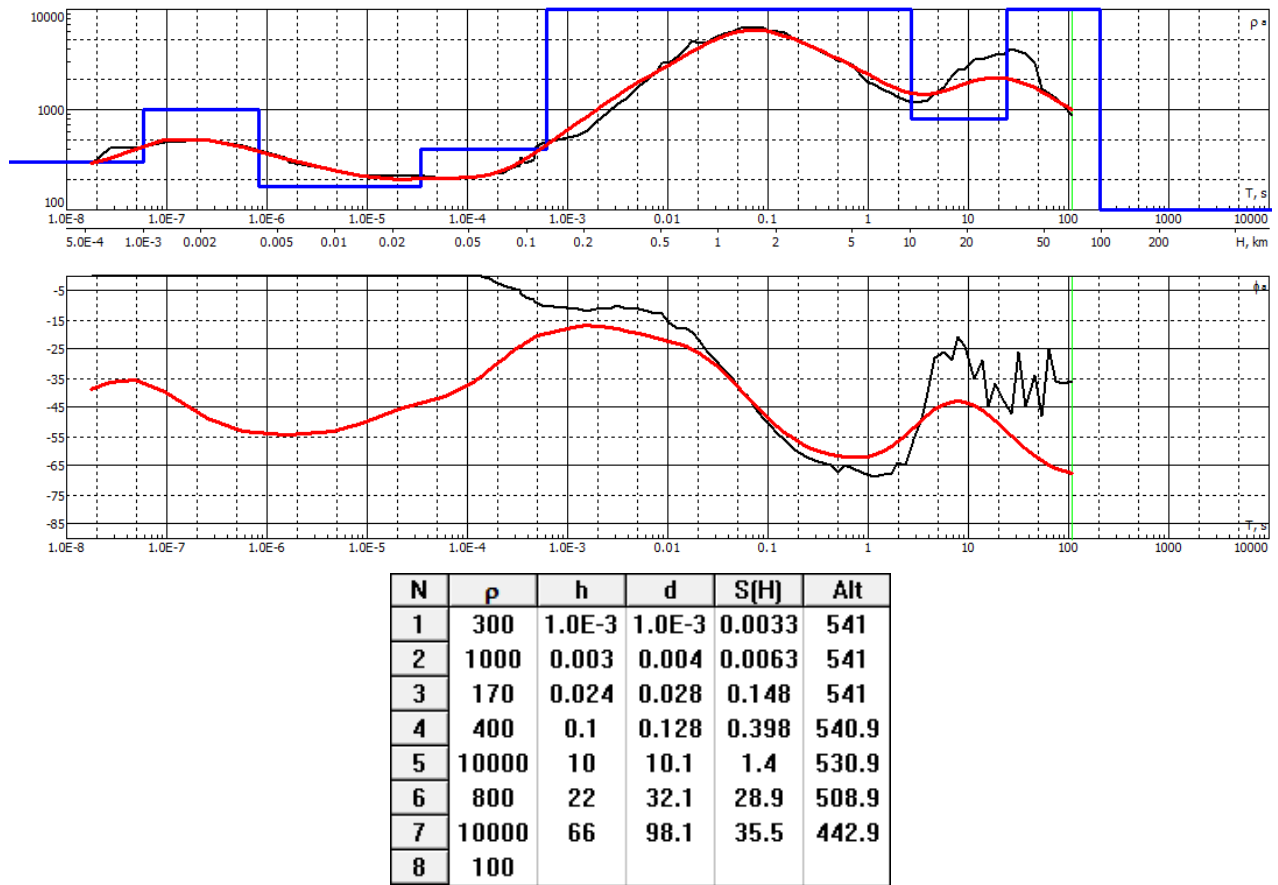


Figure 5.14: Station EL04 – average apparent resistivity and phase curves and 1D geoelectric model (blue and table).

5.2 EL38c – Andrelândia

Figure 5.15 presents the apparent resistivity and phase curves (TM and TE) for Station EL38c, with noise appearing for frequencies above 0.01 Hz. The curves go downward for one frequency decade and then go up, as the basement is reached.

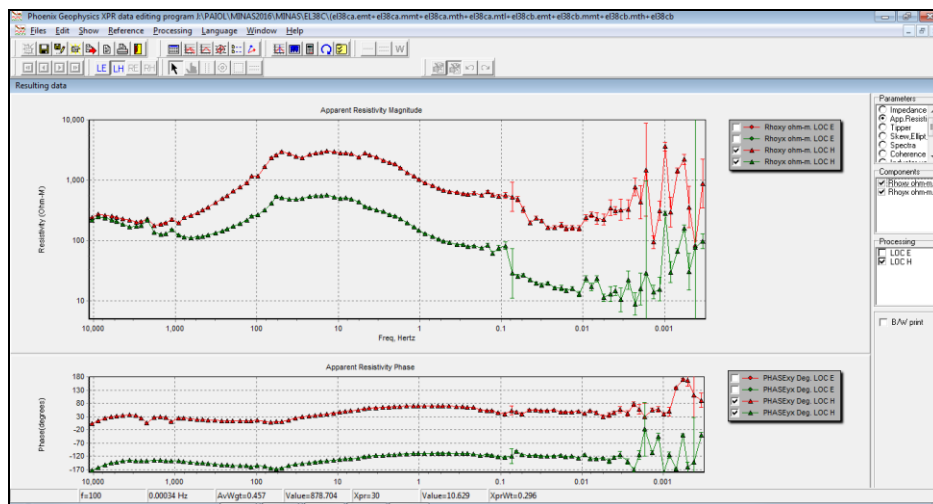


Figure 5.15: apparent resistivity and phase curves (TM and TE) for Station EL38c.

5.3 EL39c – Andrelândia

In this area it was observed outcroppings of yellowish and coarse quartzite grains, and also of reddish and altered muscovite shale.

Figure 5.16 presents the four apparent resistivity curves and its geometric average, which was inverted, resulting on the model presented in Figure 5.17, which shows a 52 m sediments layer above the basement.

Figure 5.18 presents the apparent resistivity and phase curves (TM and TE) for Station EL39c, with noise appearing for frequencies above 0.01 Hz. The curves start flat and in less than one decade go upward, what is indicative of a shallow basement.

Figure 5.19 presents the combined ER and MT curves, with expected maximum (yellow) and minimum (gray) limits for the 1D apparent resistivity curves at site EL04. Probably, the actual apparent resistivity curve will be situated within these two boundaries.

Figure 5.20 presents the apparent resistivity and phase curves (TM and TE modes) rotated for alignment with the dominant strike. Figure 5.21 presents these same curves rotated for 1D modeling (minimum separation of XY and YX curves). It is clear the good overlap of the curves, meaning that the 1D model is well adjusted. Figure 5.22 present these two curves rotated for 1D modeling and the corresponding MT geoelectric model.

Figure 5.23 presents the overlapping apparent resistivity and phase curves of stations EL38 and 39, rotated for 1D modeling, where it can be seen how similar is the deep geoelectric structure of both stations.

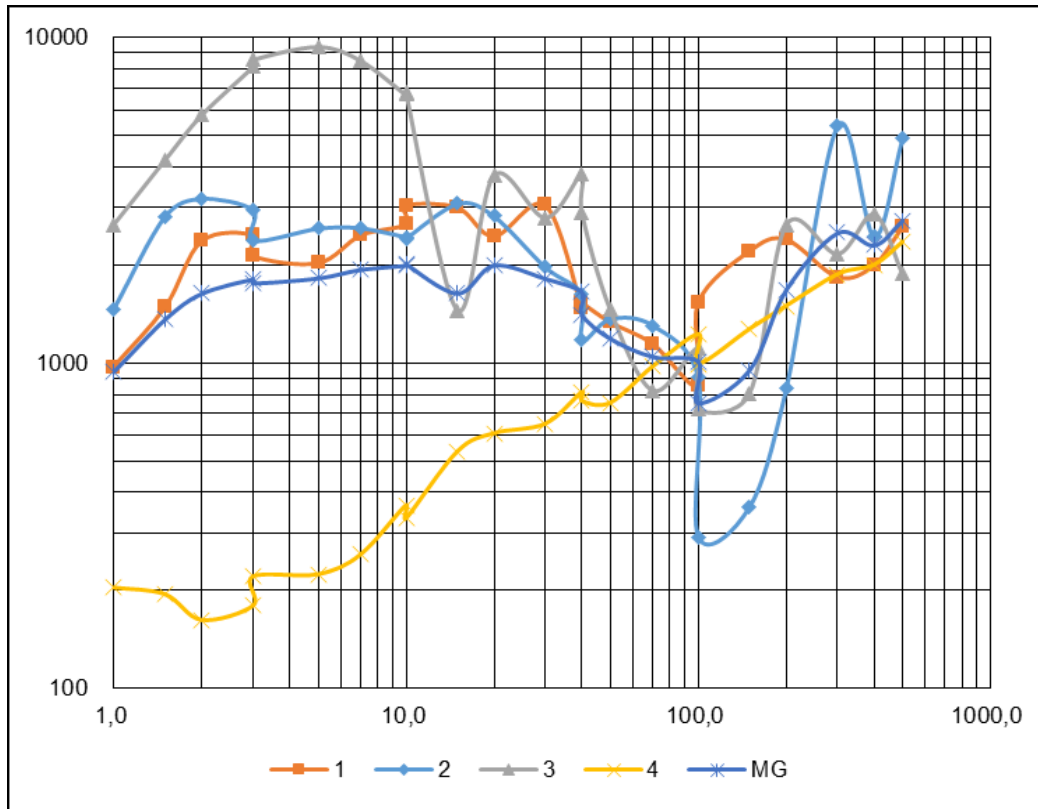
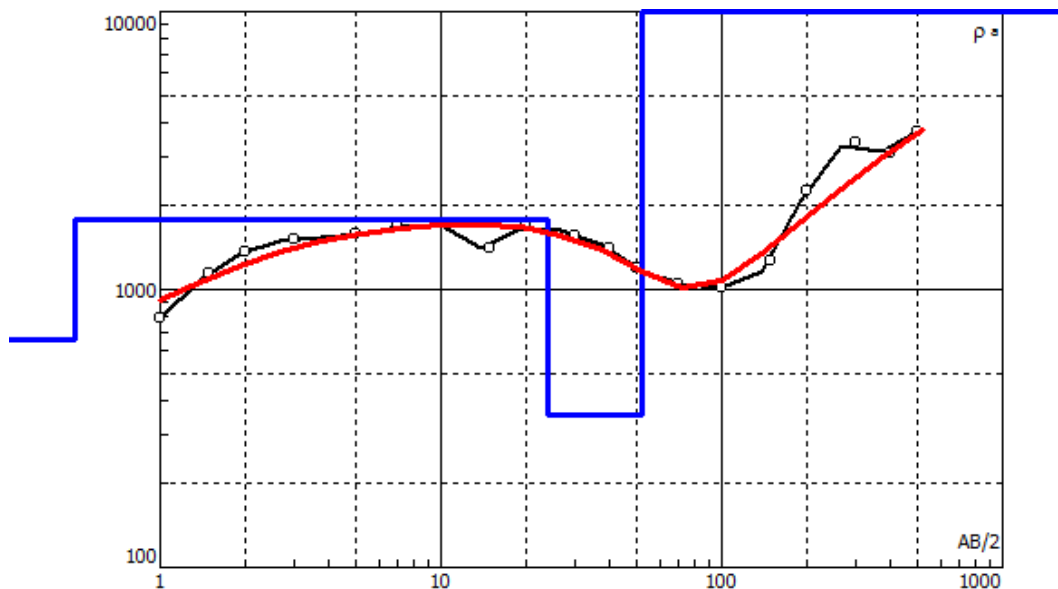


Figure 5.16: four shallow apparent resistivity curves and its geometric average at site EL39.



N	ρ	h	d	Alt
1	663	0.5	0.5	-0.5
2	1792	23.5	24	-24.04
3	355	27.9	52	-51.97
4	10000			

Figure 5.17: average apparent resistivity curve of the shallow ground layers – measured (black) and calculated (red) and geoelectric model (black).

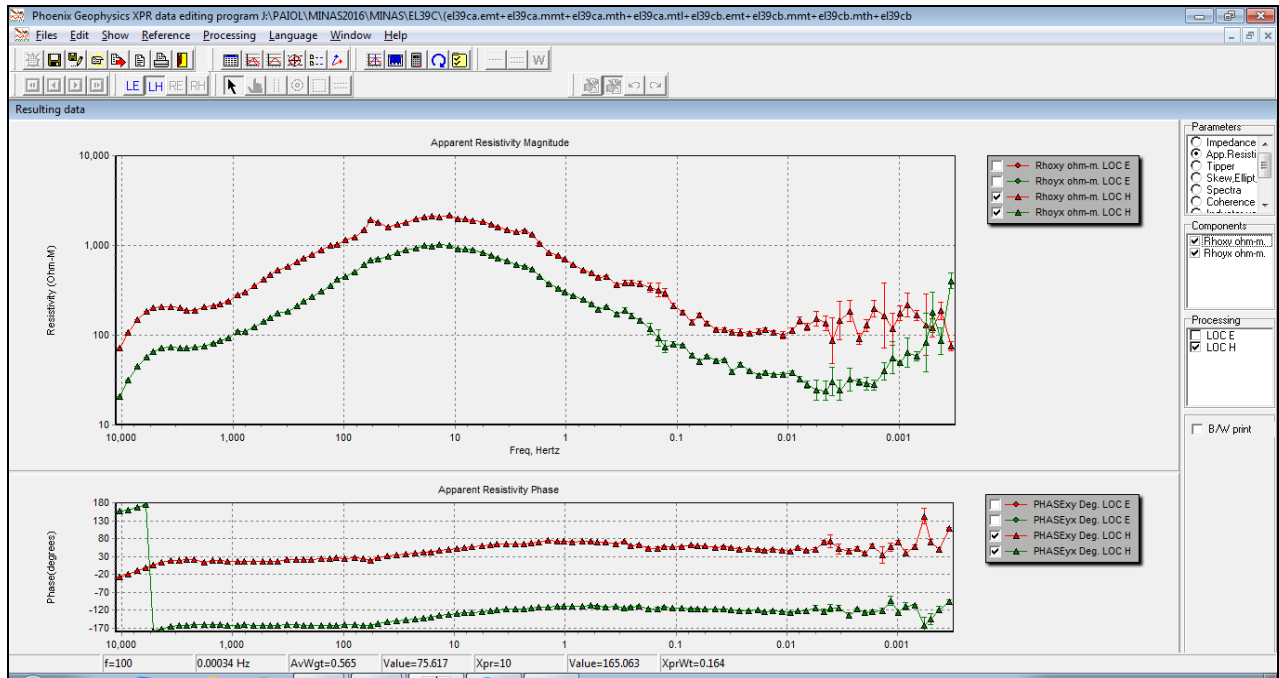


Figure 5.18: apparent resistivity and phase curves (TM and TE) for Station EL39c.

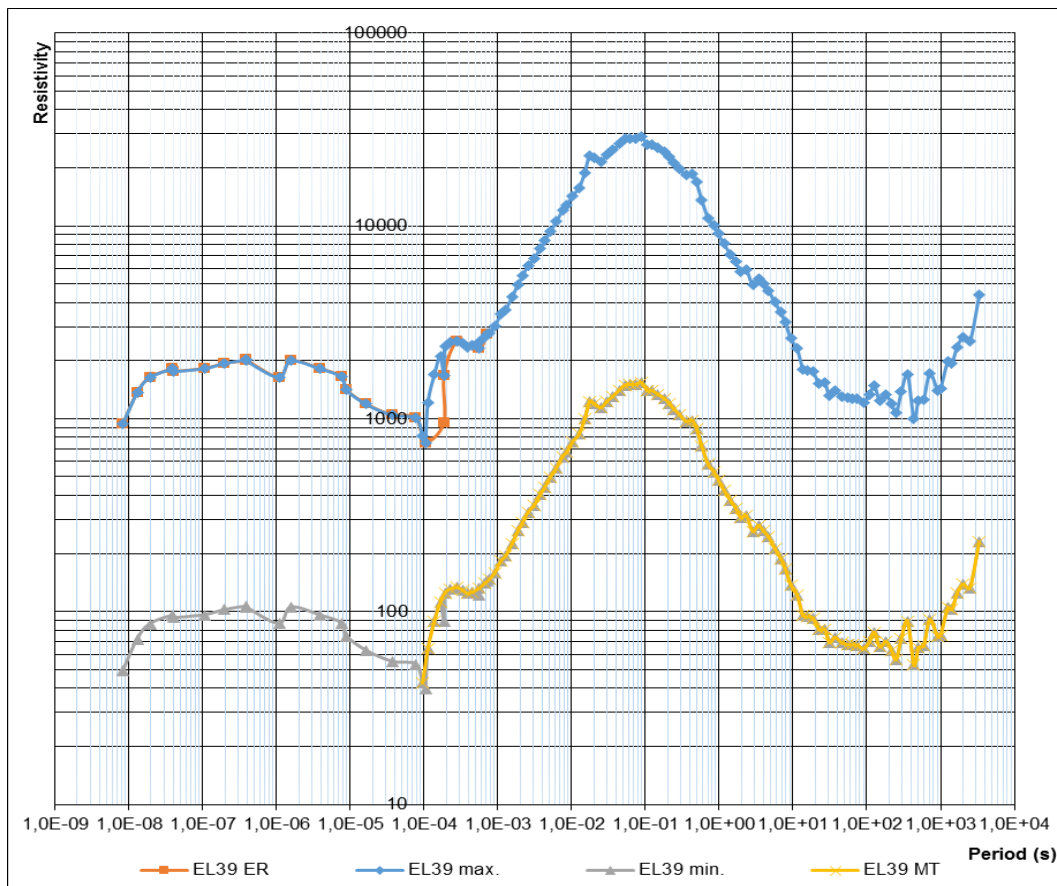


Figure 5.19: combined ER and MT curves – expected maximum (blue) and minimum (gray) boundaries for apparent resistivity curves at site EL39c.

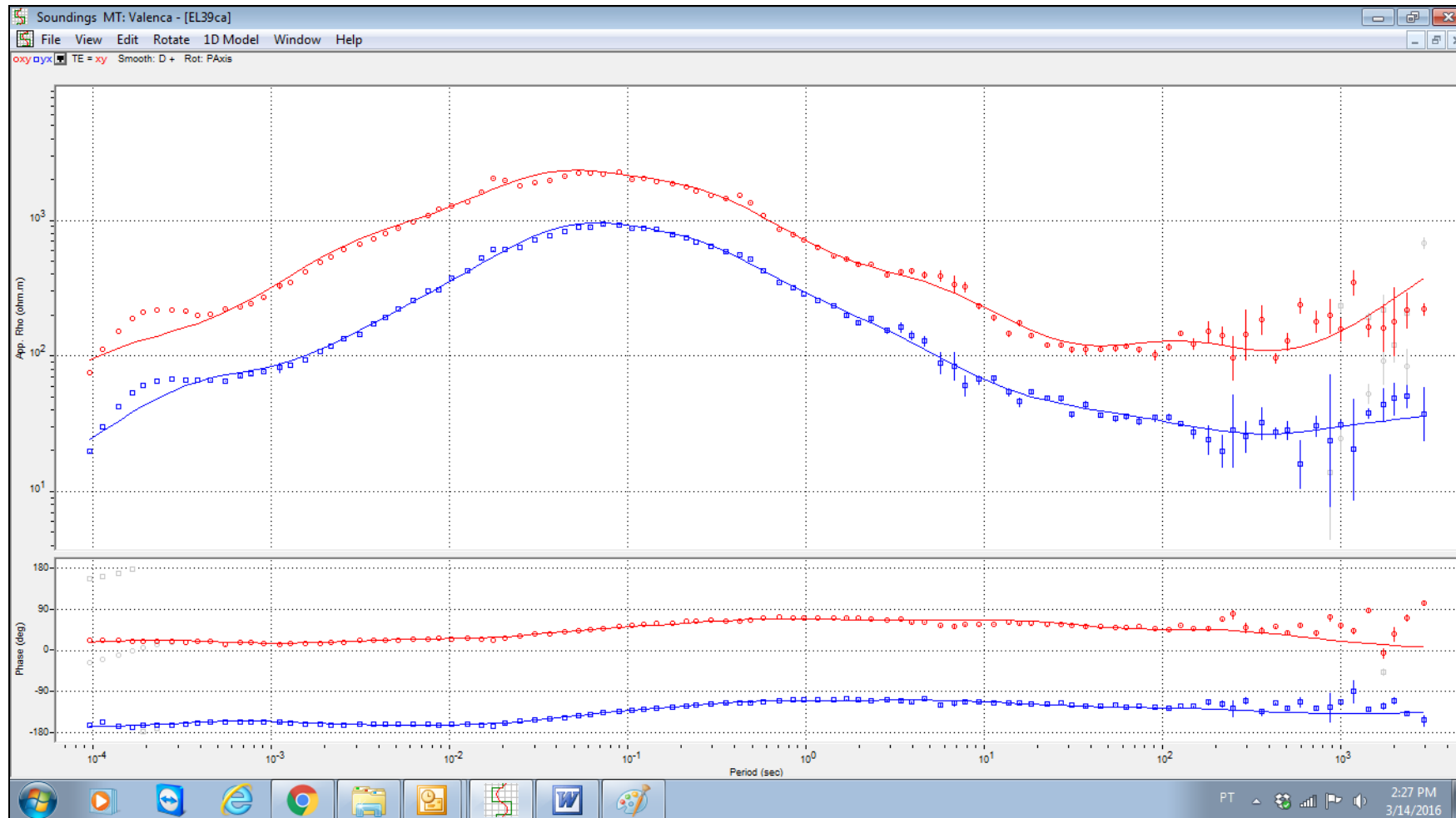


Figure 5.20: station EL39 - apparent resistivity and phase curves (TM and TE modes) rotated for alignment with the dominant strike - measured (points) and smoothed (lines).

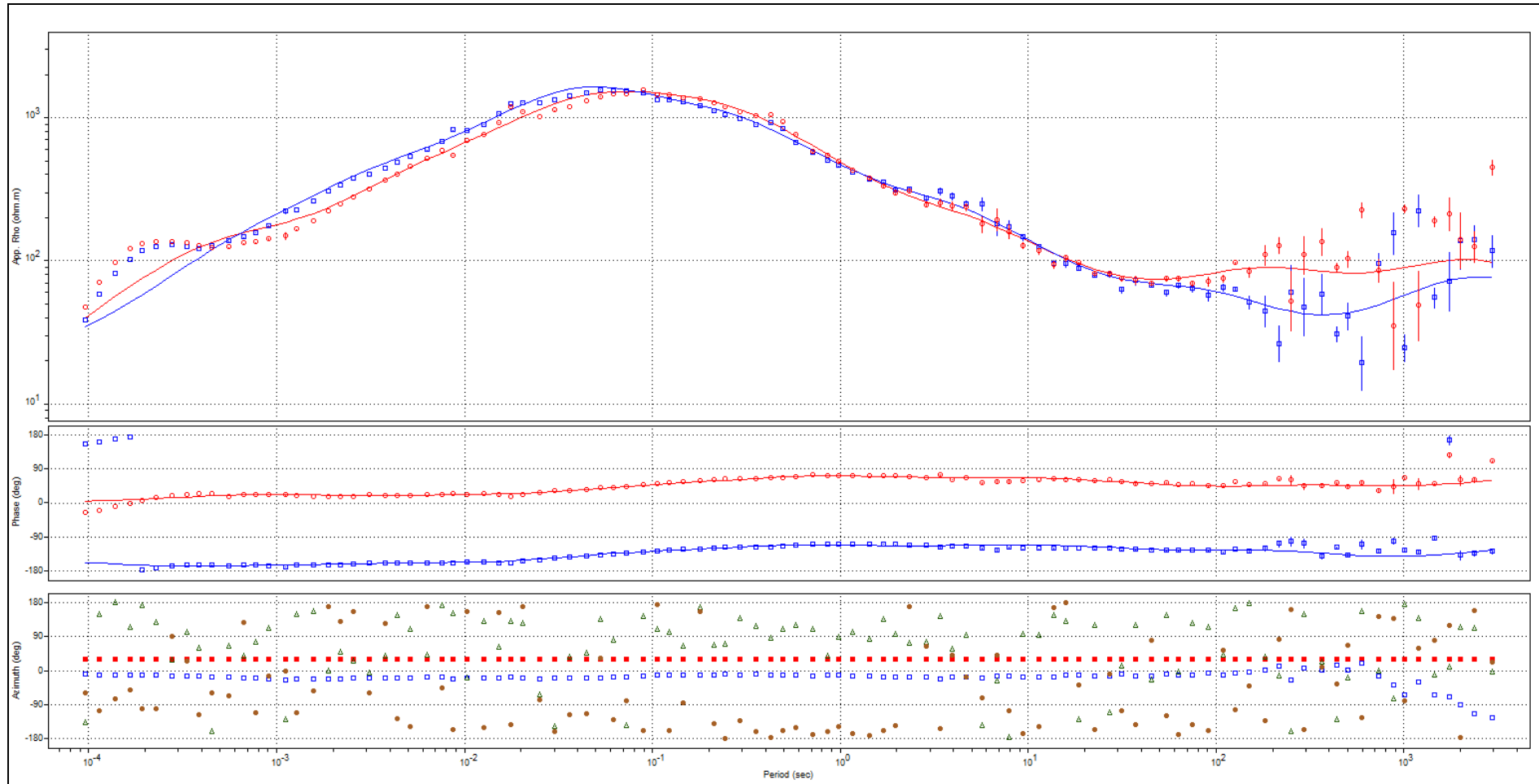


Figure 5.21: station EL39 - apparent resistivity and phase curves rotated for 1D modeling - measured (points) and smoothed (lines).

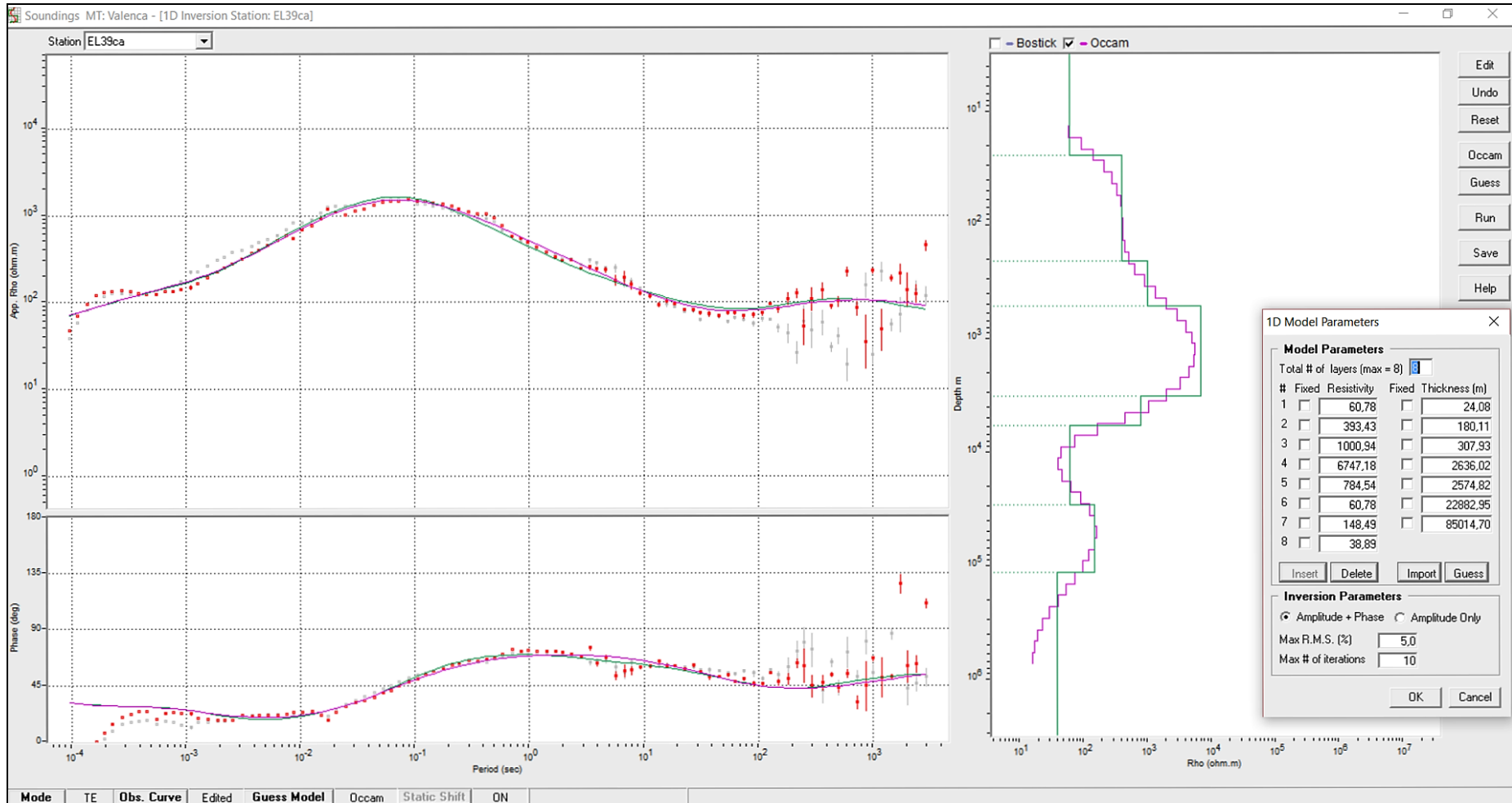


Figure 5.22: station EL39 - apparent resistivity and phase curves rotated for 1D modeling and the MT geoelectric model.

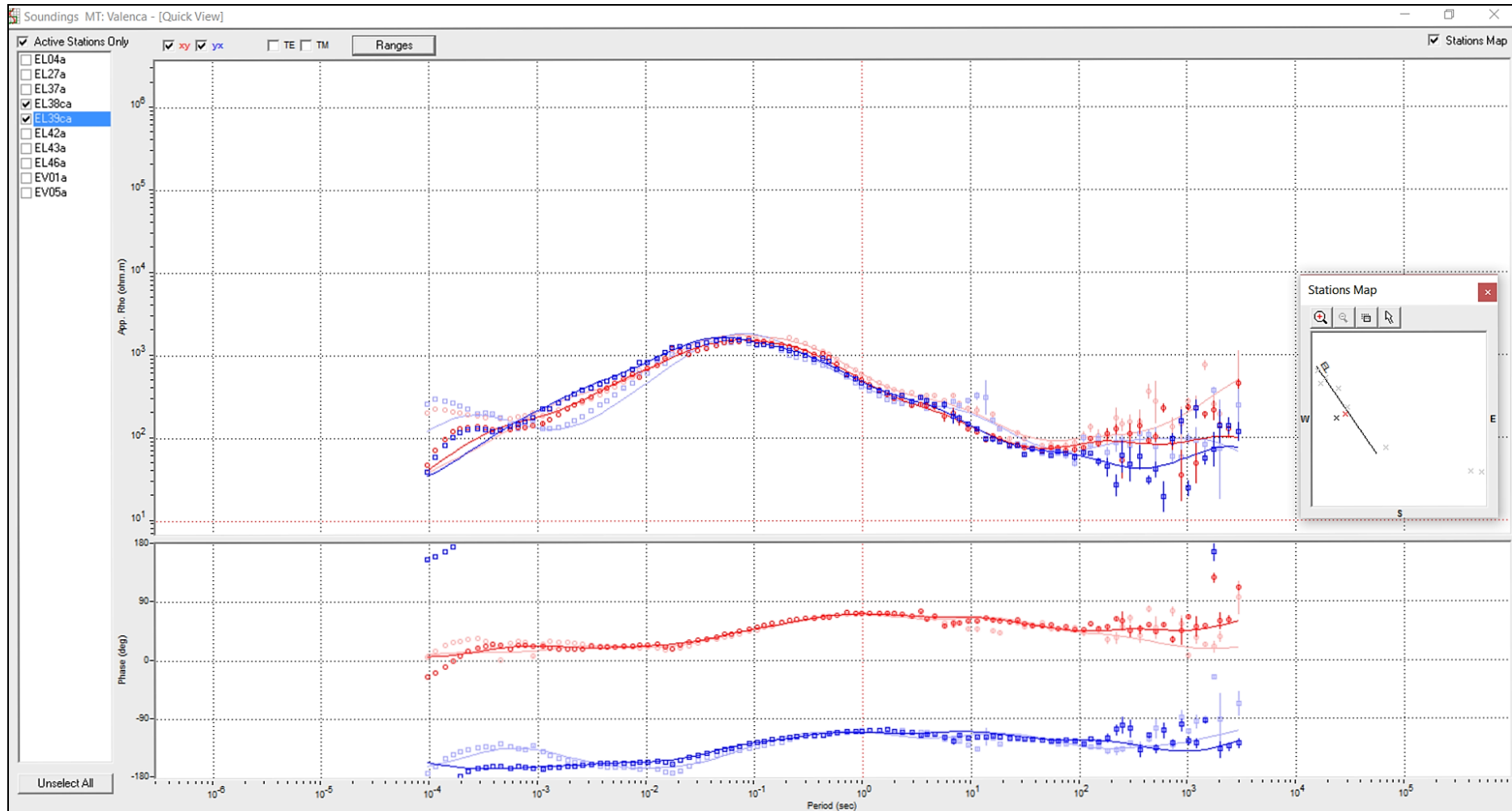


Figure 5.23: stations EL38 and 39 – the overlap of the apparent resistivity and phase curves rotated for 1D modeling show how similar is the deep geoelectric structure of both stations.

5.3.1 Combined (ER + MT) Model

Figure 5.24 presents the average 1D apparent resistivity and phase and geoelectric model (blue and table) calculated by the inversion of the combined apparent resistivity curve (ER + AMT + MT).

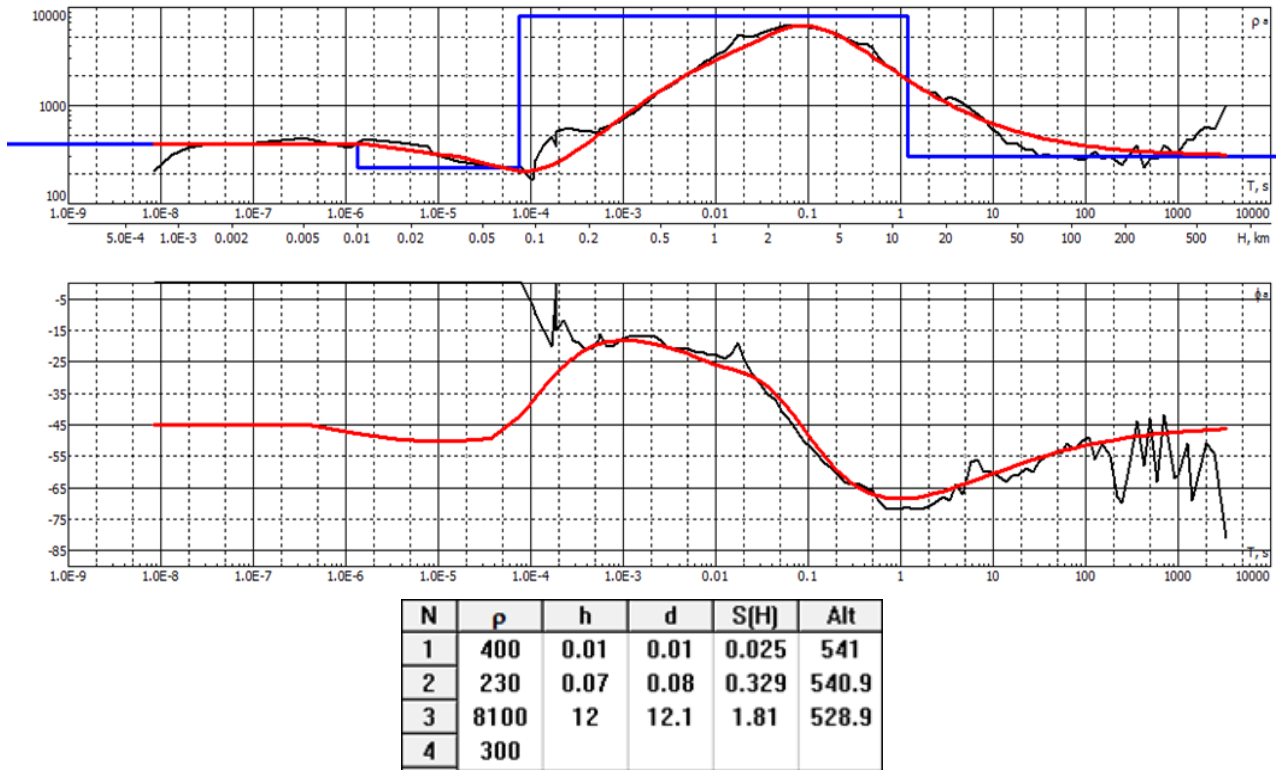


Figure 5.24: Station EL39c – average apparent resistivity and phase curves and 1D geoelectric model (blue and table).

5.4 EL43 – São Vicente de Minas

Photo 5.1 shows the area, which is undulated. Figure 5.8 presents the four apparent resistivity curves and its geometric average, which was inverted, resulting on the model presented in Figure 5.9. This models shows a 58 m sediments layer above the basement.

Figure 5.10 presents the apparent resistivity and phase curves (TM and TE) for Station EL43, with noise appearing for frequencies close to 0.1 Hz. The curves are well separated, showing a strong 2D geoelectric structure. The geoelectric structure of this station is quite different from the other stations, and probably is due to a specific local geologic formation that enhances the conductivity in one direction (TE mode), possibly shales and maybe graphite veins.

Figure 5.11 presents the apparent resistivity and phase curves, rotated to TM and TE modes, and its geometric average curve. Figure 5.12 presents the apparent resistivity and phase curves (XY and YX), rotated by 45° as referred to TM and TE modes (yellow). The rotated curve presents higher resistivities than the non-rotated average curve (gray).

This last average is the one to be used for the construction of the 1D geoelectric model, because when we parallel two apparent resistivity curves, we are paralleling resistivities of different depths (as the horizontal axis it Period, and not Depth). So, the best way to diminish these errors is by applying a rotation in order to approximate both curves.

Figure 5.13 presents the combined ER + MT apparent resistivity curve for site EL43 (yellow). For this station there was no need of adjustment between the ER and MT curves, what may be interpreted as a situation where there was no static-shift deviation on these soundings.

Figure 5.14 presents the apparent resistivity and phase curves (TM and TE modes), and Figure 5.15 presents these same two curves rotated for 1D modeling. It can be seen that due to the wide separation of the TE and TM modes, the two curves change significantly of pattern after the rotation. Figure 5.16 presents the apparent resistivity and phase curves rotated for 1D modeling and the corresponding MT geoelectric model.



Photo 5.2: view of Station EL43.

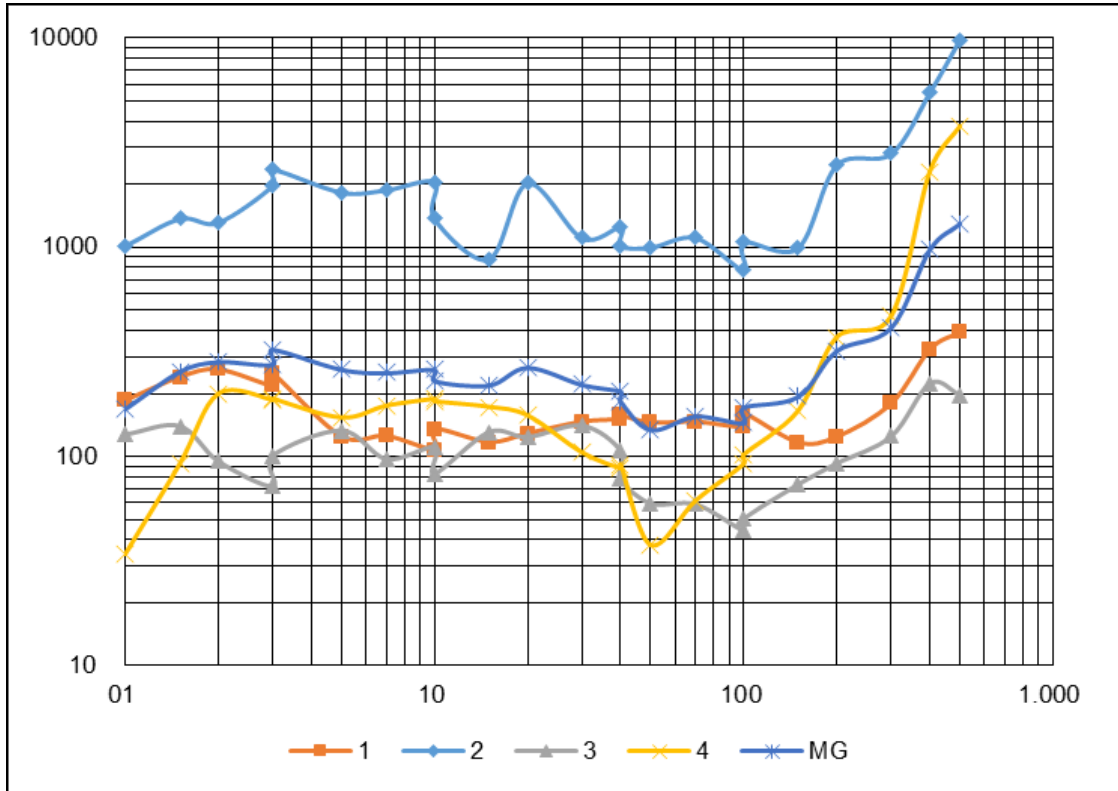
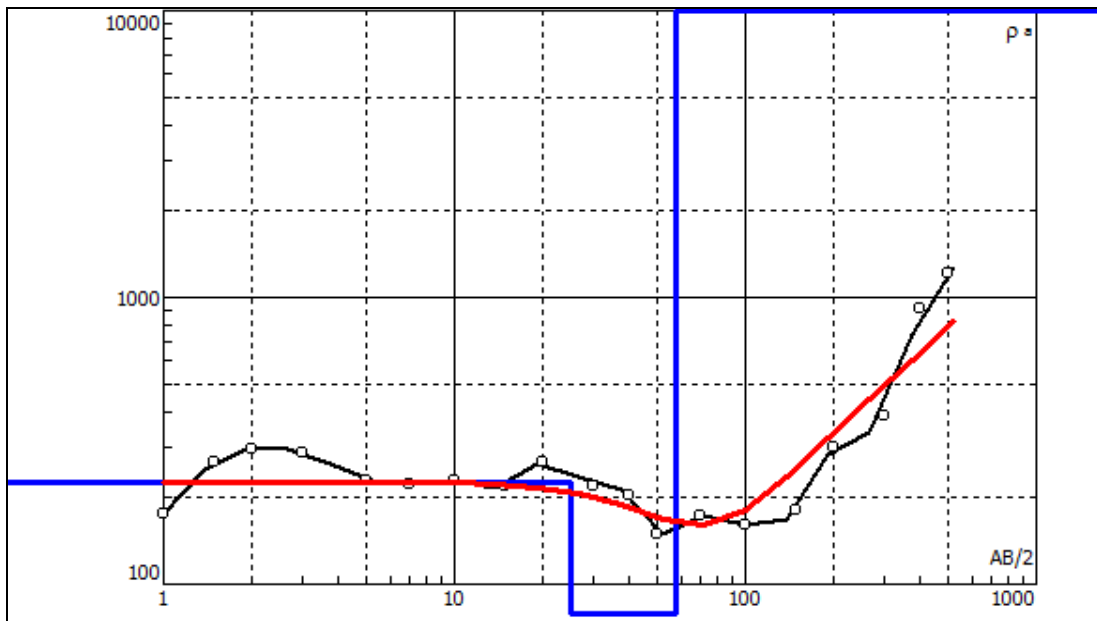


Figure 5.8: four shallow apparent resistivity curves and its geometric average at site EL43.



N	ρ	h	d	Alt
1	226	25	25	-25
2	70	33	58	-58
3	10000			

Figure 5.9: average apparent resistivity curve of the shallow ground layers – measured (black) and calculated (red) and geolectric model (black).

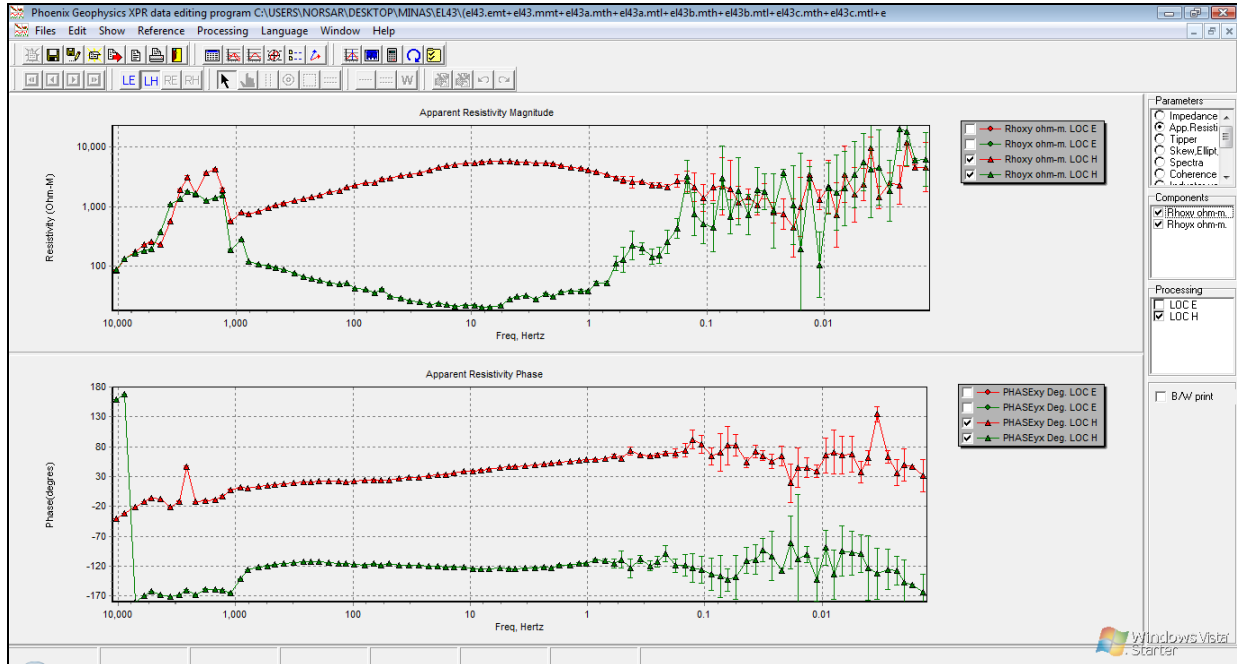


Figure 5.10: Station EL43 - TM (red) and TE (green) modes apparent resistivity and phase curves.

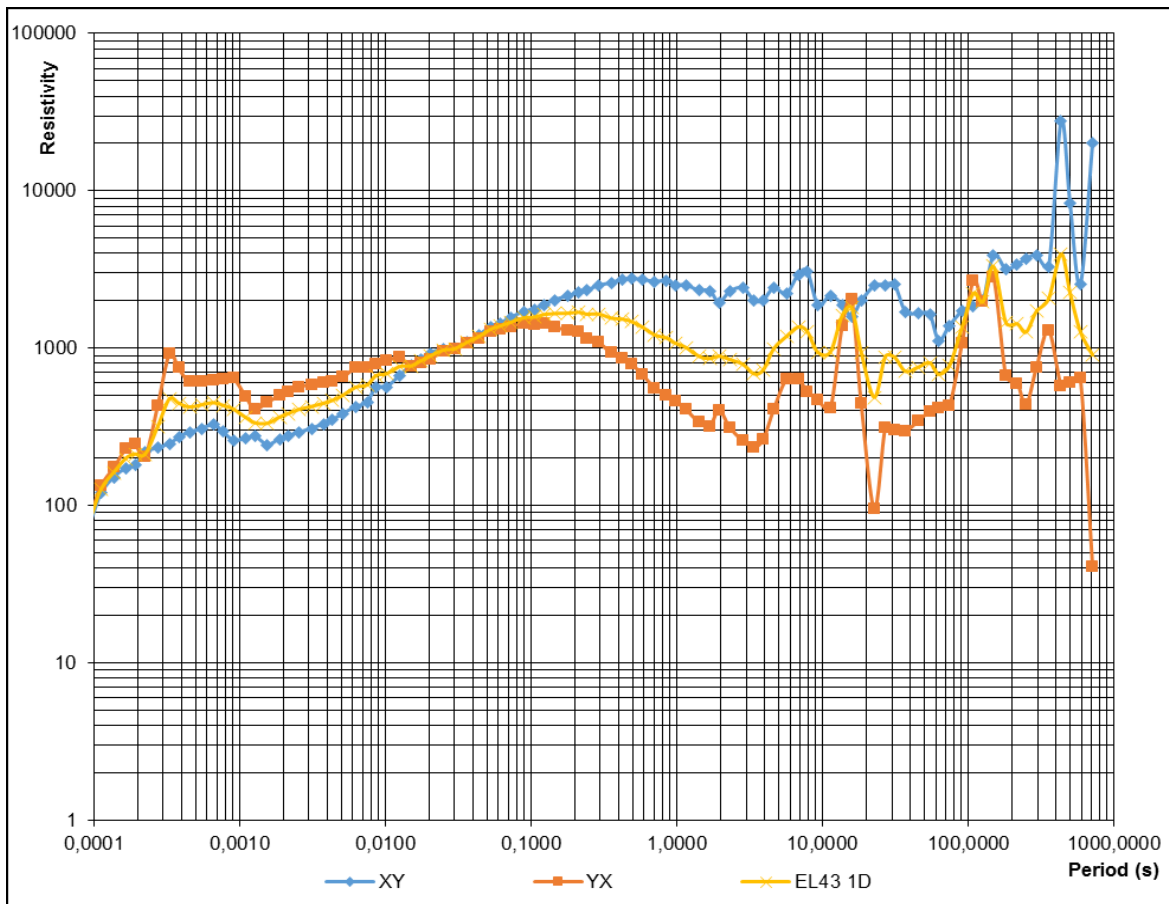


Figure 5.12: Station EL43 - apparent resistivity curves (XY and YX), rotated by 45° (referred to TM and TE modes) and 1D average curve (yellow).

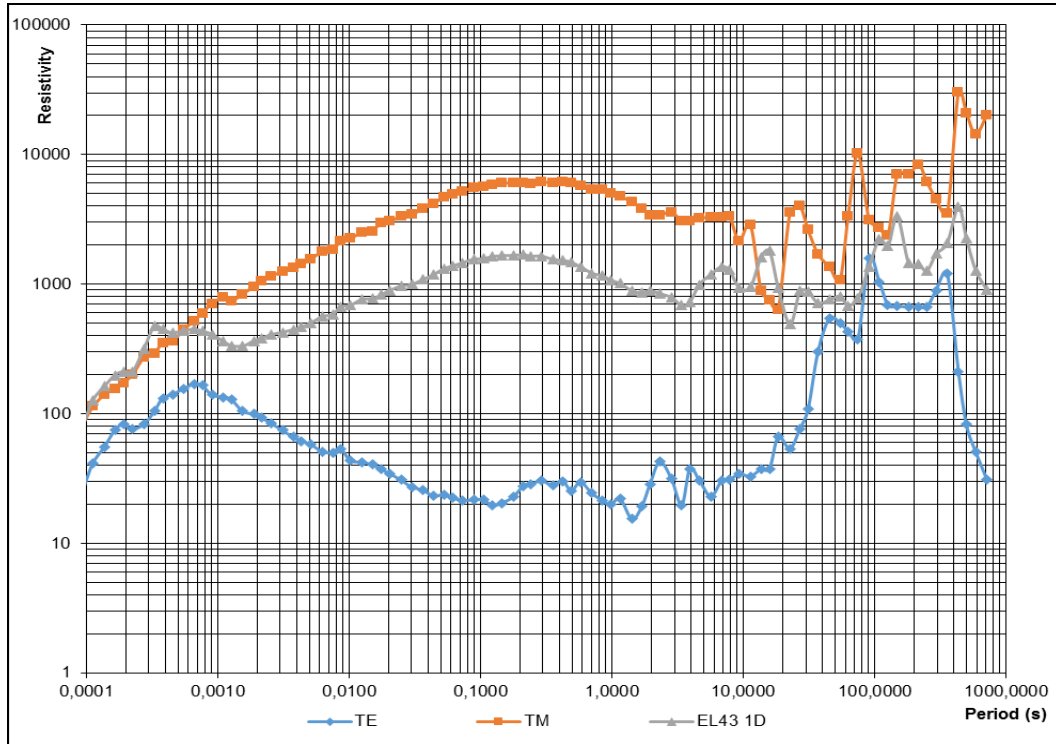


Figure 5.11: Station EL43 - TM (orange) and TE (blue) modes apparent resistivity curves and 1D average curve (gray).

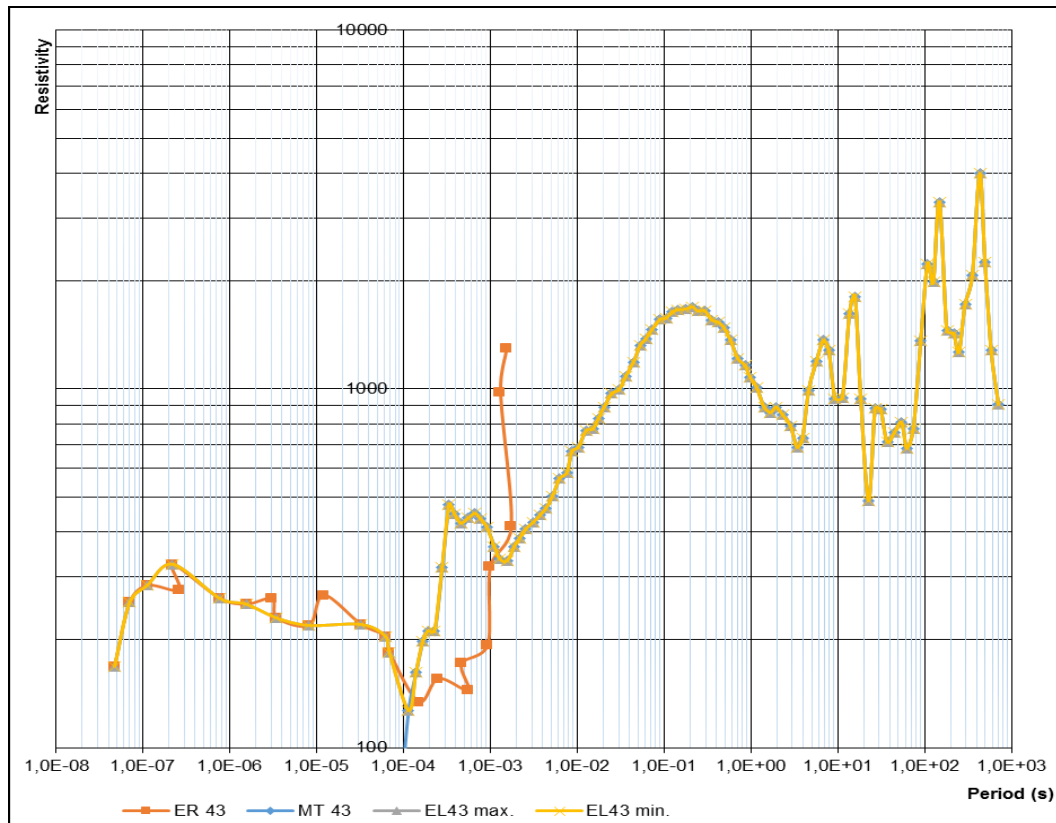


Figure 5.13: Station EL43 - combined ER and MT apparent resistivity curve (yellow) with no static shift correction.

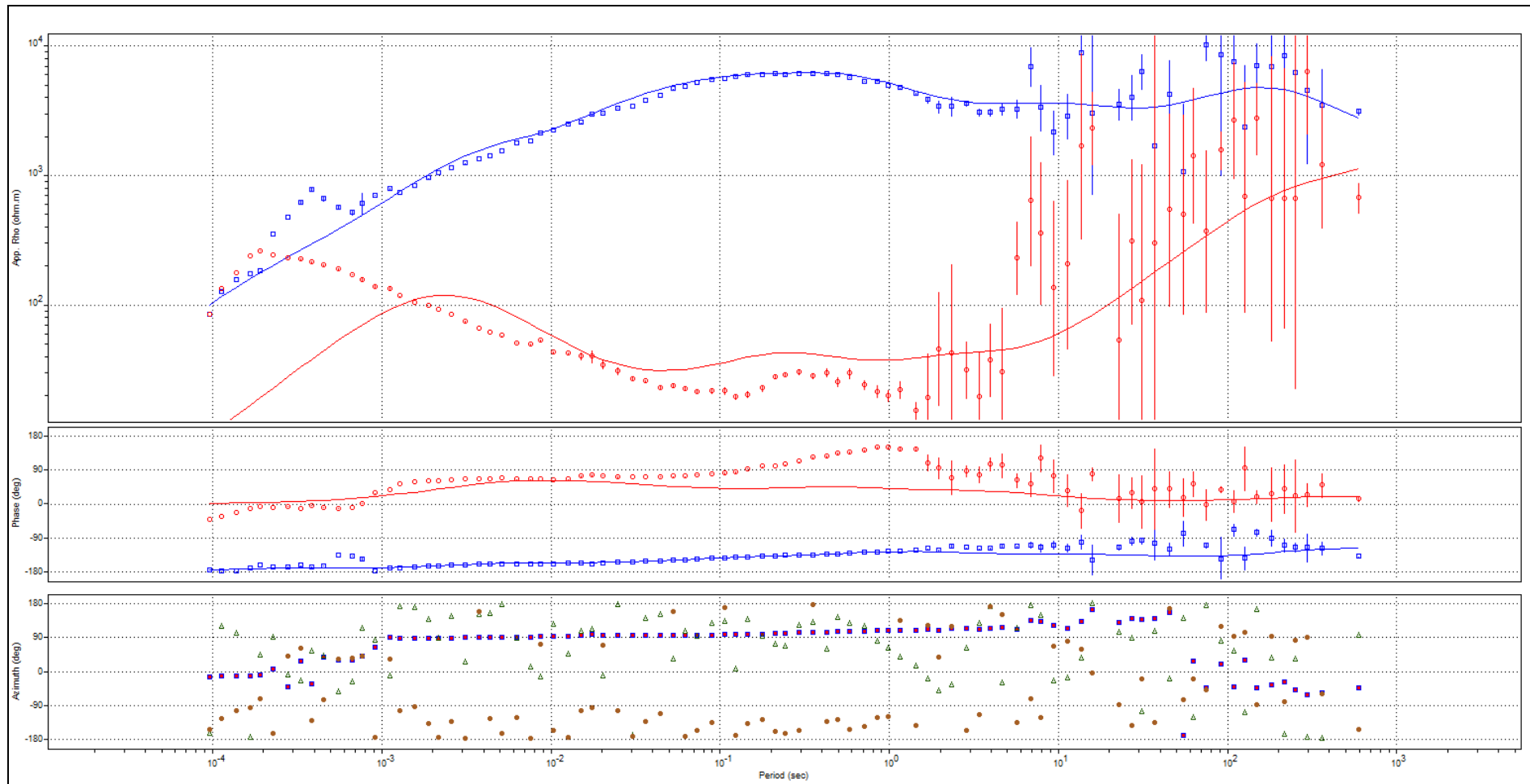


Figure 5.14: Station EL43 - apparent resistivity and phase curves (TM and TE modes) - measured (points) and smoothed (lines).

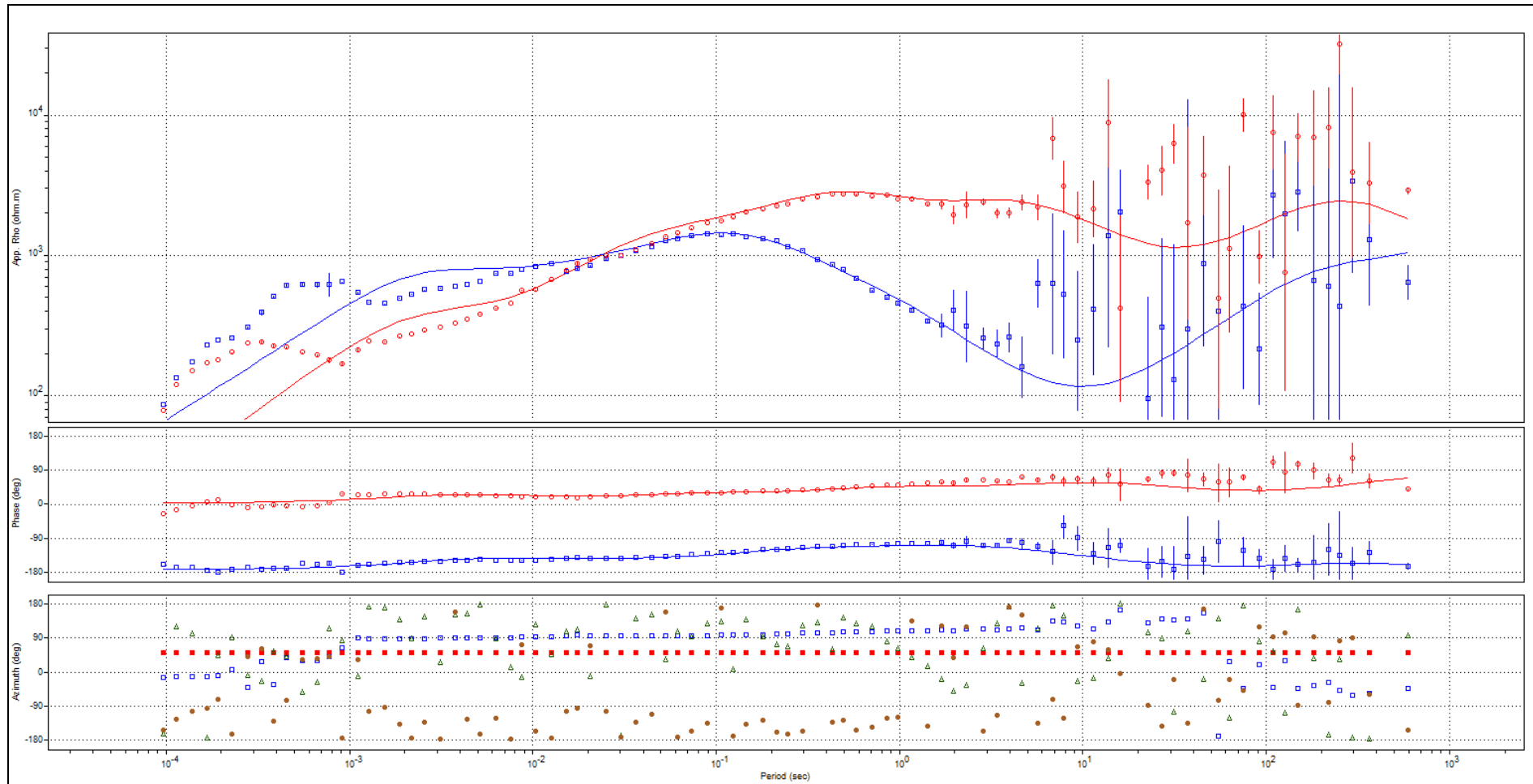


Figure 5.15: Station EL43 - apparent resistivity and phase curves rotated for 1D modeling - measured (points) and smoothed (lines).

5.4.1 Combined (ER + MT) Model

Figure 5.17 presents the 1D geoelectric model (blue) and apparent resistivity and phase - measured (black) and calculated (red). For the construction of this curve it was not needed any static-shift correction, as the end of the ER curve and the beginning of the MT curve matched well.

The table summarizes the crust geoelectric model calculated by the inversion of the apparent resistivity curve (ER + AMT + MT).

The geoelectric model shows a 100 m sediments layer followed, possibly, by 400 m of shales above the high resistivity basement.

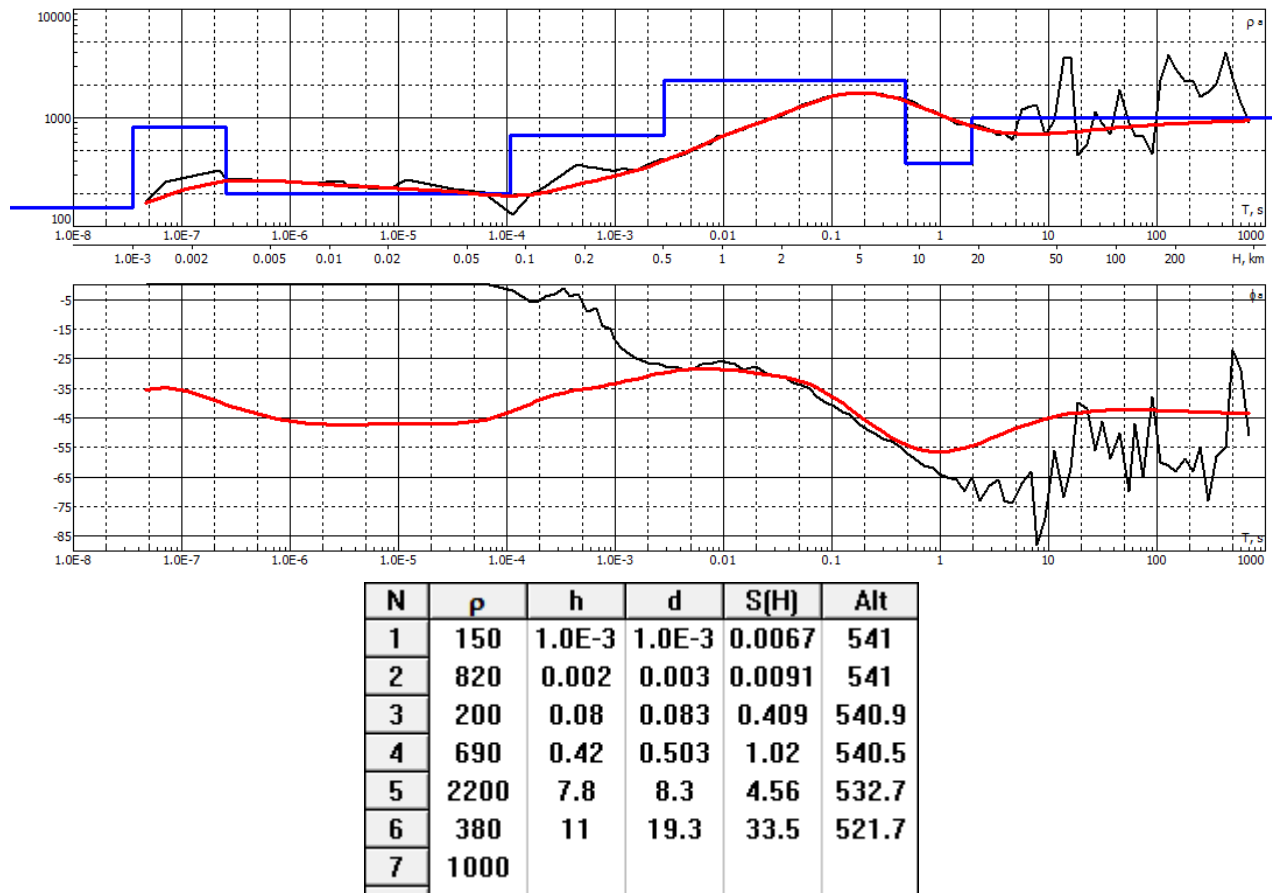


Figure 5.17: site EL43 – complete 1D apparent resistivity and phase curves average (black) and adjusted (red) and geoelectric model (blue and table).

5.5 EL42 – São Vicente de Minas

Photo 5.3 shows the area, which is reasonably flat, does not show rocky outcrops, and has a brown to reddish brown sandy soil.

Figure 5.33 presents the four apparent resistivity curves and its geometric average, which was inverted, resulting on the model presented in Figure 5.34. This models shows a 52 m sediments layer above the basement,

Figure 5.35 presents the apparent resistivity and phase curves (TM and TE) for Station EL42, with noise appearing for frequencies close to 0.1 Hz. The curves are well separated, showing a strong 2D geoelectric structure.

Figure 5.36 presents the combined ER + MT curves with the expected maximum (gray) and minimum (yellow) boundaries for apparent resistivity curves at site EL42. Probably the actual apparent resistivity curve of this site will be situated between the two limits.

Figure 5.37 presents the apparent resistivity and phase curves rotated for 1D modeling and Figure 5.38 presents these two curves with the corresponding MT geoelectric model. It can be seen that the two curves are overlapped, what means a good 1D model.



Photo 5.3: view of Station EL42.

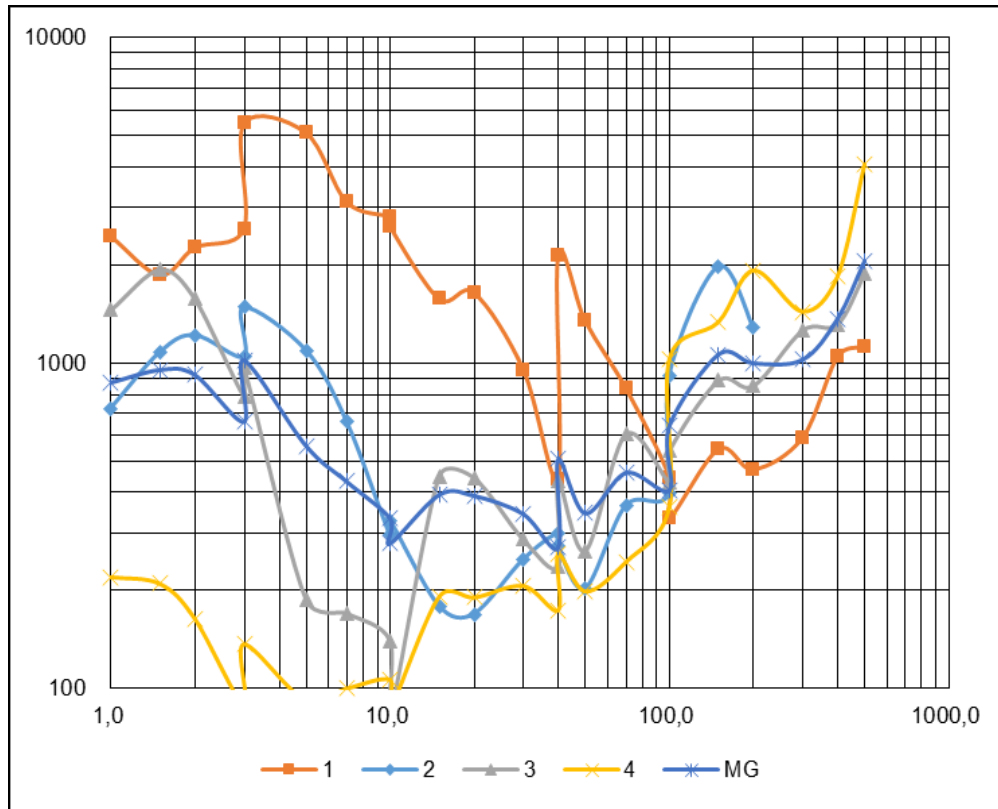


Figure 5.33: four shallow apparent resistivity curves and its geometric average at site EL42.

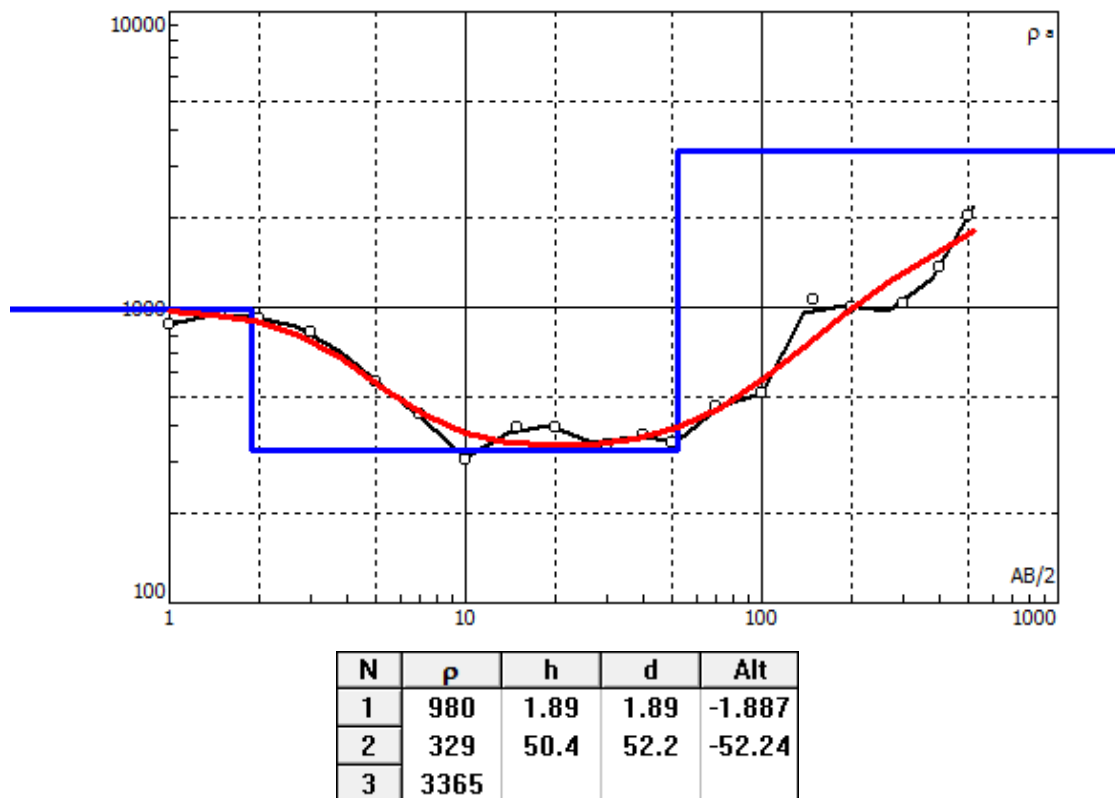


Figure 5.34: average apparent resistivity curve of the shallow ground layers – measured (black) and calculated (red) and geoelectric model (black).

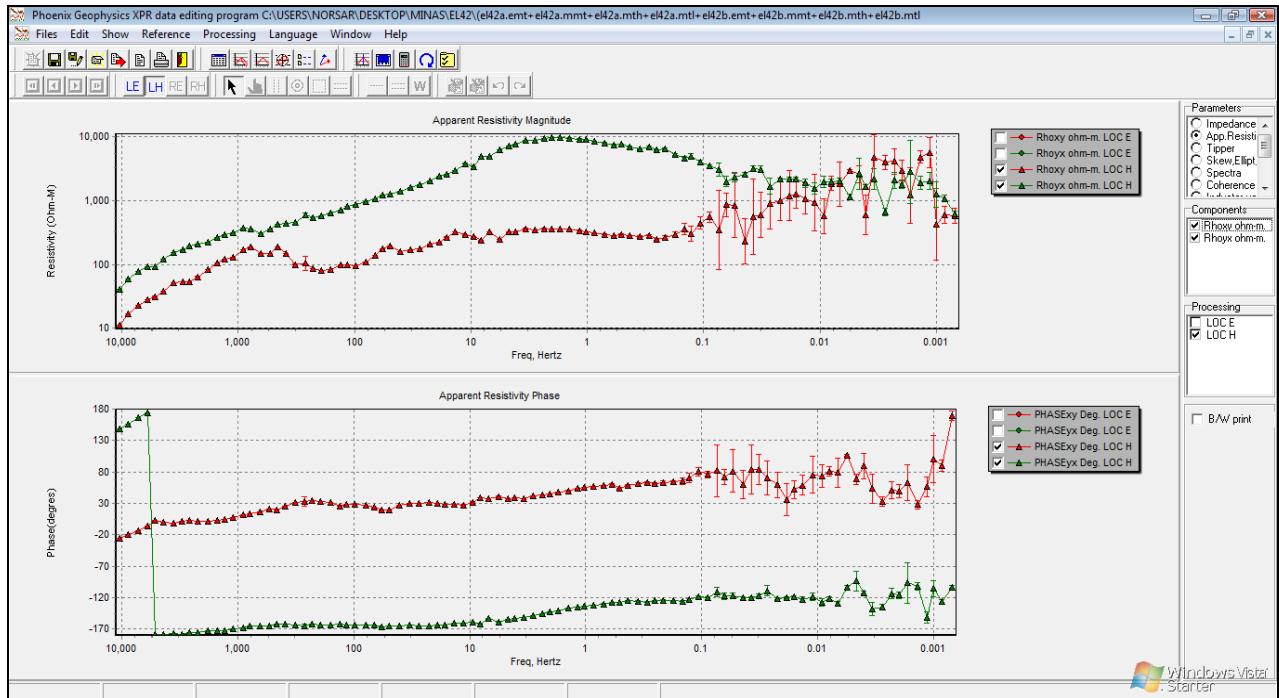


Figure 5.35: apparent resistivity and phase curves (TM and TE) for Station EL42.

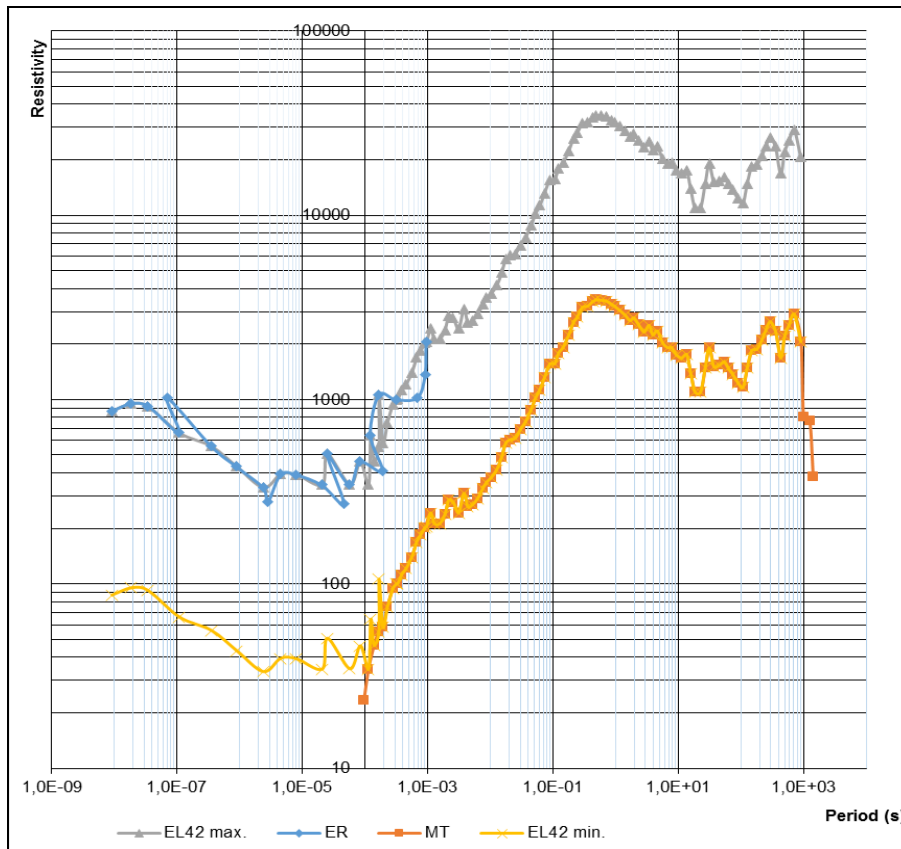


Figure 5.36: combined ER + MT curves – expected maximum (gray) and minimum (yellow) boudaries for apparent resistivity curves at site EL42.

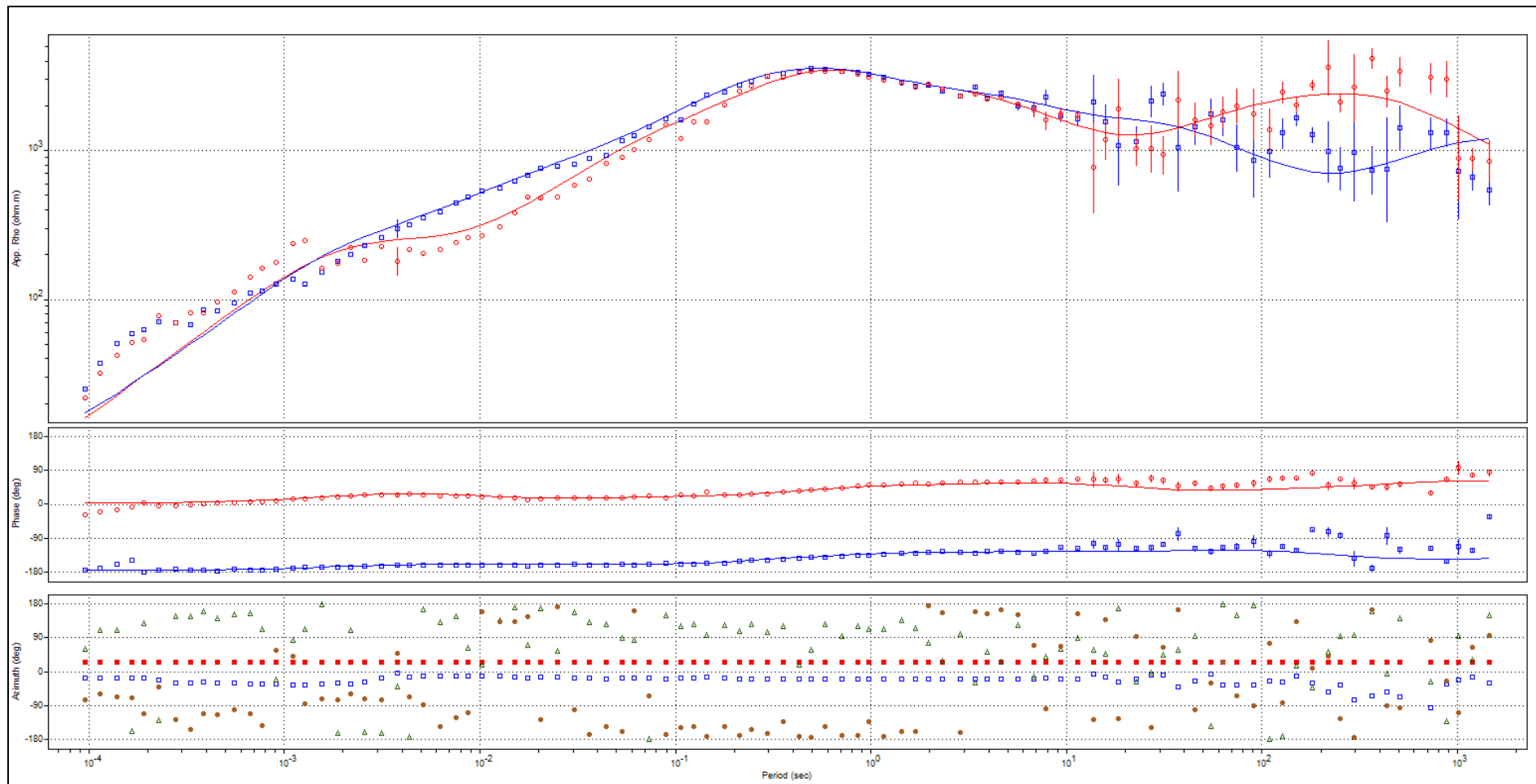


Figure 5.37: station EL42 - apparent resistivity and phase curves rotated for 1D modeling - measured (points) and smoothed (lines).

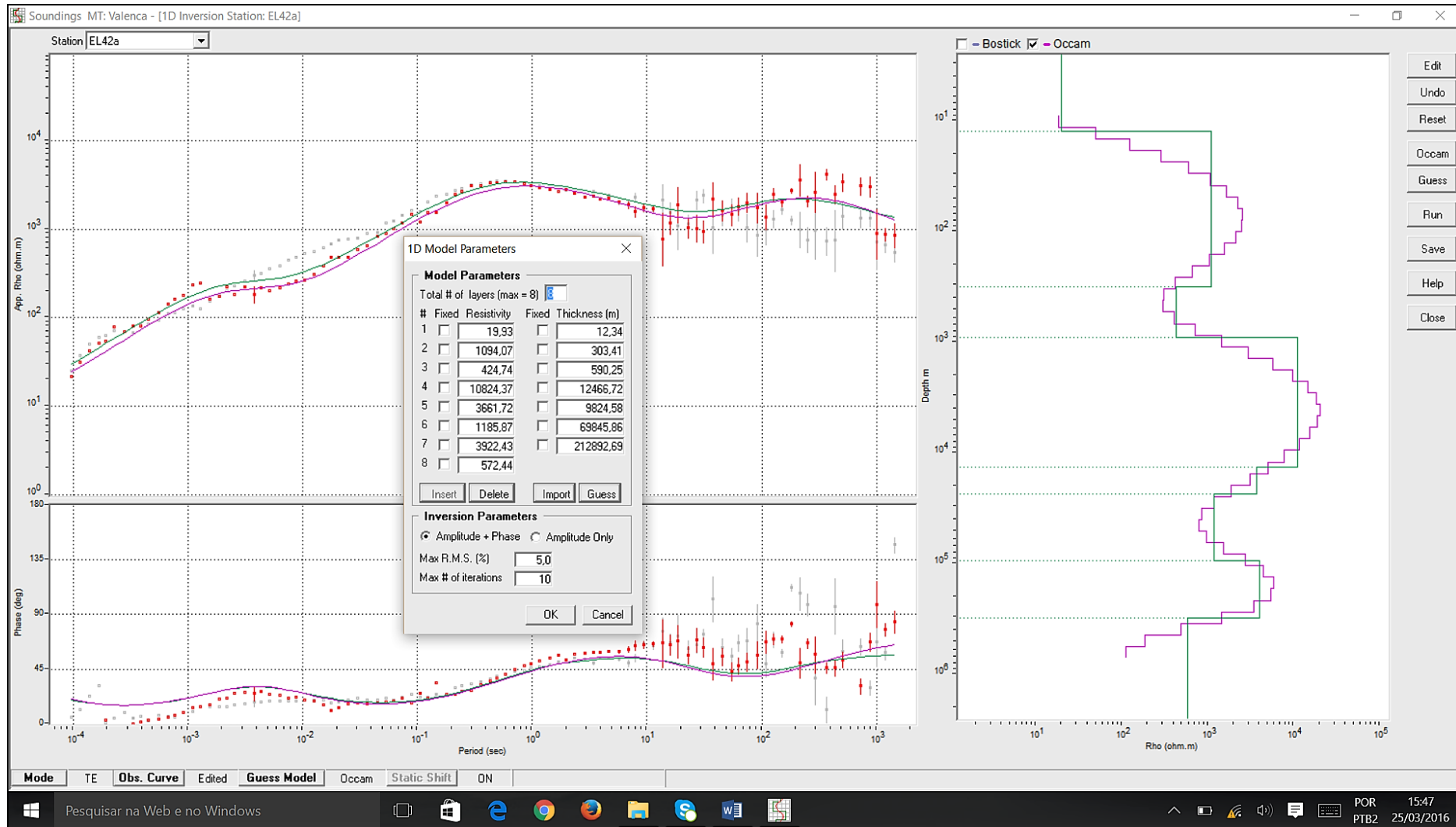


Figure 5.38: station EL42 - apparent resistivity and phase curves rotated for 1D modeling and geoelectric model.

5.5.1 Combined (ER + MT) Model

Figure 5.39 presents the average combined apparent resistivity and phase curves (ER + AMT + MT) and the 1D geoelectric model (blue and table).

The geoelectric model shows a thin overburden (35 m) above a deep and high resistivity basement, what indicates that this site has no condition to host a HVDC ground electrode.

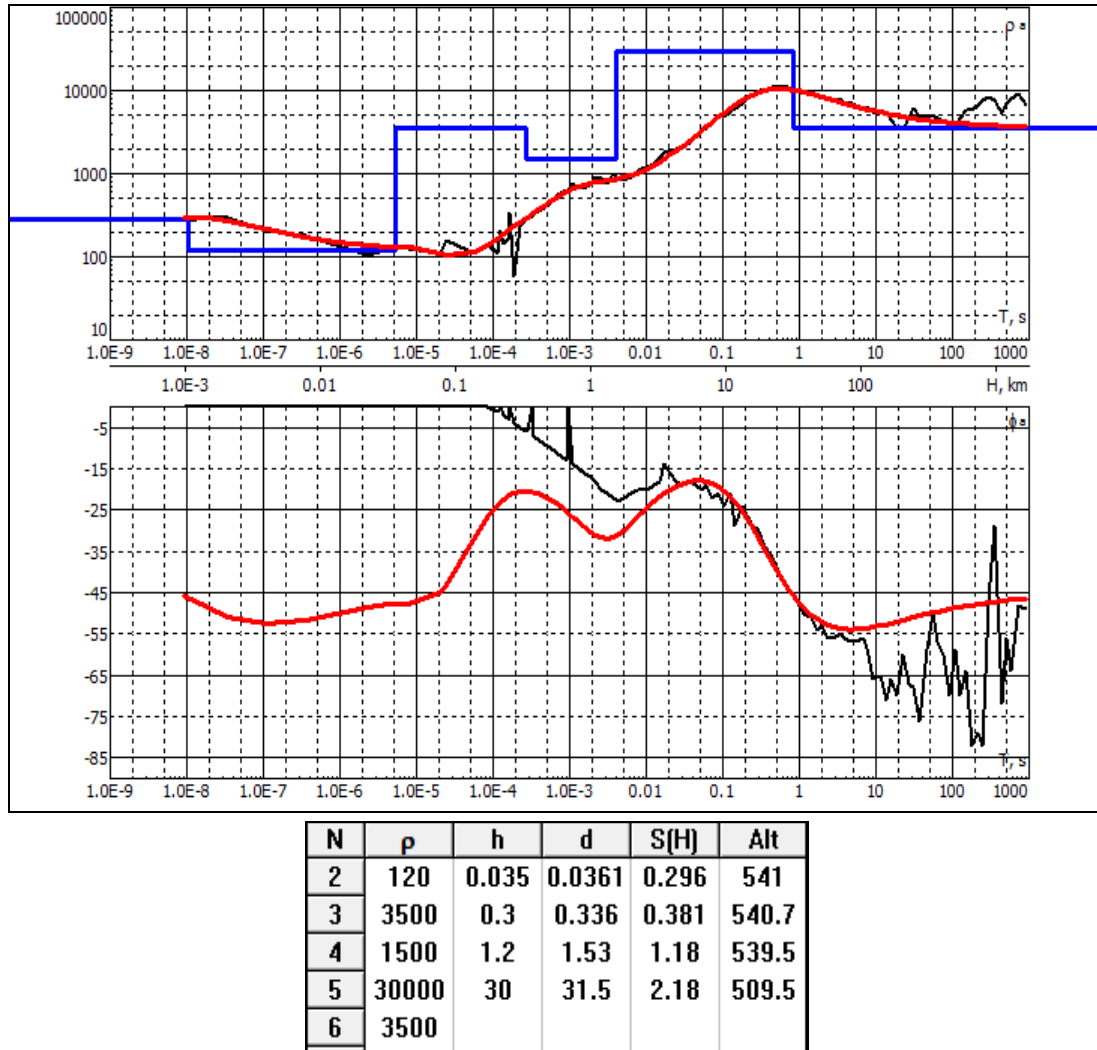


Figure 5.39: Site EL42 - average apparent resistivity and phase curves and 1D geoelectric model (blue and table).

5.6 EL46 – Carrancas

In this site the soil is brown sandy without outcrops. However, in the lower regions near water springs and drainage channels, it was observed the presence of a dark clayey layer (organo clay).

Figure 5.40 presents the four apparent resistivity curves and its geometric average, which was inverted, resulting on the model presented in Figure 5.41. This models shows a high resistivity ground, from soil surface.

Figure 5.42 presents the apparent resistivity and phase curves (TM and TE) for Station EL43, with noise appearing for frequencies close to 0.1 Hz. The curves present a half-decade flat start and then go upward. Photo 5.8 shows the area, which is reasonably flat and wide.

Figure 5.43 presents the combined ER + MT curves, with expected maximum (gray) and minimum (yellow) boundaries for apparent resistivity curves at site EL46. The actual apparent resistivity curve will be situated within these two limits.

Figure 5.44 presents the apparent resistivity and phase curves rotated for 1D modeling.



Photo 5.4: view of Station EL46.

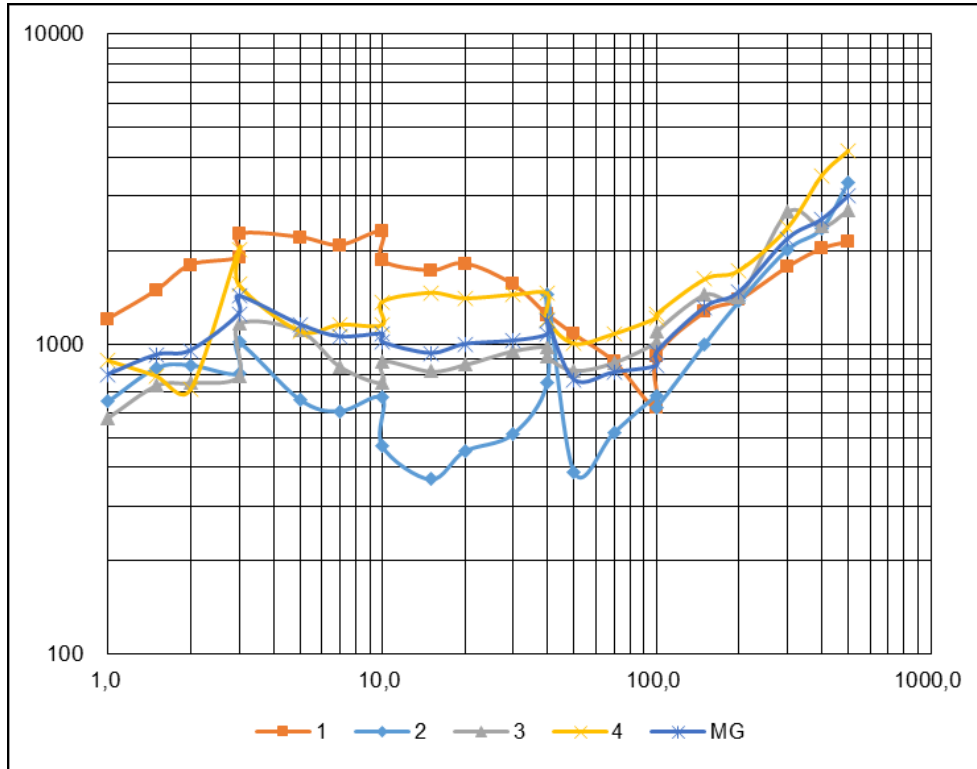


Figure 5.40: four shallow apparent resistivity curves and its geometric average at site EL46.

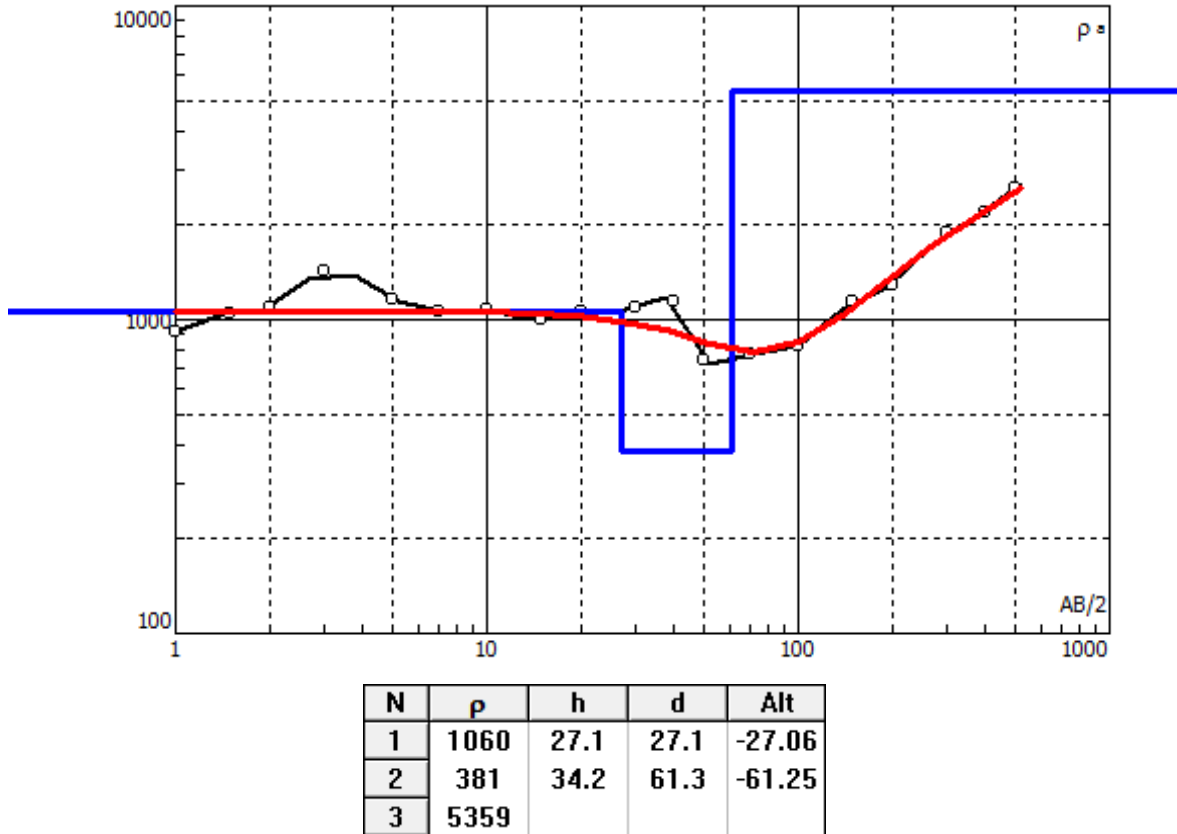


Figure 5.41: average apparent resistivity curve of the shallow ground layers – measured (black) and calculated (red) and geoelectric model (black).

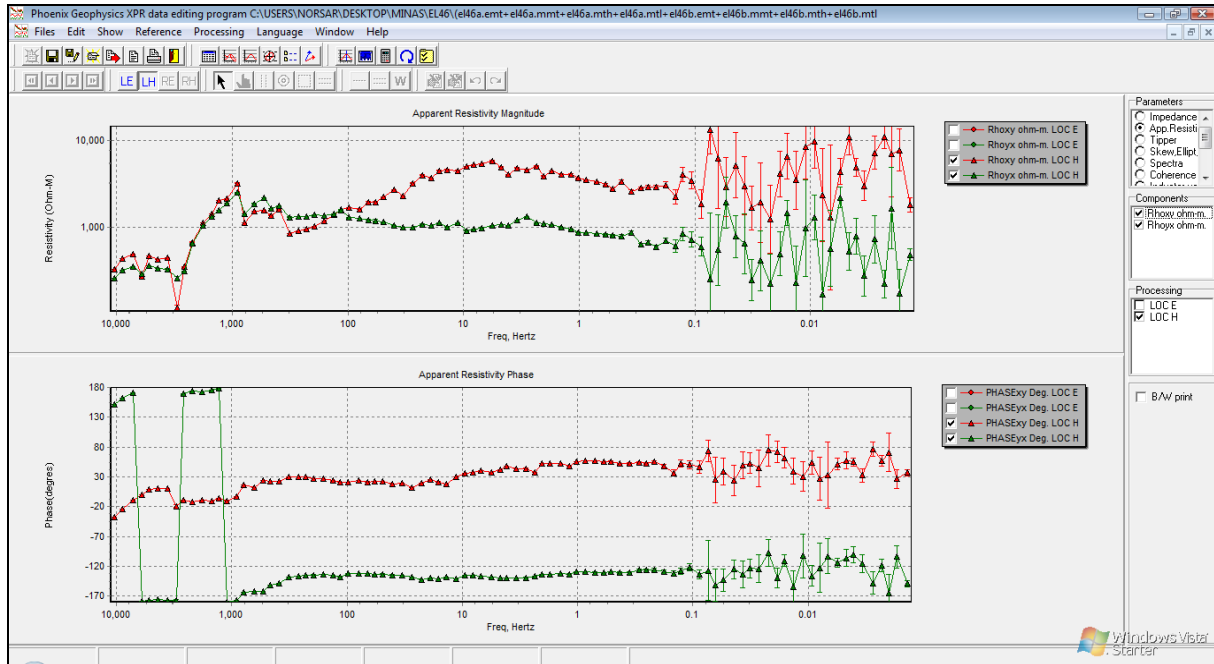


Figure 5.42: apparent resistivity and phase curves (TM and TE) for Station EL46.

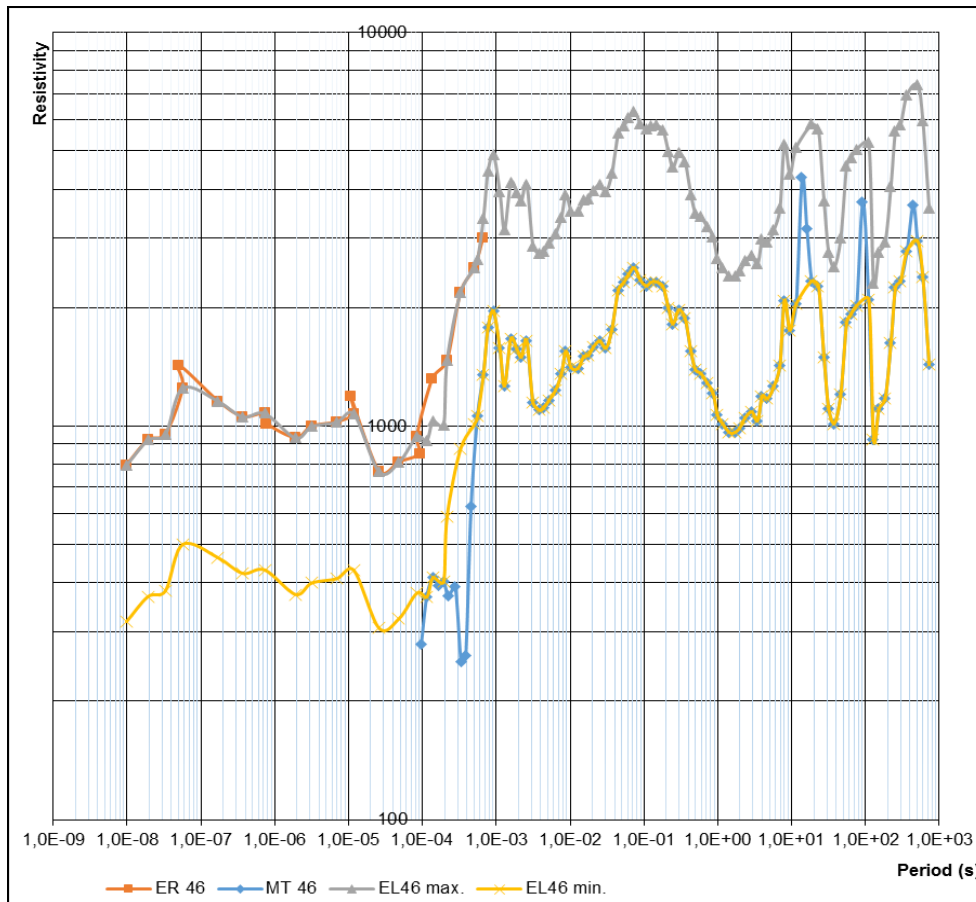


Figure 5.43: Combined ER and MT curves – expected maximum (gray) and minimum (yellow) boundaries for apparent resistivity curves at site EL46.

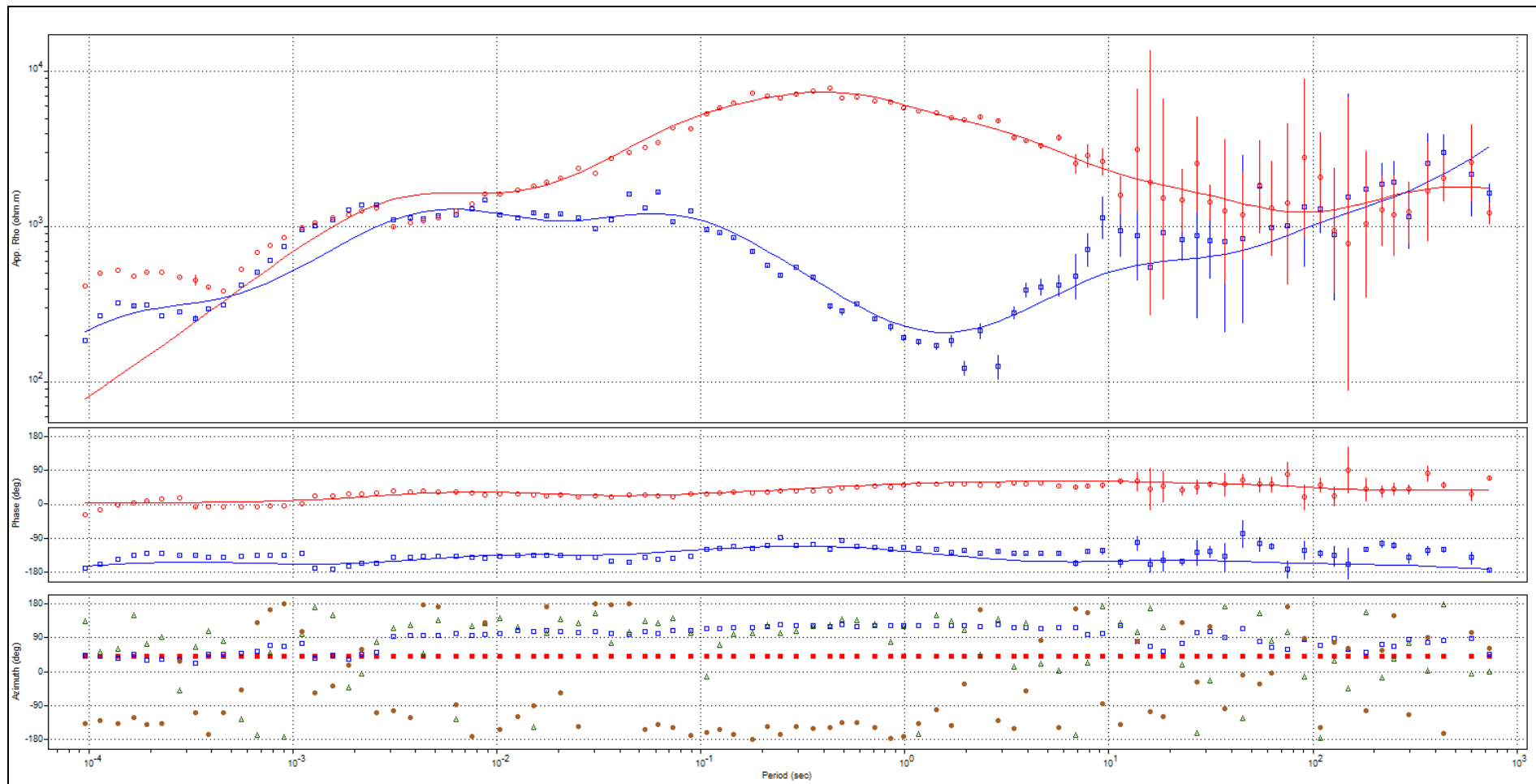


Figure 5.44: station EL46 - apparent resistivity and phase curves rotated for 1D modeling - measured (points) and smoothed (lines).

5.6.1 Combined (ER + MT) Model

Figure 5.45 presents the average combined apparent resistivity and phase curves (ER + AMT + MT) and the 1D geoelectric model (blue and table).

The geoelectric model shows a deep and high resistivity basement, what indicates that this site has no condition to host a HVDC ground electrode.

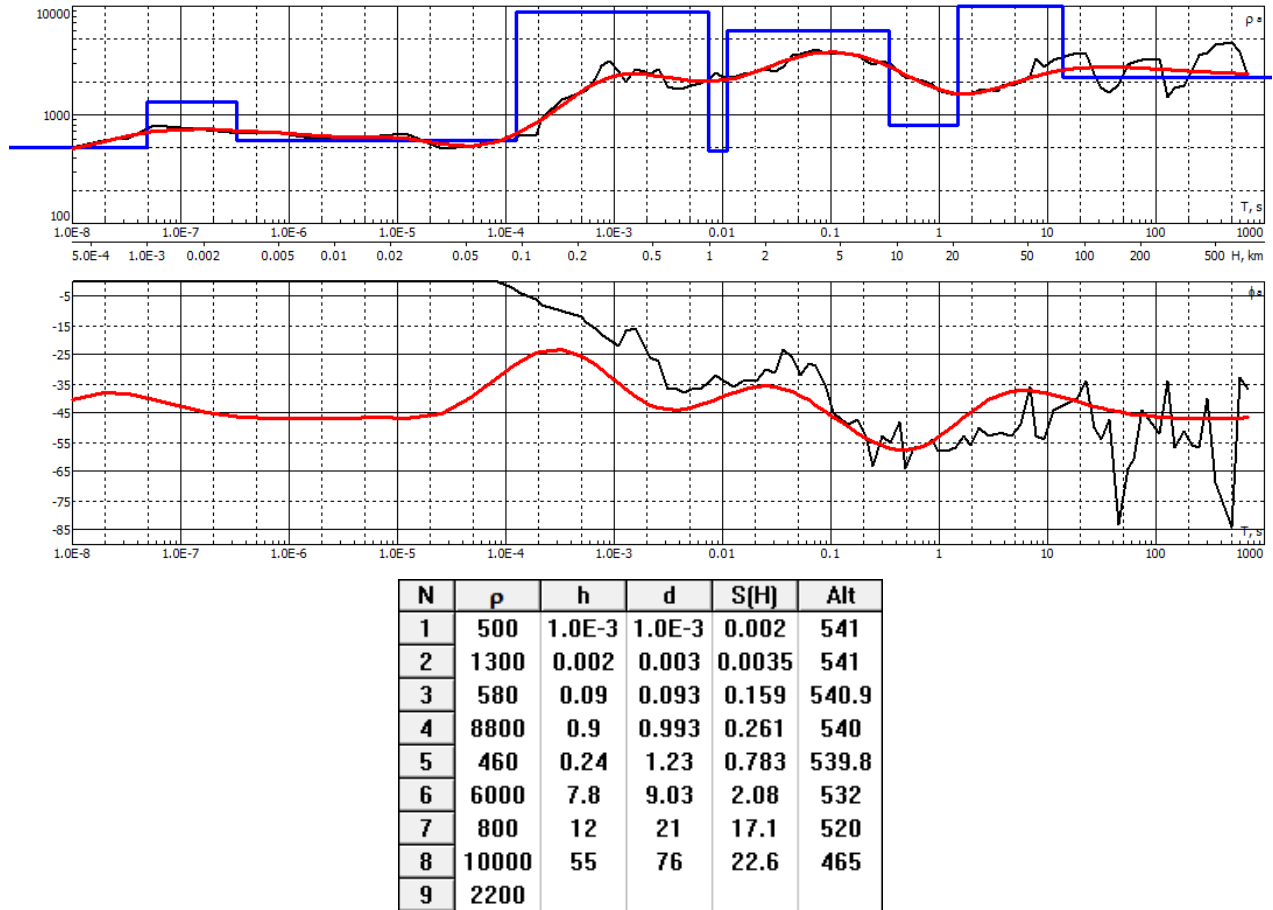


Figure 5.45: Site EL46 - average apparent resistivity and phase curves and 1D geoelectric model (blue and table).

6 ELECTRODE SIMULATION

From the five sites surveyed (EL04, EL39, EL43, EL42 and EL46), only site EL43 have shown the possibility of hosting the ground electrode, with resistance below the limit of 0.35 Ω m, even though with a big electrode.

For these five sites it was done complementary electroresistivity surveys, by means of four Schlumberger soundings at each station with current probes spacing up to 1000 m. These soundings were combined with the MT soundings for the construction of a combined apparent resistivity curve. These curves were inverted resulting on the geoelectric models.

For the determination of the horizontal electrode minimum perimeter, the following parameters shall be considered:

- one electrode sector out and maximum current of 3325 A;
- 0.5 A/m² current density at the coke-ground interface, for diminishing the risk of electrosmosys phenomena;
- a coke section of 0.5 x 0.5 m, with the consideration that the top face of the coke trench will not dissipate current to the ground.

With these premises it can be calculated the needed linear extension of electrode, and thus the minimum diameter for a single ring electrode:

$$L = (8/7) \times 2 \times 3325/1.5 = 5067 \text{ m} \rightarrow D = L/\pi = 1612 \text{ m.}$$

The single ring horizontal electrode 1.6 km diameter is thus the base case. The area that allows for such electrode with resistance below 0.35 Ω m will be a natural candidate to host the electrode.

It was made a simulation of two 1 km wide electrodes in parallel, one at site 38 and the other at site 39. The equivalent resistance of 0.59 Ω showed that this is not a good electrode configuration.

The following electrode configurations were evaluated for the surveyed sites (see Figures 6.1 to 6.7):

- single ring horizontal electrode 1.6 km diameter;
- double ring horizontal electrode with 1400/1120 m diameter;
- double ring vertical electrode with 1400/1120 m diameter (64 wells 30 m deep);
- double ring horizontal electrode with 1200/960 m diameter;
- double ring vertical electrode with 1200/960 m (64 wells 30 m deep);
- double ring horizontal electrode with 960/720 m diameter;
- double ring vertical electrode with 960/720 m diameter (64 wells 30 m deep).

It was found that for wide electrodes, the vertical configuration results on higher resistances than the horizontal configuration.

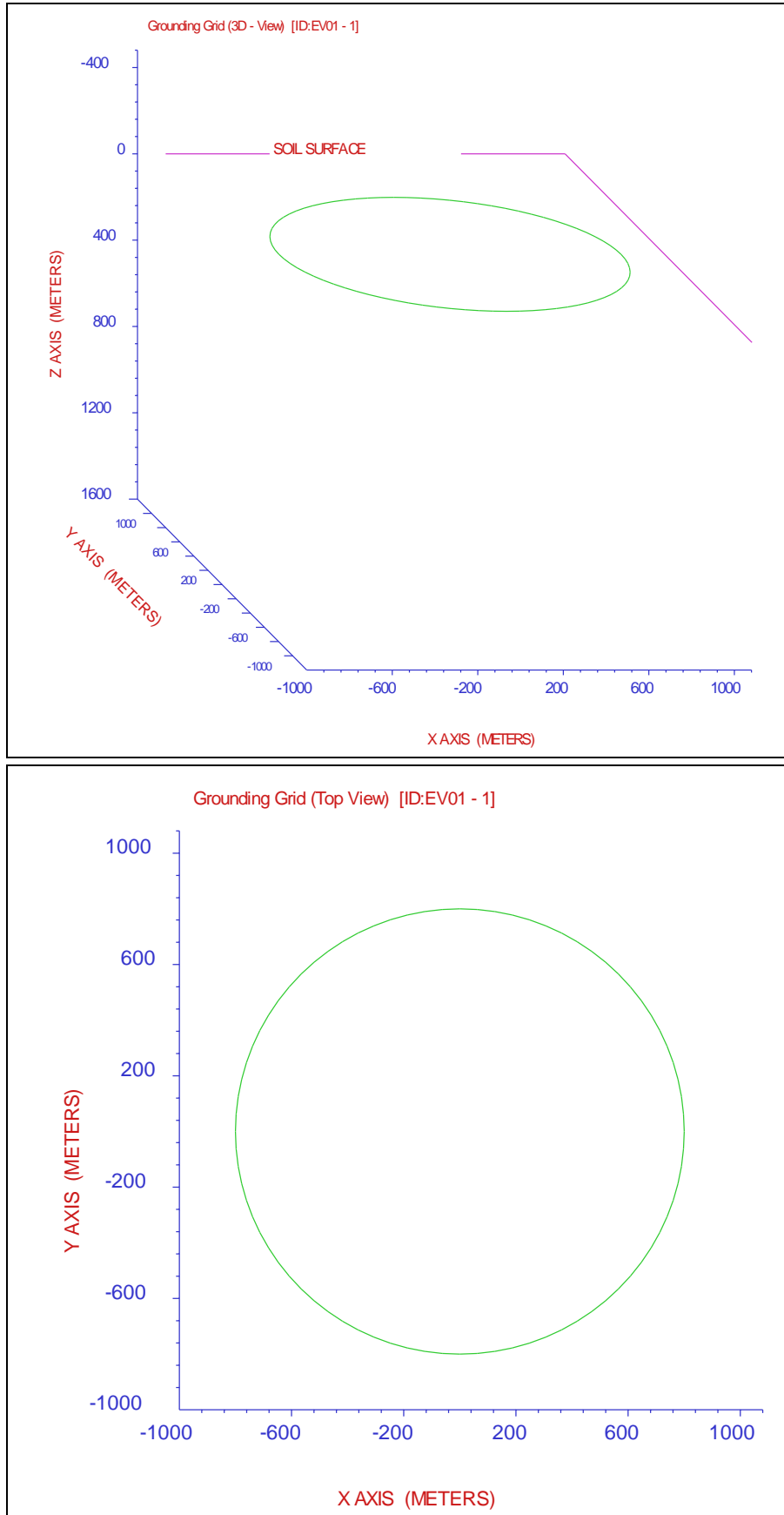


Figure 6.1: single ring 1.6 km wide ground electrode (3D and top view).

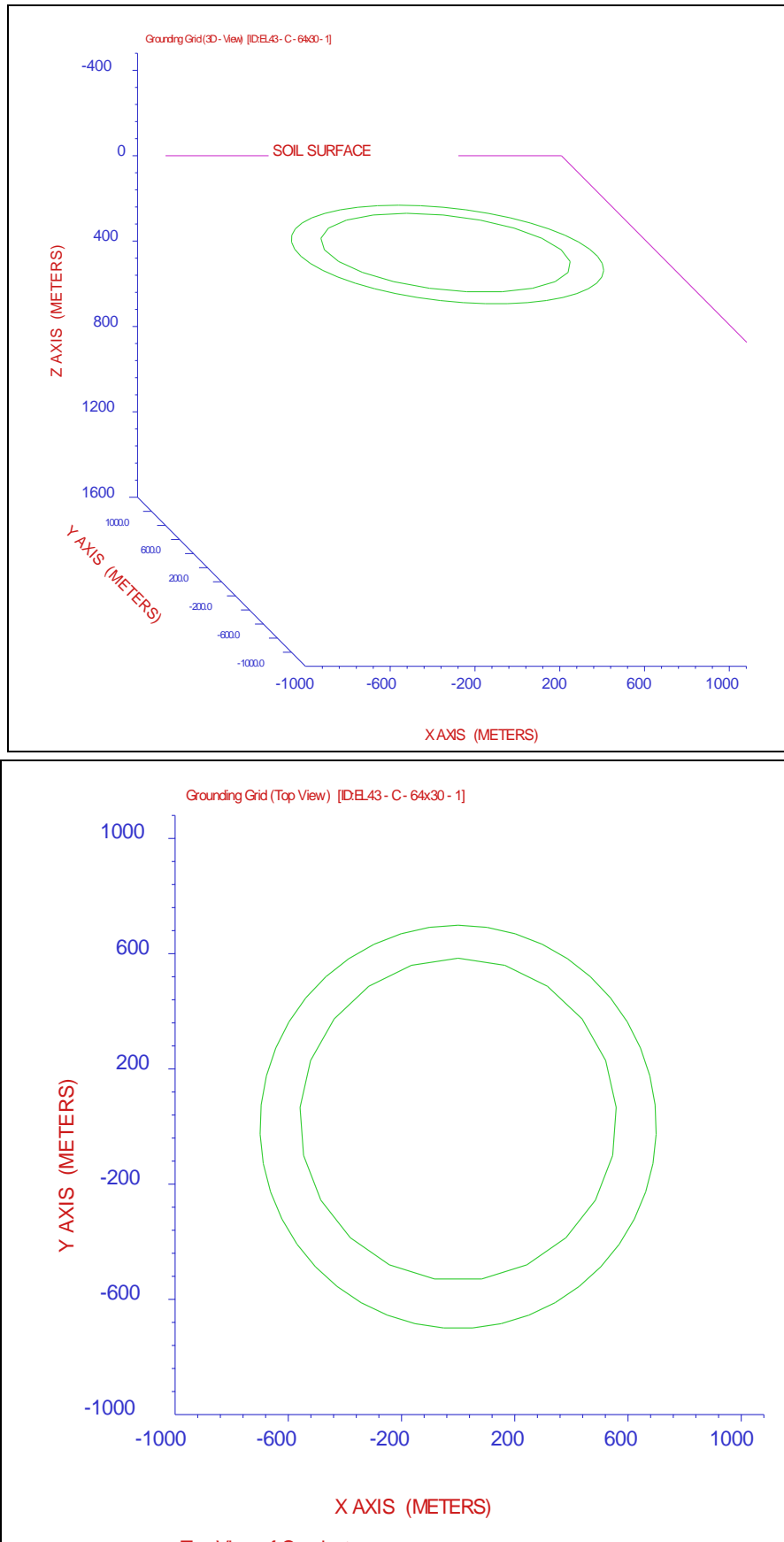


Figure 6.2: double ring horizontal electrode with 1400/1120 m diameter (3D and top view).

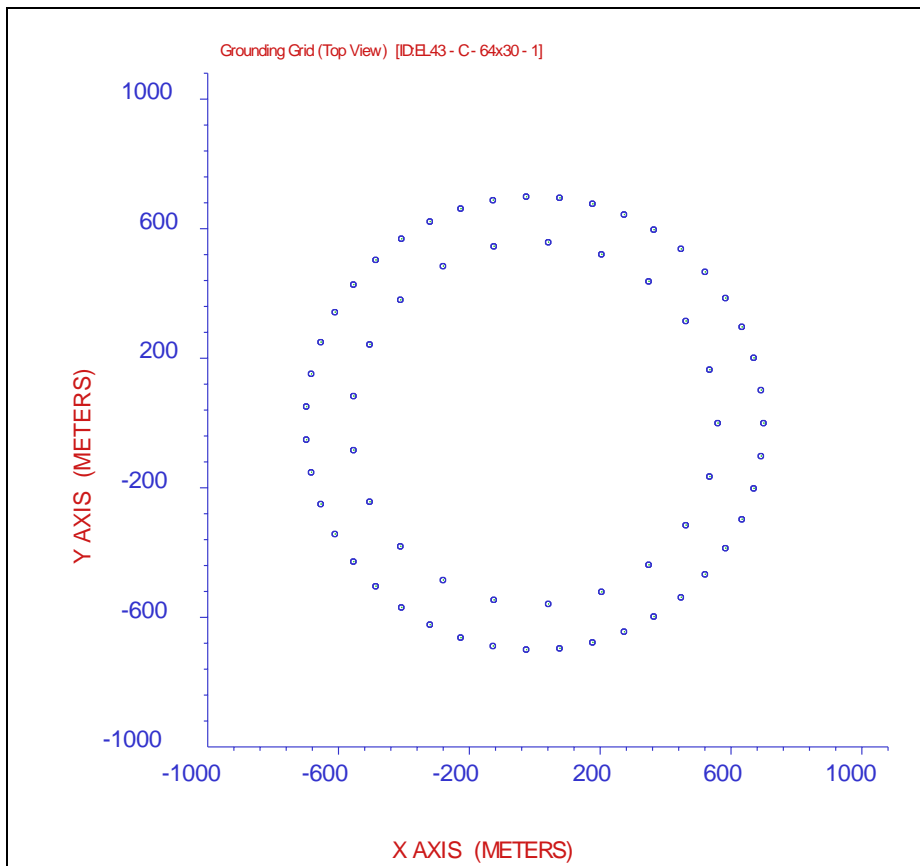
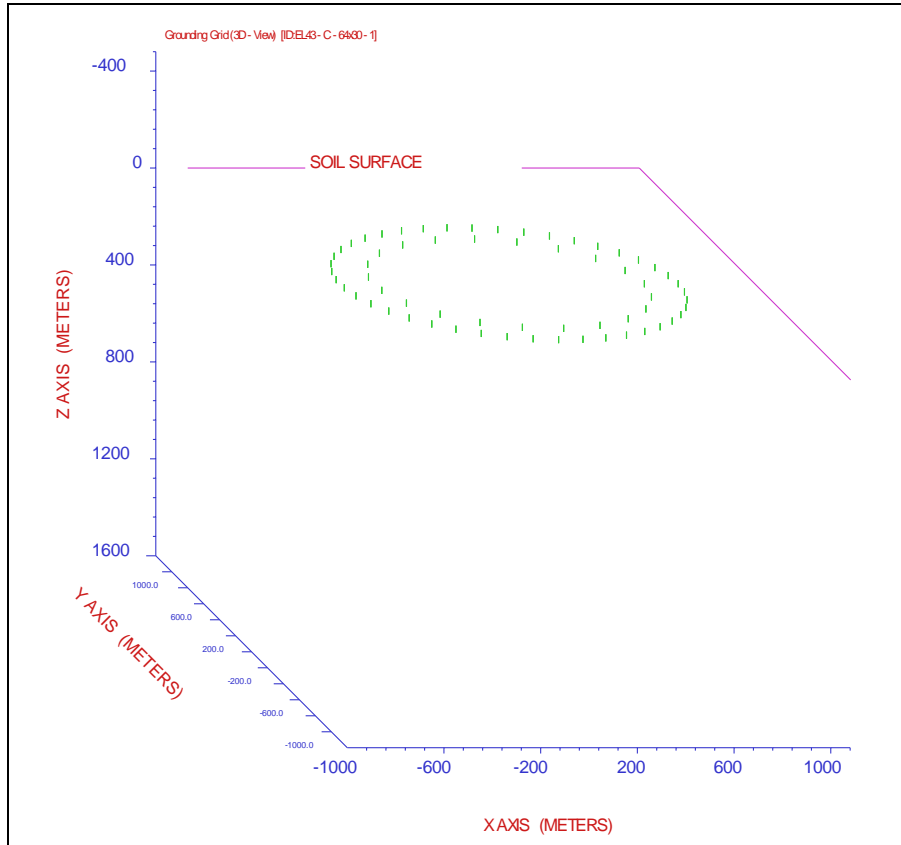


Figure 6.3: double ring vertical electrode with 1400/1120 m diameter (3D and top view).

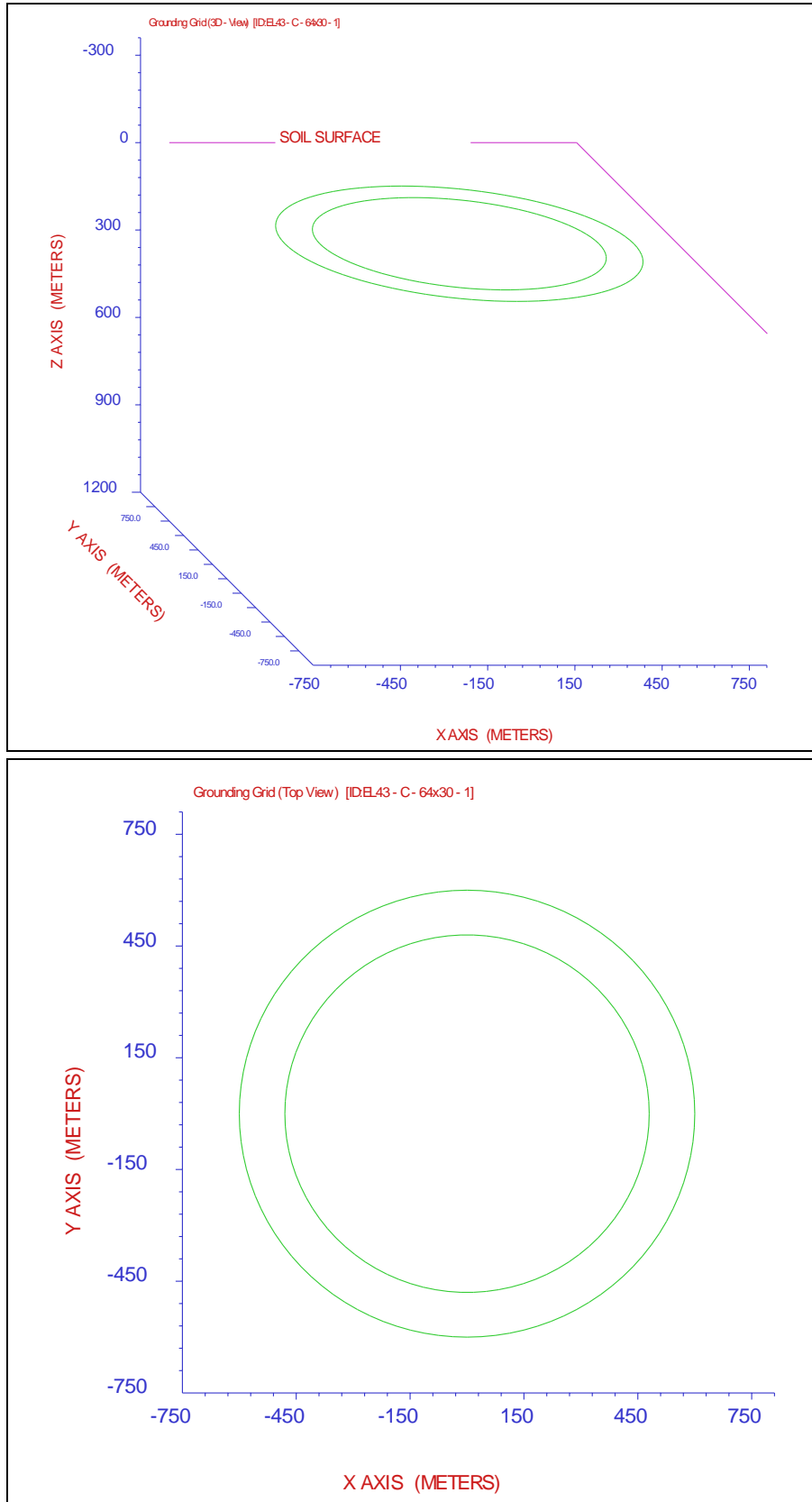


Figure 6.4: double ring horizontal electrode with 1200/960 m diameter (3D and top view).

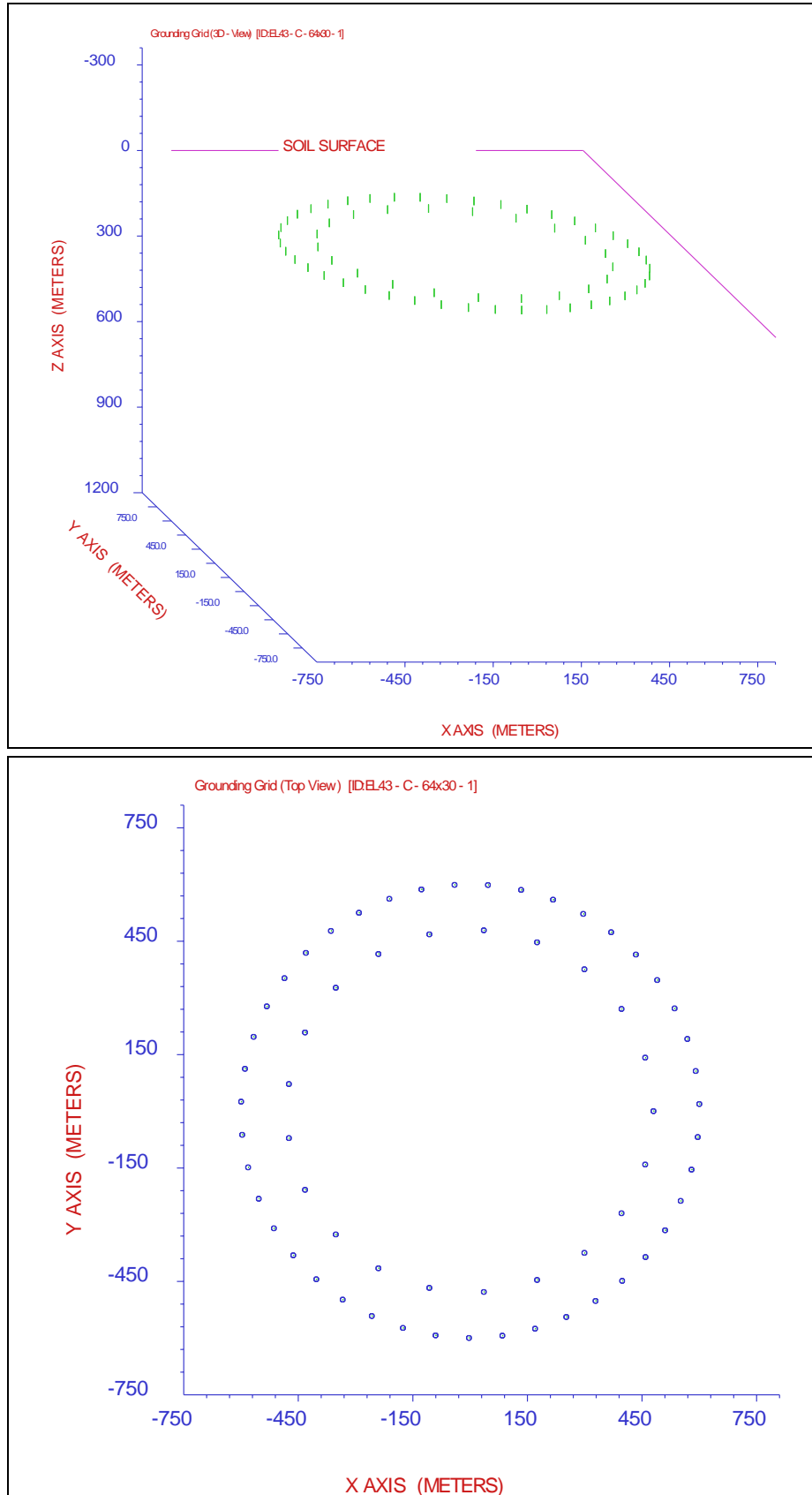


Figure 6.5: double ring vertical electrode with 1200/960 m (3D and top view).

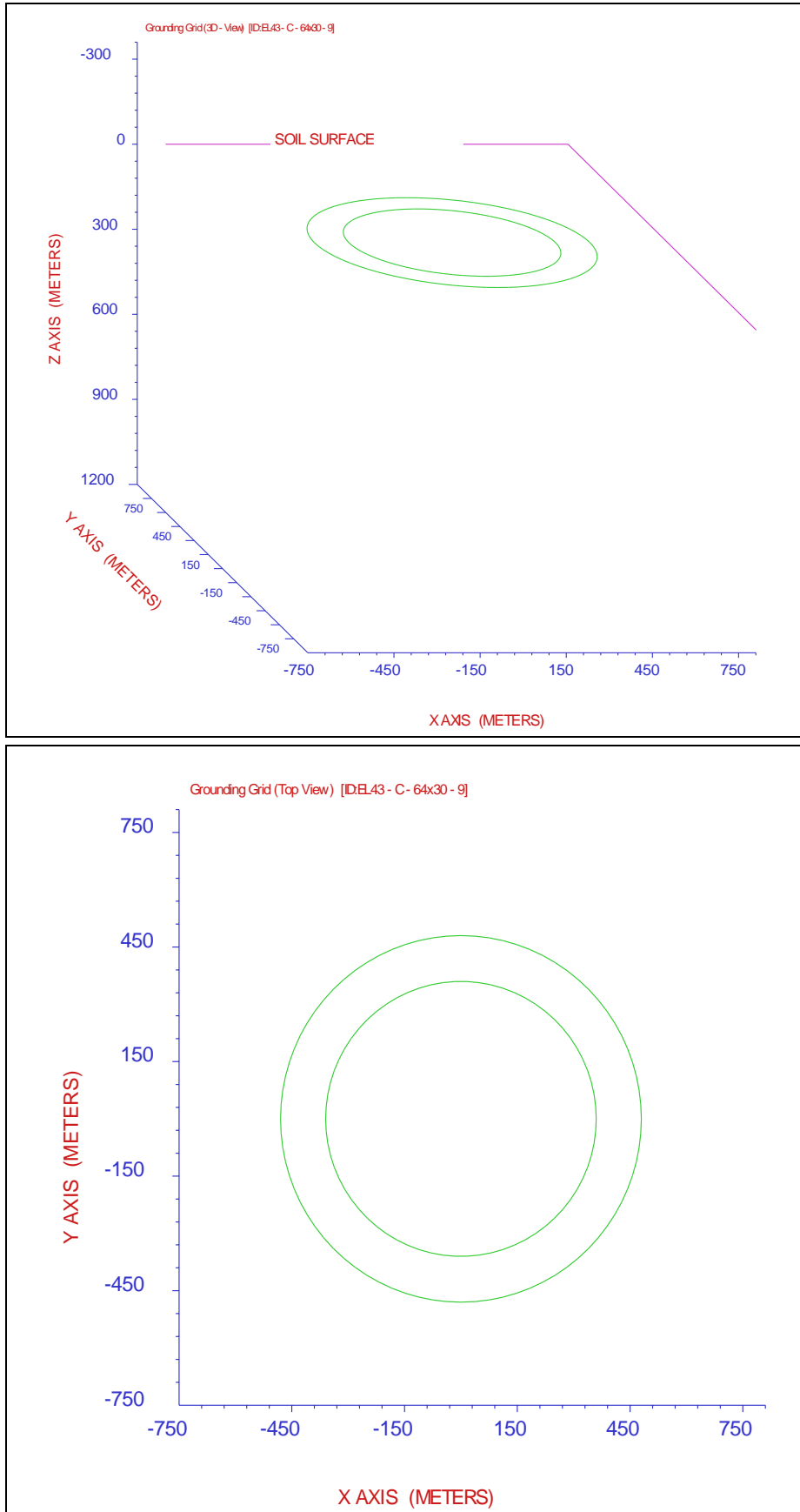


Figure 6.6: double ring horizontal electrode with 960/720 m diameter (3D and top view).

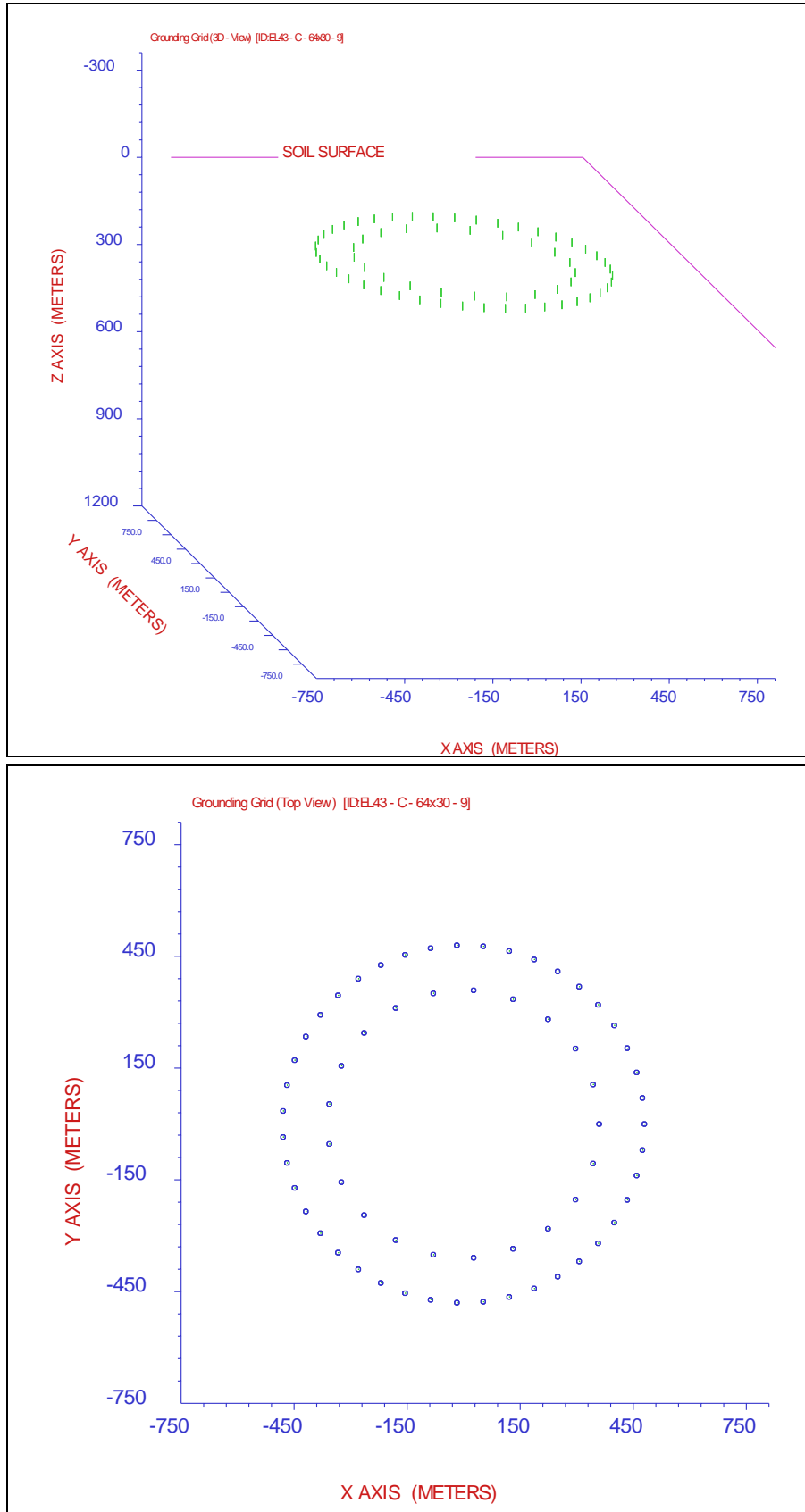


Figure 6.7: double ring vertical electrode with 960/720 m diameter (3D and top view).

6.1 Station 39

The simulation of the single ring horizontal electrode 1.6 km diameter at site EL39 resulted on the electrode resistance of 0.84 Ω , more than twice the maximum electrode resistance of 0.35 Ω .

6.2 Station 43

The following simulations were done for site EL43, which resulted on the following electrode resistances:

- single ring horizontal electrode 1.6 km diameter - 0.30 Ω ;
- double ring horizontal electrode with 1400/1120 m diameter - 0.32 Ω ;
- double ring vertical electrode with 1400/1120 m diameter (64 wells 30 m deep) - 0.35 Ω ;
- double ring horizontal electrode with 1200/960 m diameter – 0.35 Ω ;
- double ring vertical electrode with 1200/960 m (64 wells 30 m deep) - 0.37 Ω ;
- double ring horizontal electrode with 960/720 m diameter – 0.41 Ω ;
- double ring vertical electrode with 960/720 m diameter (64 wells 30 m deep) - 0.37 Ω .

The above two horizontal electrode configurations marked yellow attend the electrode resistance below 0.35 Ω .

6.3 Station 42

The simulation of the single ring horizontal electrode 1.6 km diameter at site EL42 resulted on the electrode resistance of 0.67 Ω , about twice the maximum electrode resistance of 0.35 Ω .

6.4 Station 46

The simulation of the single ring horizontal electrode 1.6 km diameter at site EL46 resulted on the electrode resistance of 1.11 Ω , about three times the maximum electrode resistance of 0.35 Ω .

===== < G R O U N D I N G (SYSTEM INFORMATION SUMMARY) > =====

Run ID.....: EL39 - 1
 System of Units: Metric
 Earth Potential Calculations.....: None
 Type of Electrodes Considered.....: Main Electrode ONLY
 Soil Type Selected.....: Multi-Layer Horizontal
 SPLITS/FCDIST Scaling Factor.....: 1.0000

MULTI-LAYER EARTH CHARACTERISTICS USED BY PROGRAM

LAYER No.	TYPE	REFLECTION COEFFICIENT	RESISTIVITY (ohm-meter)	THICKNESS (METERS)
1	Air	0.00000	0.100000E+11	Infinite
2	Soil	-0.999990	400.000	10.0000
3	Soil	-0.269841	230.000	70.0000
4	Soil	0.944778	8100.00	12000.0
5	Soil	-0.928571	300.000	Infinite

CONFIGURATION OF MAIN ELECTRODE

Original Electrical Current Flowing In Electrode...: 3325.0 amperes
 Current Scaling Factor (SPLITS/FCDIST/specified)...: 1.0000
 Adjusted Electrical Current Flowing In Electrode...: 3325.0 amperes
 Number of Conductors in Electrode.....: 80
 Resistance of Electrode System.....: 0.83900 ohms

SUBDIVISION

Grand Total of Conductors After Subdivision.: 80
 Total Current Flowing In Main Electrode.....: 3325.0 amperes
 Total Buried Length of Main Electrode.....: 5025.3 meters

EARTH POTENTIAL COMPUTATIONS

Main Electrode Potential Rise (GPR).....: 2789.7 volts

Table 6.1: Station EL39 – base case - single ring horizontal electrode 1.6 km diameter.

===== < G R O U N D I N G (SYSTEM INFORMATION SUMMARY) > =====

Run ID.....: EL43 - 1
 System of Units: Metric
 Earth Potential Calculations.....: None
 Type of Electrodes Considered.....: Main Electrode ONLY
 Soil Type Selected.....: Multi-Layer Horizontal
 SPLITS/FCDIST Scaling Factor.....: 1.0000

MULTI-LAYER EARTH CHARACTERISTICS USED BY PROGRAM

LAYER No.	TYPE	REFLECTION COEFFICIENT	RESISTIVITY (ohm-meter)	THICKNESS (METERS)
1	Air	0.00000	0.100000E+11	Infinite
2	Soil	-0.999990	150.000	1.00000
3	Soil	0.690722	820.000	2.00000
4	Soil	-0.607843	200.000	80.0000
5	Soil	0.550562	690.000	420.000
6	Soil	0.522491	2200.00	7800.00
7	Soil	-0.705426	380.000	11000.0
8	Soil	0.449275	1000.00	Infinite

CONFIGURATION OF MAIN ELECTRODE

Original Electrical Current Flowing In Electrode...: 3325.0 amperes
 Current Scaling Factor (SPLITS/FCDIST/specified)...: 1.0000
 Adjusted Electrical Current Flowing In Electrode...: 3325.0 amperes
 Number of Conductors in Electrode.....: 80
 Resistance of Electrode System.....: 0.30353 ohms

SUBDIVISION

Grand Total of Conductors After Subdivision...: 80
 Total Current Flowing In Main Electrode.....: 3325.0 amperes
 Total Buried Length of Main Electrode.....: 5025.3 meters

EARTH POTENTIAL COMPUTATIONS

Main Electrode Potential Rise (GPR).....: 1009.2 volts

Table 6.7: Station EL43 – base case single ring horizontal electrode 1.6 km diameter.

===== < G R O U N D I N G (SYSTEM INFORMATION SUMMARY) > =====

Run ID.....: EL43 - C - 64x30 - 1
 System of Units: Metric
 Earth Potential Calculations.....: None
 Type of Electrodes Considered.....: Main Electrode ONLY
 Soil Type Selected.....: Multi-Layer Horizontal
 SPLITS/FCDIST Scaling Factor.....: 1.0000

MULTI-LAYER EARTH CHARACTERISTICS USED BY PROGRAM

LAYER No.	TYPE	REFLECTION COEFFICIENT	RESISTIVITY (ohm-meter)	THICKNESS (METERS)
1	Air	0.00000	0.100000E+11	Infinite
2	Soil	-0.999990	150.000	1.00000
3	Soil	0.690722	820.000	2.00000
4	Soil	-0.607843	200.000	80.0000
5	Soil	0.550562	690.000	420.000
6	Soil	0.522491	2200.00	7800.00
7	Soil	-0.705426	380.000	11000.0
8	Soil	0.449275	1000.00	Infinite

CONFIGURATION OF MAIN ELECTRODE

Original Electrical Current Flowing In Electrode...: 3325.0 amperes
 Current Scaling Factor (SPLITS/FCDIST/specified)...: 1.0000
 Adjusted Electrical Current Flowing In Electrode...: 3325.0 amperes
 Number of Conductors in Electrode.....: 64
 Resistance of Electrode System.....: 0.31823 ohms

SUBDIVISION

Grand Total of Conductors After Subdivision...: 85
 Total Current Flowing In Main Electrode.....: 3325.0 amperes
 Total Buried Length of Main Electrode.....: 7899.8 meters

EARTH POTENTIAL COMPUTATIONS

Main Electrode Potential Rise (GPR).....: 1058.1 volts

Table 6.6: Station EL43 - double ring horizontal electrode with 1400/1120 m diameter.

===== < G R O U N D I N G (SYSTEM INFORMATION SUMMARY) > =====

Run ID.....: EL39 - 1
 System of Units: Metric
 Earth Potential Calculations.....: None
 Type of Electrodes Considered.....: Main Electrode ONLY
 Soil Type Selected.....: Multi-Layer Horizontal
 SPLITS/FCDIST Scaling Factor.....: 1.0000

MULTI-LAYER EARTH CHARACTERISTICS USED BY PROGRAM

LAYER No.	TYPE	REFLECTION COEFFICIENT	RESISTIVITY (ohm-meter)	THICKNESS (METERS)
1	Air	0.00000	0.100000E+11	Infinite
2	Soil	-0.999990	120.000	35.0000
3	Soil	0.933702	3500.00	300.000
4	Soil	-0.400000	1500.00	1200.00
5	Soil	0.904762	30000.0	30000.0
6	Soil	-0.791045	3500.00	Infinite

CONFIGURATION OF MAIN ELECTRODE

=====

Original Electrical Current Flowing In Electrode...: 3325.0 amperes
 Current Scaling Factor (SPLITS/FCDIST/specified)...: 1.0000
 Adjusted Electrical Current Flowing In Electrode...: 3325.0 amperes
 Number of Conductors in Electrode.....: 80
 Resistance of Electrode System.....: 0.66555 ohms

SUBDIVISION

=====

Grand Total of Conductors After Subdivision...: 80
 Total Current Flowing In Main Electrode.....: 3325.0 amperes
 Total Buried Length of Main Electrode.....: 5025.3 meters

EARTH POTENTIAL COMPUTATIONS

=====

Main Electrode Potential Rise (GPR).....: 2213.0 volts

Table 6.2: Station EL42 – base case - single ring horizontal electrode 1.6 km diameter.

===== < G R O U N D I N G (SYSTEM INFORMATION SUMMARY) > =====

Run ID.....: EL39 - 1
 System of Units: Metric
 Earth Potential Calculations.....: None
 Type of Electrodes Considered.....: Main Electrode ONLY
 Soil Type Selected.....: Multi-Layer Horizontal
 SPLITS/FCDIST Scaling Factor.....: 1.0000

MULTI-LAYER EARTH CHARACTERISTICS USED BY PROGRAM

LAYER No.	TYPE	REFLECTION COEFFICIENT	RESISTIVITY (ohm-meter)	THICKNESS (METERS)
1	Air	0.00000	0.100000E+11	Infinite
2	Soil	-0.999990	500.000	1.00000
3	Soil	0.444444	1300.00	2.00000
4	Soil	-0.382979	580.000	90.0000
5	Soil	0.876333	8800.00	900.000
6	Soil	-0.900648	460.000	240.000
7	Soil	0.857585	6000.00	7800.00
8	Soil	-0.764706	800.000	12000.0
9	Soil	0.851852	10000.0	55000.0
10	Soil	-0.639344	2200.00	Infinite

CONFIGURATION OF MAIN ELECTRODE

=====

Original Electrical Current Flowing In Electrode...: 3325.0 amperes
 Current Scaling Factor (SPLITS/FCDIST/specified)...: 1.0000
 Adjusted Electrical Current Flowing In Electrode...: 3325.0 amperes
 Number of Conductors in Electrode.....: 80
 Resistance of Electrode System.....: 1.1161 ohms

SUBDIVISION

=====

Grand Total of Conductors After Subdivision.: 80
 Total Current Flowing In Main Electrode.....: 3325.0 amperes
 Total Buried Length of Main Electrode.....: 5025.3 meters

EARTH POTENTIAL COMPUTATIONS

=====

Main Electrode Potential Rise (GPR).....: 3711.2 volts

Table 6.3: Station EL46 – base case - single ring horizontal electrode 1.6 km diameter.

7 CONCLUSION

From the 8 stations surveyed, only station EL43 has the geologic conditions to host a HVDC ground electrode. The following simulations were done for site EL43, which resulted on electrode resistances below 0.35 Ω :

- base case - single ring horizontal electrode 1.6 km diameter - 0.30 Ω ;
- double ring horizontal electrode with 1400/1120 m diameter - 0.32 Ω .

The single ring horizontal electrode 1.6 km diameter occupies a bigger area but demands less excavation and less materials (coke and FeSiCr anodes) than the double ring electrode.

Unhappily it was not found any other site that can be considered a second option for hosting the electrode.

Photos 6.1 and 6.2 show that site EL43 is reasonably flat, except for a hill in the NW direction. A field survey will be needed in order to adjust the perimeter of the electrode as flat as possible. This perimeter does not need to be exactly circular, and a non circular electrode will allow for a flatter perimeter.

Site EL43 shows a significant anisotropy in the ground structure, presenting a resistivity profile similar to a sedimentary basin in the direction of the main geologic strike of the area, and a high resistivity profile in the transversal direction. This happens, probably, due to shales (a metamorphic rock that has a significant carbon content), and possibly to graphite veins. This anisotropy will result on asymmetric electrode equipotentials on soil surface.

For the basic design of the electrode at site EL43 it will be needed complementary geophysical and geotechnical surveys. The geophysical survey will be a shallow resistivity campaign of about 35 Schlumberger soundings along the previewed electrode perimeter (considering the 1.6 km ring). The geotechnical survey will be SPT soundings down to the basement and wells drilling for induction profiling, for the determination of the water table level and of the actual resistivity along the wells extension. The induction profiling of a few wells will allow for the adjustment of the static shif of the ER and MT soundings.

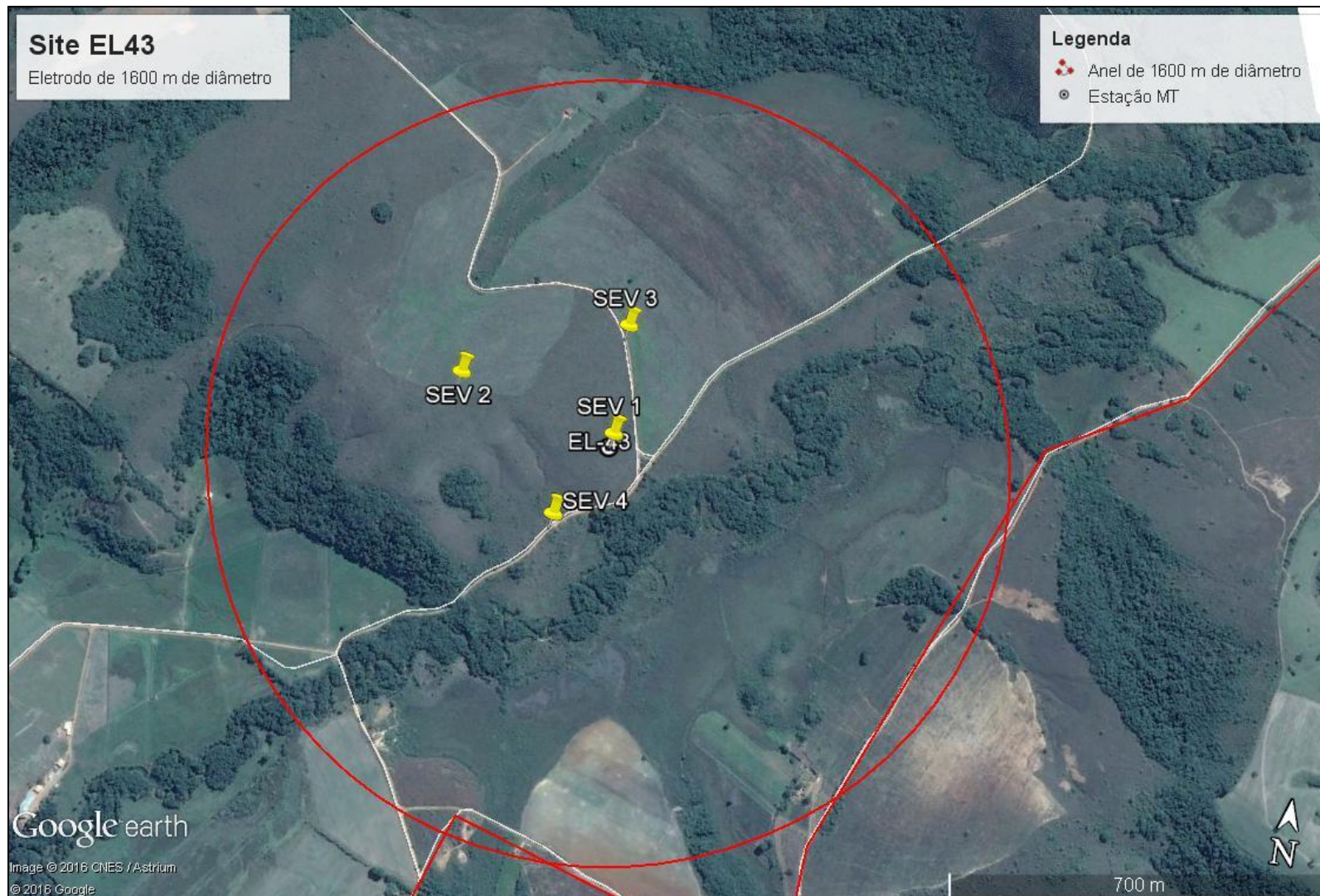


Photo 7.1: top view of a ring 1600 m wide centered at MT station 43, with Schlumberger sounding points.

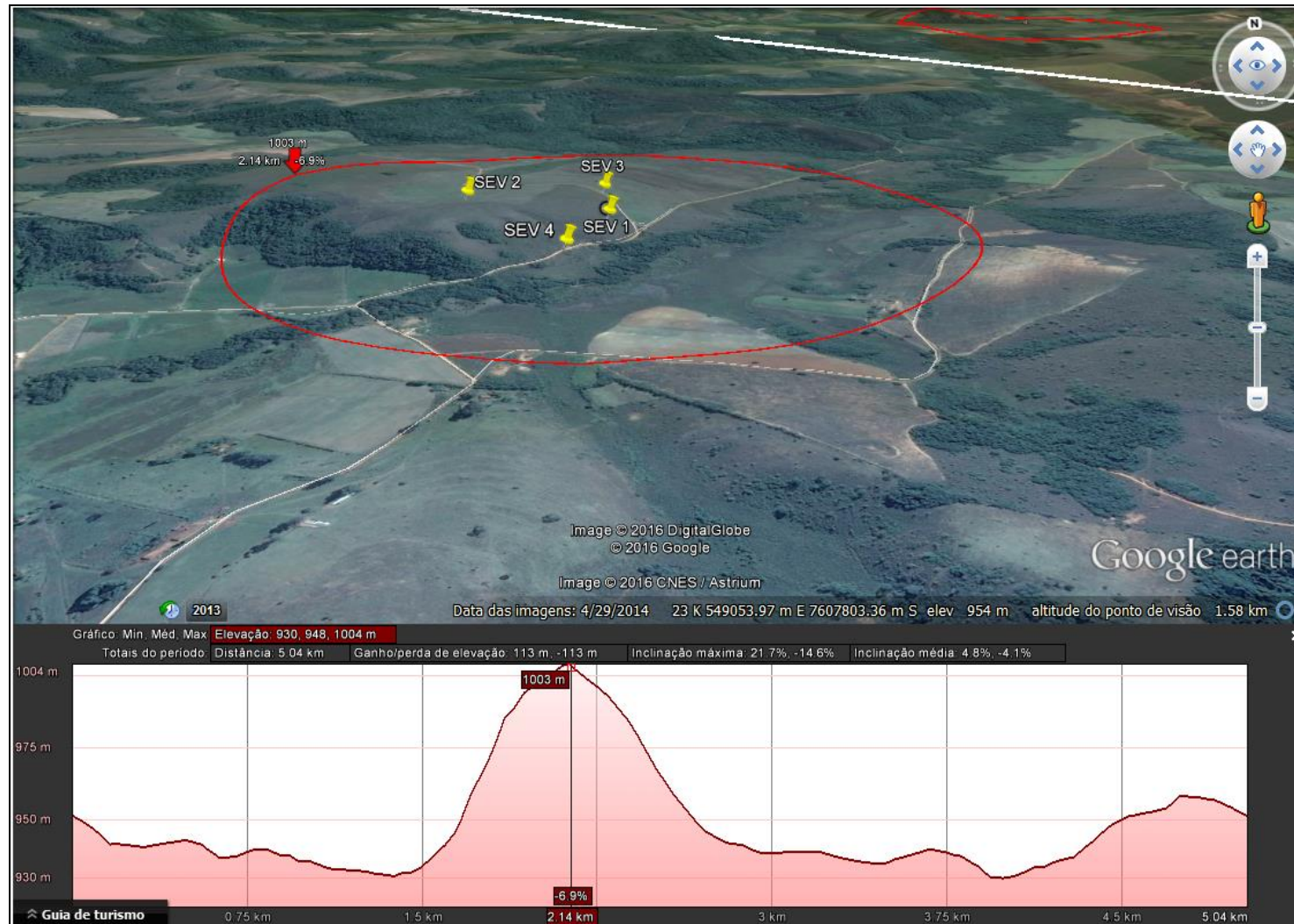


Photo 7.2: angle view of Station 43 with perimeter profile.

CSEPDI

**BELO MONTE HVDC SYSTEM
BIPOLE II – RJ - GROUND ELECTRODE
“DESKTOP STUDY”**

